The MDM2 oncoprotein antagonizes Poly(ADP-ribosyl)ation

Dissertation

for the award of the degree

"Doctor of Philosophy" (Ph.D.)

Division of Mathematics and Natural Sciences

of the Georg-August-Universität Göttingen

within the doctoral program Molecular Medicine

of the Georg-August University School of Science (GAUSS)

submitted by

Celeste Giansanti

from Sant'Angelo in Pontano, Italy

Göttingen, 2022

TABLE OF CONTENTS

ABBREVIATIONS

°C	Degree celsius
µg	Microgram
µl	Microliter
µM	Micromolar
ADPr	ADP-ribosylation
APS	Ammonium persulphate
ATM	Ataxia Telangiectasia Mutated
ATR	Ataxia Telangiectasia And Rad3-Related
BAX	BCL2-associated X Protein
BCA	Bicinchoninic acid
BER	Base Excision Repair
bp	Base pair
BRCT	BRCA1 C Terminus
BSA	Bovine serum albumin
CD	Catalytic Doman
CHK1	Checkpoint kinase 1
CHK2	Checkpoint kinase 2
CldU	5-chloro-2′-deoxyuridine
CtBP	C-terminal-binding protein 1 CtBP
Ctrl	Control
DAPI	4′,6-diamidino-2-phenylindole
ddH_2O	Double-distilled H_2O
DDR	DNA damage response
DMEM	Dulbecco´s Modified Eagle Medium
DMSO	Dimethyl sulfoxide
DSB	DNA double-strand break
DTT	Dithiotreitol
EDTA	Ethylenediaminetetraacetic acid
EdU	5-ethynyl-2'-deoxyuridine
e.g.	for example (Latin *exempli gratia*)
EtOH	Ethanol
FBS	Fetal bovine serum
FSRN	Fork Speed Regulatory Network
GAPDH	Glyceraldehyde-3-phosphate dehydrogenase

h	hour
H2AX	Histone variant 2A.X
H_2O_2	Hydrogen peroxide
H3	Histone 3
HCl	Hydrochloric acid
HRP	Horseradish peroxidase
i	Inhibitor
IdU	5-iodo-2'-deoxyuridine
i.e.	That is (Latin *id est*)
KCl	Potassium chloride
kDa	Kilodalton
MAR	Mono(ADP-ribose)
MDM2	Murine double minute 2 homolog
MgCl2	Magnesium chloride
mM	millimolar
mut	Mutant
NaCl	Sodium chloride
NAD^+	Nicotinamide adenine dinucleotide
NER	Nucleotide Excision Repair
NES	Nuclear export signal
ng	Nanogram
NLS	Nuclear localization signal
nM	Nanomolar
ns	Not significant
PAGE	Polyacrylamide gel electrophoresis
PAR	Poly(ADP-ribose)
PARP	Poly(ADP-ribose) polymerase
PBS	Phosphate buffered saline
PCNA	Proliferating cell nuclear antigen
PFA	Paraformaldehyde
Phospho	Phosphorylated
Pol ι	DNA polymerase iota
PRC2	Polycomb Repressor Complex 2
PRIMPOL	Primase and DNA directed polymerase
PROTAC	Proteolysis targeting chimera
PTM	Posttranslational Modification

PUMA	p53-upregulated mediator of apoptosis
RECQ1	ATP-dependent DNA helicase Q1
rev	Reverse
RING	Really Interesting New Gene
ROI	Region of interest
RPA	Replication protein A
RT	Room temperature
RT-qPCR	Real-time quantitative PCR
SDS	Sodium dodecyl sulphate
SDS-PAGE	SDS-polyacrylamide gel electrophoresis
Ser-ADPr	Serine ADP-ribosylation
siRNA	Small interfering RNA
SSBR	Single Stranded Break Repair
ssDNA	Single stranded DNA
TLS	Translesion Synthesis
Tris	Tris(hydroxymethyl)-aminomethan
WIP1	Wild-Type P53-Induced Phosphatase 1
WGR	tryptophan-glycine-arginine-rich
WWE	Tryptophan- Tryptophan-Glutamate
ZF/Zn	Zinc Finger

1. ABSTRACT

MDM2 is a target gene product and a negative regulator of the tumor suppressor p53. Additionally, MDM2 interferes with the progression of DNA replication forks. Poly(ADP-Ribose) Polymerase 1 (PARP1) is the main ADP-ribosyltransferase in human cells. It regulates DNA replication fork progression and DNA damage tolerance. In this thesis work, we studied the interplay between MDM2 and PARP1, and the functional consequences of it, with a particular focus on DNA replication. We found that p53 activation reduced PARP1 protein levels by the induction of MDM2. MDM2 directly interacts with PARP1, leading to inactivation, ubiquitination and proteasome-mediated degradation of the latter. In the same context, MDM2 significantly enhanced the rate of DNA synthesis. This depended on PARP1 inactivation, since transient overexpression of PARP1 brought DNA replication fork progression back to control levels, and simultaneous MDM2 induction and PARP1 inhibition did not further increase newly synthetized DNA track lengths, strongly suggesting an epistatic relation. When a replication fork encounters an obstacle, fork reversal can occur, meaning that the canonical three-way replication fork is rearranged to a four-way junction. Since PARP1 is required for the stabilization of these structures, we quantified the frequency of reversed forks by electron microscopy. We found that MDM2 accumulation strongly reduced fork reversal. In order to further determine the mechanistic base of the acceleration of DNA replication forks, we investigated the impact of two factors involved in the restart of stalled replication forks, which have been linked to PARP1. These are the helicase RECQ1, which mediates the resolution of reversed replication forks, and the primase/polymerase PRIMPOL, which restarts DNA synthesis downstream replication roadblocks. Strikingly, either RECQ1 or PRIMPOL depletion disabled MDM2-mediated acceleration of the nascent DNA elongation. We then explored whether the enhanced restart at stalled DNA replication forks would provoke genome instability by analyzing the formation of micronuclei. As expected, MDM2-dependent inactivation of PARP1 promoted micronuclei formation. In addition, it also exacerbated the cytotoxicity of the Topoisomerase I inhibitor camptothecin, highlighting a potential clinical relevance of this pathway. In conclusion, MDM2 does not only provide negative feedback on p53; it also antagonizes PARP1 to govern DNA replication fork progression, thus enhancing the tolerance of cells towards DNA damage.

2. INTRODUCTION

2.1 P53: forty years of research

In the 1970s, a substantial part of cancer research was focused on the study of oncogenic viruses. Early on, it became clear that oncogenic retroviruses promoted tumorigenic transformation by overexpressing 'hijacked' cancer-promoting cellular proteins (Stehelin et al., 1976). Oncogenic DNA viruses seemed to operate differently. The hypothesis was that these viruses contained their own oncogenes encoding viral components that indirectly induce cellular oncogenic factors. Simian virus 40 (SV40) was typically used as a prototype oncogenic DNA virus to infect experimental animals. Upon infection, few viral proteins were synthesized and readily recognized by the host immune system that produced antibodies against them. Notably, these viral antigens were also the viral oncoproteins (Levine and Oren, 2009).

It was during the attempt of immunoprecipitating one of these SV40 oncoproteins, using the sera from infected animals, that a non-viral protein with a molecular weight of 53 kDa was co-precipitated (Lane and Crawford, 1979). In the same year, this factor was identified by other laboratories with similar modalities: Daniel Linzer and Arnold Levine at Princeton (USA), Pierre May at the Cancer Research Institute (Villejuif, France), Robert Carroll at New York University (USA), and Alan Smith at the Imperial Cancer Research Fund London (UK) (Kress et al., 1979; Linzer and Levine, 1979; Melero et al., 1979; Smith et al., 1979). Three additional findings exposed this 53kDa protein as a tumor-associated factor: (i) it was found in teratocarcinoma-derived cells (Linzer and Levine, 1979), (ii) antibodies against it were produced by animals immunized with non-virally transformed cancer cells (DeLeo et al., 1979), (iii) it was found in cells transformed by the retrovirus Abelson murine leukemia virus (Rotter et al., 1980). This 53 kDa protein was unanimously named p53 only in 1983 at the 1st International p53 Workshop in Oxted (UK).

After the discovery of p53, many labs tried to clone its gene. To this end, mRNA from cancer cells was used, which mostly led to cloning the mutated versions of the gene. Since mutant p53 exerts cancer-promoting effects, p53 was initially labelled as an oncogene (Eliyahu et al., 1984; Jenkins et al., 1984; Parada et al., 1984). Its tumor suppressive function emerged only in 1989 from three main reports: (i) Arnold Levine's laboratory cloned the correct WT p53 coding gene (TP53) (Finlay et al., 1989), (ii) Bert Vogelstein's lab found that p53 was frequently inactivated by mutations in both TP53 alleles in human colorectal cancers (Baker et al., 1989), (iii) independently in Levine's and Oren's laboratories, it was observed that overexpression of p53 effectively repressed MYC- and HRAS-mediated oncogenesis (Eliyahu et al., 1989; Finlay et al., 1989). Additionally, the other two hallmarks of a tumor suppressor were fulfilled by p53: Germline TP53 mutations cause the hereditary Li-Fraumeni syndrome, characterized by early-

onset cancers (Malkin et al., 1990; Srivastava et al., 1990), and Trp53 (murine p53)-knockout mice develop tumors (Donehower et al., 1992; Donehower and Lozano, 2009).

P53 is not only a tumor suppressor; it is the most 'successful' tumor suppressor in that TP53 is the most frequently mutated gene in human cancers (Vogelstein et al., 2000). For this reason, it has been heavily studied in the past 40 years, with the publication of thousands of scientific works.

How does p53 work?

The biological function of p53 was first determined using a temperature-sensitive mutant of p53, by which p53 was shown to determine cell cycle arrest at G1 and G2-M (Michalovitz et al., 1990). Additionally, prolonged re-expression of p53 in the M1 leukemia cell line provoked cancer cell apoptosis, shedding new light on apoptosis as a mechanism for tumor suppression (Michalovitz et al., 1990).

Mechanistically, p53 regulates the expression of hundreds of genes encoding proteins or microRNAs. These are transcriptionally transactivated by p53 binding to consensus DNA sequences via the two p53 transactivation domains (Fields and Jang, 1990; Raycroft et al., 1990; Zhu et al., 1998). We refer to the simultaneous regulation of the expression of the responsive genes upon different stimuli as p53 response, which can vary in a cell type-, and context-dependent fashion. Many of the responsive genes encode proteins that are involved in cell cycle progression and apoptosis (Menendez et al., 2009), which explains p53 impact on cell fate. Surprisingly, also p53 non-transcriptional functions emerged more recently. Among them, there is the p53 activity at DNA replication forks that will be discussed below.

But why is TP53 the most commonly mutated gene in human cancers?

P53 has been evolutionarily selected to be induced upon one or a combination of cell stresses. There are multiple cellular stress responder pathways. Among them, p53 has the peculiarity of acting as a single node, or integrator, for different kinds of stress inputs and outputs. This means that all the pathways sensing these stresses converge on the post translational modification of one unique factor, which is p53. The same factor will then be enabled by these modifications to regulate the appropriate set of genes for a combined response. This pathway architecture permits to integrate information better than single modifications on different factors. However, the simple loss of p53, e.g., by mutation, shuts down the entire pathway. For this reason, mutations of this factor are selected in cancer cells more frequently than mutations of one of the redundant stress sensors or p53 target genes. Mutations of p53 target genes are not tumorigenic, with the exception of Mouse Double Minute 2 homolog (MDM2), the amplification of which is found in cancer, notably in sarcomas (Rayburn et al., 2005).

2.2 The p53-MDM2 negative feedback loop

In 1992, MDM2 was found to associate with p53 (Momand et al., 1992). MDM2 is one of the most strongly p53-induced genes. Its product is an E3 ubiquitin ligase that inactivates p53 by different means: (i) It blocks sterically the transactivation domain of p53 (Oliner et al., 1993), (ii) MDM2-driven ubiquitination withdraws p53 from its cognate DNA binding sites (Henningsen et al., 2021), and (iii) it mediates p53 proteasomal degradation (Haupt et al., 1997; Honda et al., 1997; Kubbutat et al., 1997). Once induced by p53, MDM2 binds, inactivates and destabilizes it, giving rise to a regulatory feedback loop (Wade et al., 2013) (Figure 1). Setting up this feedback loop, MDM2 enables the inducible nature of p53 in response to stress. Indeed, in unstressed conditions, p53 is kept at low basal levels by MDM2. This is possible because the transcription of MDM2 is regulated by two promoters, leading to the expression of two isoforms (Barak et al., 1994). The first promoter (P1) is situated upstream of exon one and mediates the constitutive expression of MDM2, while the second (P2) is located within the first intron, right downstream the p53 responsive elements, thereby enabling p53-induced transactivation (Cheng and Cohen, 2007; Zauberman et al., 1995). When the cell is exposed to stress, such as a genotoxic insult, the reduced binding of MDM2 to p53, and the diminished E3 ubiquitin ligase activity of MDM2 mediate rapid increase of p53 protein levels. Upon accumulation, p53 transactivates its cognate genes, including MDM2. In this context, MDM2 protein levels can be further regulated by the tumor suppressor $P14^{ARF}$, which inhibits the ubiquitin ligase activity of MDM2 , with consequent p53 induction (Kamijo et al., 1998). Another player in the p53-MDM2 negative feedback loop is MDM4/MDMX, which, despite lacking E3 ubiquitin ligase activity, inactivates p53 by different means: (i) by binding to its amino-terminal region, (ii) by associating with MDM2 and enhancing its E3 ligase activity (Kostic et al., 2006; Linares et al., 2003).

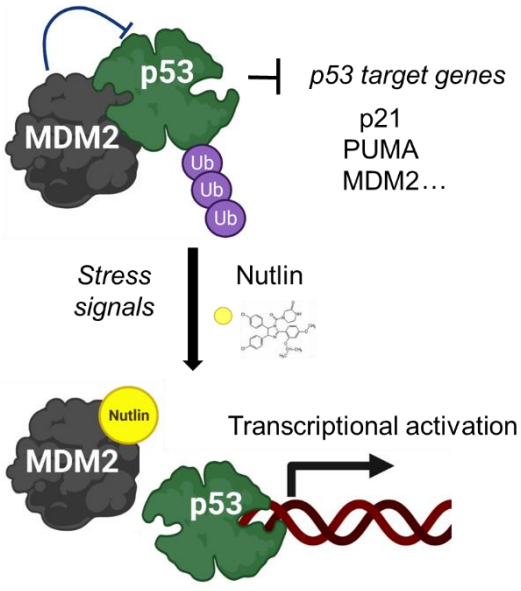

Figure 1. P53-MDM2 negative feedback loop and Nutlin pharmacodynamics.

Homeostasis of p53 levels is maintained in unstressed cells by MDM2, which ubiquitinates p53, leading to its proteasomal degradation (top panel). In response to stress signals, or to the disruption of the p53-MDM2 interaction by Nutlin, p53 transactivates its cognate genes (bottom panel).

2.3 Pharmacological inhibitors of MDM2

The research advances on p53 raised the interest toward its use for cancer therapy. Two main approaches were employed for the development of p53-based anticancer treatments. In order to target tumors with mutated TP53, research efforts focused on the development of small molecules capable of binding mutant p53 and restoring the functions of p53 in tumor cells (Boeckler et al., 2008; Bykov et al., 2002). On the other hand, to target the tumors retaining wild type p53, the effort was made to develop compounds capable of disrupting the interaction of p53 with its negative regulator MDM2. This gave rise to the class of compounds known as Nutlins (Vassilev, 2007; Vassilev et al., 2004). Among them, Nutlin-3a (referred to as Nutlin from here on) turned out to be the most potent and specific at the time (Vassilev et al., 2004). Nutlin binds to the p53-binding hydrophobic pocket of MDM2, effectively displacing p53, which accumulates and induces transcriptional transactivation of all the target genes, including the pro-apoptotic factor PUMA and the E3 ubiquitin ligase MDM2 (Figure 1). Nutlin entered clinical trials for liposarcoma patients. As expected, the drug induced p53 activation and apoptosis in the tumor. However, even if triggering tumor shrinkage in experimental animals, the drug did not improve patients' therapy, mostly due to the appearance of p53 mutations, and it caused severe adverse reactions (Ray-Coquard et al., 2012). Despite the clinical outcome, MDM2-binders have become useful research tools to study the p53 response without imposing cellular stress. Nutlin turned out to be particularly useful also for the study of MDM2. Once the p53-MDM2 interaction is disrupted, all the p53 targets are induced and among them also MDM2. The only downside to the use of Nutlin for investigating MDM2 biology is that all the p53 targets are concomitantly induced, which makes mechanistic studies on MDM2 particularly difficult. To overcome this problem, proteolysis targeting chimera (PROTAC) were recently developed. In the particular case of MDM2, a molecule named MD-224 is now commercially available. This is composed of two active domains connected by a linker: MI-1061 and a heterologous E3 ubiquitin ligase, Cereblon. MI-1061 binds MDM2, similarly to Nutlin, disrupting MDM2 binding to p53. At the same time, the Cereblon domain leads to ubiquitination and proteasomal degradation of MDM2, while p53 remains active (Li et al., 2019). This new tool enables mechanistic studies on MDM2 in the context of the p53 response. The MDM2 PROTAC had a pivotal role in the research work presented in this thesis.

2.4 Structure, posttranslational modifications, and interactome of MDM2

MDM2 protein consists of 491 amino acid residues, and it is composed of three domains: the N-terminal region, the C-terminal Really Interesting New Gene (RING) finger domain, and the central region that includes an acidic region, a nuclear localization signal (NLS), a nuclear export signal (NES), and a C4 zinc finger domain (Linke et al., 2008) (Figure 2).

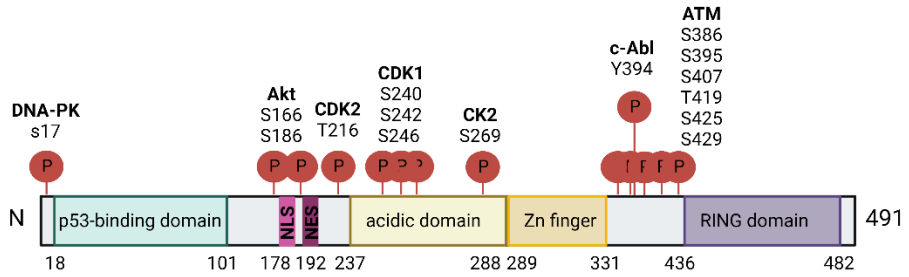

Figure 2. MDM2 domains and phosphorylation sites. The MDM2 protein comprises an N-terminal p53-binding domain, a nuclear localisation (NLS) and export signal (NES), an acidic domain, a Zinc (Zn) finger domain as well as a C-terminal RING domain. Additionally, kinases of different classes phosphorylate MDM2 at the indicated sites. Scheme adapted from Wade *et al.*, 2010.

The N-terminal domain forms a hydrophobic pocket (AA25-100) that allows binding to p53 (Kussie et al., 1996). Even though multiple structures of MDM2 regions in complex with other proteins and compounds have been published in the past, the full-length structure has not yet been solved, and the N-terminal is the best characterized of all the domains (Grasberger et al., 2005; Kallen et al., 2009; Skalniak et al., 2019; Srdanovic et al., 2022).

The RING finger domain has intrinsic E3 ubiquitin ligase activity. It mediates the transfer of ubiquitin from an E2 ubiquitin-conjugating enzyme onto target proteins, in order to mark them for proteasomal degradation. P53 is the most prominent target of MDM2 ubiquitination, along with MDM2 itself (Fang et al., 2000; Honda et al., 1997). The RING finger domain also represents the hetero-dimerization site of MDM4 (Shvarts et al., 1996).

The central acidic and zinc finger domains are key for the association with a long list of proteins, which include the Retinoblastoma (Rb) protein, the MDM2 negative regulator $p14^{ARF}$, the ribosomal proteins L5, L11 and L23, and the histone acetyltransferase and p53 activator p300 (Lindstrom et al., 2007; Zhang et al., 2003). During the p53 response, the interaction of MDM2 with p300 is important to repress DNA damage-induced p53 activation (Kobet et al., 2000). Within the central region, there are also a nuclear localization sequence (AA181-185) and a nuclear export signal (AA190-200), which allow the regulation of the protein localization (Roth et al., 1998).

MDM2 carries multiple phosphorylation sites in all the domains (Figure 2). ATM, which is activated by DNA double strand breaks (DSBs), phosphorylates MDM2 at Ser395. This phosphorylation, which is reversed by the phosphatase WIP1, disables MDM2 ubiquitin ligase activity on p53 (Lu et al., 2007; Maya et al., 2001). Other MDM2 phosphorylation events include: (i) Akt-mediated phosphorylation at Ser166, which causes MDM2 stabilization (Arcaro and Guerreiro, 2007), (ii) DNA-PKcs-mediated phosphorylation at Ser17, which leads to MDM2 dissociation from p53, thereby enabling p53 accumulation (Mayo et al., 1997), (iii) the rapamycin (mTOR) pathway downstream kinase S6K1 targets Ser163 in response to

doxorubicin to disable MDM2 ubiquitination activity (Lai et al., 2010), (iv) c-Abl phosphorylates MDM2 at Tyr394, blocking p53 ubiquitination (Goldberg et al., 2002).

The combination of different posttranslational modifications and the different factors interacting with MDM2 determine the regulation of p53, contributing to the activation of suitable transcriptional programs depending on the type of cellular stress (Levine, 2019).

2.5 Tumor suppressive activity of the p53-MDM2 system

The function of p53 as tumor suppressor is mostly ascribed to the induction of cell cycle arrest and apoptosis. p53 activity determines cell cycle arrest in G1-S and G2-M transition ensuring detection and repair of damaged DNA before initiation of DNA replication and mitosis, respectively. CDKN1A encoding the protein p21 is the primary target gene of p53 that mediates cell cycle arrest. It acts inhibiting CDK causing cell cycle arrest in G1. Another p53 target gene product that interferes with the cell cycle progression is 14-3-3-σ. It induces a G2 arrest by inhibition of the phosphatase CDC25C, which mediates progression into mitosis (Harper et al., 1995; Hermeking et al., 1997). Other p53 target genes that determine cell cycle arrest are: (i) calveolin-1 at the G0-G1 transition (Galbiati et al., 2001), (ii) BTG anti-proliferation factor 2 (BTG2) at the G1-S transition (Rouault et al., 1996), GADD45α at the G2-M transition (Wang et al., 1999). Upon severe damage, p53 induces another transcriptional program, resulting in apoptosis. P53 activates the extrinsic pathway of apoptosis by transactivating Fas Cell Surface Death Receptor encoding gene (FAS), Tumor Necrosis Factor S6 (TNFS6) (Muller et al., 1998; Munsch et al., 2000; Schilling et al., 2009), and Tumor necrosis factor-Related Apoptosis-Inducing Ligand (TRAIL) (Liu et al., 2004; Takimoto and El-Deiry, 2000). These ultimately provoke caspase-dependent apoptosis via procaspase 8. Alternatively, p53 also induces the intrinsic pro-apoptotic pathway by transactivating Bcl-2-Associated X protein (BAX) (Miyashita and Reed, 1995), p53 Upregulated Modulator of Apoptosis (PUMA) (Nakano and Vousden, 2001), and NOXA (Shibue et al., 2003). These trigger the release of cytochrome c from the mitochondria, which recruits the p53 target gene product Apoptosis-Peptidase Activating Factor-1 (APAF-1) (Fortin et al., 2001; Robles et al., 2001) and procaspase 9 to start the cascade of effector caspases, i.e., caspase-3 and caspase-7, the effectors of cell death. Additionally, upon extensive DNA damage p53 supports cellular senescence, a form of cell cycle arrest in which the cells retain their metabolic activity, but do not divide. This is mediated by p21 induction, Promyelocytic Leukemia protein (PML) (Pearson et al., 2000), Plasminogen Activator Inhibitor-1 (PAI1) (Kortlever et al., 2006), and E2F7 that initiates the senescence program (Aksoy et al., 2012; Brookes et al., 2002; Lin et al., 1998; Roninson, 2002).

In addition to these roles in cell cycle arrest, apoptosis and senescence, p53 is known to promote DNA damage repair regulating the expression of a subunit of the enzyme

ribonucleotide reductase (RNR), and factors involved in different DNA damage repair pathways. During unperturbed DNA replication, RNR is localized in the cytoplasm, where it catalyzes the production of deoxyribonucleotide triphosphates (dNTPs), which then diffuse into the nucleus. In 2000, Tanaka *et al.* discovered that upon DNA damage, p53 induces the expression of p53R2, which is a subunit of the RNR, but localized in the nucleus. This allows dNTP production directly in the nucleus, facilitating DNA damage repair (Tanaka et al., 2000). Additionally, p53 supports Nucleotide Excision Repair (NER) via induction of DNA Damage-Binding protein 2 (DDB2) (Tan and Chu, 2002) and Xeroderma Pigmentosum, complementation group C (XPC) proteins (Adimoolam and Ford, 2002). Interestingly, p53 also activates the DNA polymerase δ cofactor Proliferating Cell Nuclear Antigen (PCNA) (Shivakumar et al., 1995), which is involved in DNA damage tolerance pathways including Translesion DNA Synthesis (TLS), and in the recruitment of repair factors (Essers et al., 2005). Moreover, p53 can directly induce TLS by activating DNA polymerase eta (Pol η) (Lerner et al., 2017), further triggering the DNA damage checkpoint (Liu and Chen, 2006).

In this way, p53 stops the survival and the proliferation of cells with mutated DNA that could undergo tumorigenesis. However, it acts destroying damaged cells or promoting repair, rather than preventing the damage from occurring. Such activity would be more in line with the definition of p53 as the “guardian of the genome” (Lane, 1992), and with some evidences that support the notion of p53 exerting its tumor suppressive activity at least in part by precluding DNA damage formation.

Firstly, p53 knockout mice develop normally and start showing tumors at four-six months of age (Donehower et al., 1992). Reintroduction of p53 expression in mice with inducible p53 only temporarily arrested the growth of established lung tumors (Junttila et al., 2010). Furthermore, simultaneous targeted deletions of the key p53 target genes CDKN1A/p21, and BBC3/Puma, did not phenocopy p53 deletion, suppressing T cell lymphomas formation (Valente et al., 2013). Similarly, an acetylation-deficient p53 mutant that does not induce cell cycle arrest or apoptosis can still prevent the formation of T cell lymphomas in mice (Li et al., 2012). Along the same line, p53 depletion did not protect cancer cells from apoptosis. Loss of p53, instead, enhanced doxorubicin-, cisplatin-, and topoisomerase inhibitors-induced cytotoxicity in the HCT116 cell line (Bunz et al., 1999; Yeo et al., 2016), and sensitized cancer cells to the knock down of genes involved in nucleotide synthesis (Bartz et al., 2006), DNA replication (Krastev et al., 2011), and/or repair of DNA double strand breaks (Xie et al., 2012).

Our lab observed that p53 activation by Nutlin promoted resistance toward the nucleoside analogue gemcitabine (Kranz and Dobbelstein, 2006), UV-irradiation (Kranz et al., 2008), and Wee1 inhibitors (Li et al., 2015). Since p53 protected the cells against chemotherapeutics interfering with DNA replication, this effect was initially ascribed to the p53-induced G1 arrest.

This notion was supported by previous reports suggesting that p53 activity is reduced during DNA replication (Gottifredi et al., 2001; Mattia et al., 2007). However, in 2016, our lab surprisingly reported the induction of p53 target genes during S phase (Klusmann et al., 2016). This observation opened a new perspective over p53 role in DNA replication.

2.6 The impact of the p53-MDM2 system on DNA replication: the model and the missing pieces

In 2016, our lab reported that p53 induction increases the processivity of DNA replication forks (Klusmann et al., 2016; Klusmann et al., 2018; Wohlberedt et al., 2020). This was observed not only in cancer cell lines, but also in fibroblasts and mouse thymocytes, comparing p53-proficient and p53-deficient genotypes (Klusmann et al., 2016). Other labs confirmed these findings in other systems. P53 was reported to enhance nascent DNA elongation rate by limiting topological stress (Yeo et al., 2016), inducing TLS (Lerner et al., 2017), and fork restart (Roy et al., 2018), or activating pCDKN1A/p21, which was thought to promote DNA synthesis by its interaction with PCNA (Mansilla et al., 2016). However, others reported different and contradictory results. P53 was shown to compromise DNA replication fork progression through the induction of idling cycles (Hampp et al., 2016), and accumulation of CDKN1A/p21 (Mansilla et al., 2013).

A new piece was added to the puzzle when the depletion of the p53 target MDM2 was reported to impair DNA synthesis (Klusmann et al., 2016). This strongly suggested the direct involvement of MDM2 in the p53-mediated regulation of DNA replication. In 2018 our lab also reported that MDM2 supports DNA replication performing overlapping functions with the Polycomb Repressor Complex (PRC), thanks to its ubiquitin ligase activity. In particular, chromatin modification by MDM2 and PRC1 was proved to support DNA replication through the avoidance of DNA:RNA hybrids (R-loops) (Klusmann et al., 2018). However, the impact of MDM2 on replication was only studied in a p53 null background, through knock down experiments, and it was never tested in the context of the p53 response. This was due to the fact that MDM2 depletion quickly raises the p53 levels, causing cell cycle arrest and apoptosis, precluding any study on DNA replication. The development of the MDM2 PROTAC represented a breakthrough in the field, finally allowing to study MDM2 role in the DNA replication in the context of the p53 response.

2.7 The dangers of high speed in DNA replication

At the time of the finding of p53 increasing DNA replication fork progression, accelerated DNA replication fork speed was associated with reduced fork stalling and replication stress, which ultimately support genome stability. Therefore, the observation that the “guardian of the genome” was enhancing fork speed was considered a remarkable prove of p53 action to

prevent genome instability and oncogenic transformation. In 2018, this notion was challenged by the studies performed in Prof. Jiri Bartek's lab. The observed increase in nascent DNA elongation rate, upon inhibition of Poly(ADP-Ribose) Polymerase 1 (PARP1), proved that the increase in DNA replication fork progression has deleterious effects on genome stability when overcoming a certain threshold (Maya-Mendoza et al., 2018).

The current accepted model is that DNA replication fork progression should be finely regulated to maintain a limited speed. Overcoming this limit means inaccurate replication, with engagement of error-prone DNA damage tolerance mechanisms, and accumulation of single stranded DNA stretches, which boost replication stress and genomic instability (Merchut-Maya et al., 2019).

These new understandings called for a re-investigation and a re-interpretation of the impact of the p53-MDM2 system on DNA replication fork progression.

2.8 Poly(ADP-Ribose) Polymerase 1 (PARP1)

PARP1 is the founding member of the ADP-ribosyltransferases (ARTs), which comprises 17 members. PARP1, along with PARP2 and PARP3, is activated by DNA breaks and is involved in DNA damage response (Azarm and Smith, 2020; Pandey and Black, 2021; Ray Chaudhuri and Nussenzweig, 2017).

As all the ARTs, PARP1 is catalyzing the ADP-ribosylation of proteins (see paragraph below). PARP1 is conserved in eukaryotes. The human PARP1 is composed of six domains. In the N-terminal domain, there are three zinc fingers (ZF1, ZF2, and ZF3), which allow DNA binding and enzyme activation (Langelier et al., 2011; Langelier et al., 2010). Then, there is the BRCT (BRCA1 C terminus) domain, also known as auto-modification domain, this is an evolutionarily conserved protein domain that is important for protein-protein interaction and serves as acceptor site in auto-modification. The BRCT domain is followed by the WGR (tryptophan–glycine–arginine) domain, which is a regulatory domain. Finally, there is the PARP catalytic domain at the C-terminus (Figure 3A) (Bork et al., 1997; Iwashita et al., 2005; Nishikimi et al., 1982; Ray Chaudhuri and Nussenzweig, 2017). This includes two subdomains: a helical domain (HD) and an ADP-ribosyltransferase (ART) domain. The HD structure determines PARP1 catalytic activity. In the native folded position, it blocks NAD^+ binding, impairing catalytic activity. This is supported by the observation that the PARP1 mutant lacking HD is constitutively active (Dawicki-McKenna et al., 2015). Upon binding to DNA breaks, the HD unfolds, allowing NAD^+ entry and enzymatic activity (Langelier et al., 2018).

The full-length PARP1 structure has not yet been determined. Atomic structures of PARP1 have been solved for each isolated domain, or for two consecutive domains. One recent crystal structure analysis of PARP1 showed the three peptide segments corresponding to ZF1, ZF3,

and WGR-CD domains in complex with DNA. However, in this structure, the ZF2 and BRCT domains are missing (Langelier et al., 2012).

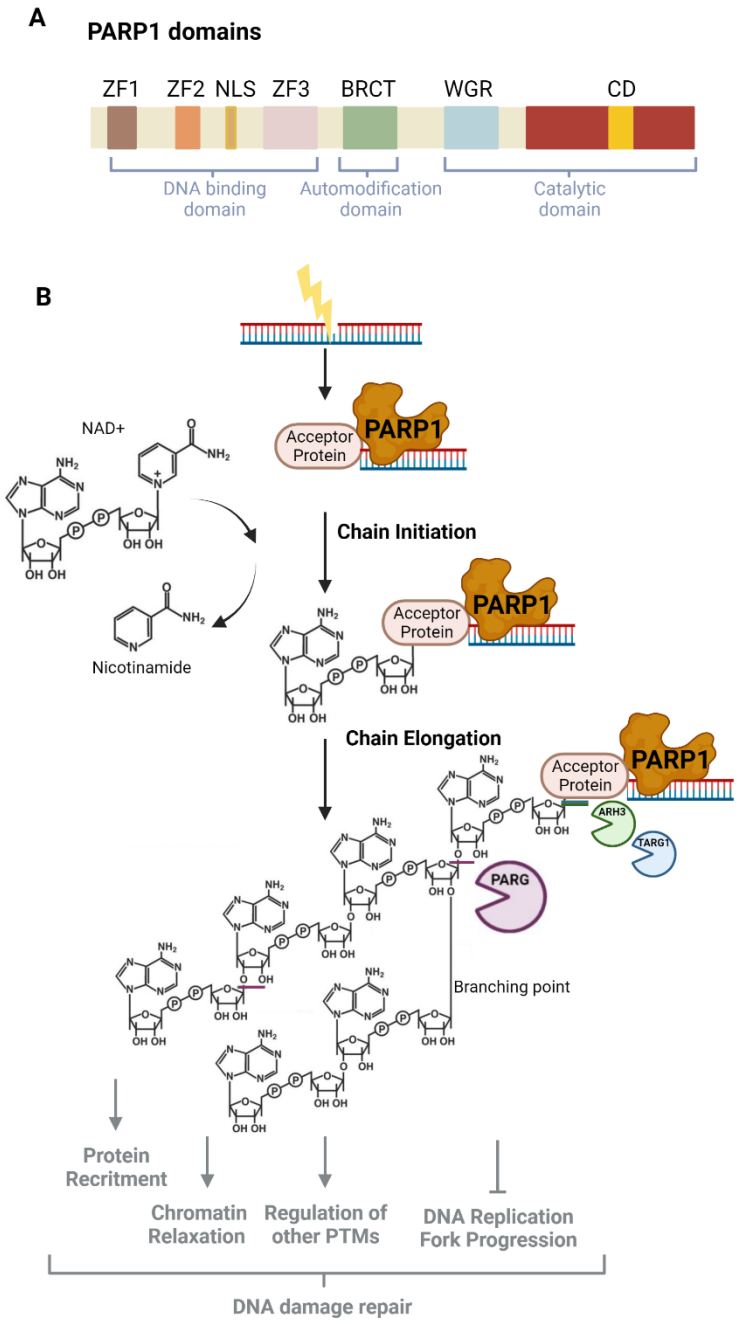

Figure 3. PARP1 domains and function at DNA breaks.

(A) Schematic representation of PARP1 domains. PARP1 DNA-binding domain is composed by three zinc finger motifs (ZF1–3), and a nuclear localization signal (NLS). This is followed by the BRCA1 C terminus (BRCT) domain, also named auto-modification domain. The carboxy-terminal contains the Trp-Gly-Arg (WGR) domain and the catalytic domain (CD). **(B)** PARP1 binding to DNA breaks triggers ADP-ribosylation on itself and acceptor proteins, using NAD^+ and releasing nicotinamide (chain initiation). PARP1 can polymerize the ADP-ribose to form Poly(ADP)ribose (PAR) chains (chain elongation). These are catabolized by PAR glycohydrolase (PARG), while the first attached ADP ribose is removed by ADP-ribosylhydrolase 3 (ARH3) or O-acyl-ADP-ribose deacylase 1 (OARD1/TARG1). PAR-mediated recruitment of DNA repair factors leads to chromatin remodeling, regulates other PTMs and slows down DNA replication fork progression to allow DNA damage repair. Adapted from Ray Chaudhuri and Nussenzweig, 2017.

2.9 Protein ADP-ribosylation

ADP-ribosylation of proteins is a widespread posttranslational modification (PTM) catalyzed by ARTs (Gibson and Kraus, 2012). In humans, PARP1 is the main ART (Kim et al., 2005). The ADP-ribosylation reaction takes place in two distinct steps: the chain initiation and the elongation. The chain initiation consists of the transfer of an ADP-ribose moiety from NAD^+ to the side chain of an amino acid of a target protein, with the release of nicotinamide (Figure 3). The attachment of a single ADP-ribose is referred to as Mono(ADP-ribosyl)ation (MARylation)

(Palazzo et al., 2021). The amino acids Aspartate, Glutamate, Serine, Tyrosine, Arginine and Cysteine can act as acceptor residues, forming O-, N- and S-glycosidic bonds with the ADP-ribose, respectively (Crawford et al., 2018). The chain initiation is followed by the elongation that consists of the polymerization of ADP-ribose units on the first attached ADP-ribose, using the ribose hydroxyl oxygen of the preceding unit. This polymerization is called Poly(ADP-ribosyl)ation (PARylation) and can be carried out in a linear or branched fashion, forming α-O-glycosidic (1″-2′) ribose-ribose bonds or α-O-glycosidic (1‴-2″) ribose-ribose bonds, respectively (Alemasova and Lavrik, 2019). The conjugation site, the chain length, and the branching determine the functional outcome of this modification. PARylation of proteins has been shown to affect electrostatic interactions, to regulate intracellular phase separation and to represent a biochemical scaffold that mediates the recruitments of various PAR-interacting factors, known as “PAR readers” (Leung, 2014; Leung, 2020). For this reason, ADP-ribosylation is involved in the regulation of many cellular processes, e.g., DNA damage repair, DNA replication, transcription, cell division, chromatin organization (Gupte et al., 2017). ADP-ribosylation is a high-turnover reaction. This PTM is reversed by multiple factors, referred to as “ADP-ribosylation erasers”. PARG (Poly(ADP-ribose) glycohydrolase) is responsible for the catabolism of poly(ADP-ribose), hydrolyzing the glycosidic bonds between ADP-ribose units of PAR chains to release ADP-ribose monomers. PARG presents both exoglycosidase and endoglycosidase activities. However, PARG processivity diminishes with PAR shortening, and it is unable to remove MARylation marks (Hatakeyama et al., 1986; Slade et al., 2011). Amino acid-specific ADP-ribose-acceptor hydrolases turned out to be responsible for MARylation removal in human cells. They are the macrodomain-containing proteins MACROD1 and MACROD2, the terminal ADP-ribose protein glycohydrolase 1 (TARG1), and the ADP-ribose hydrolase (ARH) family members ARH1 and ARH3. In addition, phosphodiesterases can also process ADP-ribose (O'Sullivan et al., 2019). Among these MAR erasers, ARH3 is the only one that has been shown to remove the O-glycosidic bond linking the ADP-ribose to the serine residues (Palazzo et al., 2021).

2.10 PARP1 as a pharmacological target

The idea of using PARP1 inhibitors (PARPi) for clinical purposes arose from the observation that loss of PARP1 was specifically toxic for tumors with deficiency in the hereditary breast cancer genes BRCA1 and BRCA2 (Bryant et al., 2005; Farmer et al., 2005). The interaction between PARP1 and the BRCA genes represents an example of synthetic lethality, meaning that the perturbation of either gene alone is nontoxic, even though the perturbation of both genes simultaneously results in the loss of cell viability (Setton et al., 2021). Subsequently, PARP1 inhibitors were proven to be effective to treat also tumors deficient for other components of the DNA repair machinery, e.g., ATM (Mak et al., 2020). Since this

breakthrough, pharmacological inhibition of PARP1/2 represents one of the most successful targeted therapies of cancer (Lord and Ashworth, 2017). Currently, PARP1/2 inhibitors are approved for the treatment of DNA repair-deficient breast, ovarian, pancreatic, and prostate cancers (Rose et al., 2020). However, the mechanism at the base of the synthetic lethality remains unclear, and many hypothesis have been formulated in the past years.

PAR formation leads to the recruitment of PAR readers that are fundamental components of multiple DNA damage repair pathways, including Non Homologous End Joining (NHEJ) and micro homology mediated end joining (MMEJ) (Ray Chaudhuri and Nussenzweig, 2017). Given the role of BRCA1 and BRCA2 in the alternative pathway for DNA Double Strand Break (DSB) repair, namely Homologous Recombination (HR), one of the hypotheses attributed the synthetic lethality to the lack of DSB repair (Helleday, 2011b). However, this was only partially supported by the experimental data (Cong et al., 2021b). For instance, not all HR deficient tumors respond to PARPi in the clinic (Ledermann and Pujade-Lauraine, 2019).

It is known that the clinically used PARP1 inhibitor, namely Olaparib, leads to the “trapping” of PARP1/2 on the chromatin. As mentioned above, PARP1 itself is the main target of PARylation *in vivo*, which takes place in the auto-modification domain (Nishikimi et al., 1982). This auto-modification induces the release of the enzyme from DNA lesions, presumably through electrostatic and steric repulsion (Ahel et al., 2009). PARP1 auto modifies in cells at glutamate, aspartate and serine residues, and major sites include Glu488 and Glu491 and Ser499, Ser507, Ser519. Upon inhibition of its catalytic activity, PARP1 is unable to auto-modify, remaining “trapped” on the DNA (Longarini and Matic, 2022). The trapped PARP1 was considered to act as an obstacle to DNA replication (D'Andrea, 2018; Michelena et al., 2018; Murai et al., 2012; Pommier et al., 2016). Since BRCA proteins are important for fork protection and stability, more recent hypotheses see the PARP inhibitor-dependent fork stalling as the main cause of synthetic lethality with BRCA proteins deficiency (Lomonosov et al., 2003; Schlacher et al., 2011). However, also this hypothesis was not confirmed by the experimental data, which showed an increase rather than a decrease of DNA elongation upon PARP inhibition (Maya-Mendoza et al., 2018). In order to achieve a mechanistic understanding of the synthetic lethality, additional studies on the role of PARP1 in DNA damage repair and DNA replication are required.

2.11 The role of PARP1 in the repair of DNA damage

The involvement of PARP1 in many DNA repair pathways makes it crucial for the maintenance of genomic stability. We refer to the set of pathways that detect, signal, and repair DNA damage as the DNA Damage Response (DDR). The earliest event in the DDR is the recognition of DNA lesions by PARP1 (Ray Chaudhuri and Nussenzweig, 2017). As already mentioned, PARP1 becomes catalytically active upon binding to different DNA substrates, of which DNA single-strand breaks (SSBs) and double-strand breaks (DSBs) are the best characterized (Langelier et al., 2012). Upon DNA damage, one third of the human nuclear proteome is ADP-ribosylated (Larsen et al., 2018). In this context serine residues appear to be the predominant substrate for MARylation (Palazzo et al., 2018).

PARP1-mediated ADP-ribosylation allows DNA damage repair by (i) protein recruitment, (ii) chromatin relaxation, and (iii) interplay with other PTMs, particularly on histones (Longarini and Matic, 2022).

Many DDR factors, e.g., ATM, DNA-PKcs and the Ku proteins, are PAR readers, because they contain PAR-binding modules. These are PAR-binding consensus motifs (PBMs), PAR-binding zinc finger motifs (PBZs), macrodomain folds, WWE domains and many other modules, which allow the recruitment to sites of DNA damage via PAR recognition (Krietsch et al., 2013; Teloni and Altmeyer, 2016). Interestingly, these PAR-binding modules often overlap with functional domains, which mediate the association with oligonucleotides, protein–protein interactions, subcellular localization, and all these functions are affected by PAR binding. In these ways, synthesis and removal of ADP-ribosylation allow the regulation of DDR pathways in a spatial and time specific manner. The current knowledge about PARP1 functions in Single-Strand Break Repair (SSBR) (1), Base Excision Repair (BER) (2), Nucleotide Excision Repair (NER) (3), and DNA Double Strand Breaks (DSBs) repair (4) is summarized in the following paragraphs.

2.11.1 The role of PARP1 in Single-Strand Break Repair (SSBR)

Single-Strand DNA Breaks (SSBs) can originate from DNA replication and/or base modifications, like oxidation or generation of abasic sites. These are rapidly recognized by PARP1, triggering PARylation that recruits X-ray repair cross-complementing protein 1 (XRCC1) (El-Khamisy et al., 2003). This function as a scaffold engaging further SSBR factors, i.e., DNA ligase 3 (LIG3), DNA polymerase β and bifunctional polynucleotide kinase 3´-phosphatase (PNKP), which complete the repair process (Caldecott et al., 1994; Loizou et al., 2004; Marintchev et al., 2000; Whitehouse et al., 2001). Interestingly, XRCC1 deficiency causes hyperactivity of PARP1 that depletes the NAD^+ pools, provoking cell death.

Consequently, XRCC1 deficiencies are associated to neuropathological problems in mice and humans (Hoch et al., 2017).

Moreover, PARP1 is responsible for the repair of SSB in the form of single stranded DNA nicks that originate from the activity of the topoisomerase 1 (TOP1). When TOP1 remains linked to the DNA through a tyrosine residue, it forms TOP1 cleavage complexes (TOP1cc). These are removed by the tyrosyl-DNA phosphodiesterase 1 (TDP1) that is PARylated by PARP1, stabilizing it and enhancing its recruitment to TOP1cc. After TDP1-dependent removal of TOP1cc, SSBR, as described above, can take place (Das et al., 2014).

2.11.2 The role of PARP1 in Base Excision Repair (BER)

Damaged bases are recognized and removed by apurinic-apyrimidinic (AP) endonucleases leading to the formation of single strand DNA gaps, which are then repaired by the SSBR factors (Caldecott, 2008). So, PARP1 is involved in BER by its activity in SSBR described above. An additional role of PARP1 in BER is supported only partially by the scientific community (Dantzer et al., 2000; Dantzer et al., 1999; Pachkowski et al., 2009; Vodenicharov et al., 2000). Some reports even show PARylated PARP1 counteracting efficient BER (Orta et al., 2014; Strom et al., 2011), and, more recently, the requirement of PARP1 for the repair of a specific subset of base lesions has been suggested (Reynolds et al., 2015).

2.11.3 The role of PARP1 in Nucleotide Excision Repair (NER)

Bulkier DNA lesions that distort the DNA helix, such as large hydrocarbon adducts from tobacco smoke or UV-C-induced lesions, like cyclobutane pyrimidine dimers (CPD), are repaired by the Nucleotide Excision Repair (NER) pathway (Wilson and Kunkel, 2000). This mediates identification and excision of the region containing the damage, gap filling and ligation. PARP1 is involved in damage recognition in the global genome nucleotide excision repair (GG-NER), which is active irrespective of transcription, unlike the alternative Transcription-Coupled Nucleotide Excision Repair (TC-NER) (Sugasawa, 2019). In the GG-NER, xeroderma pigmentosum group C-complementing protein (XPC) and RAD23B recognize the lesion, via the recruitment of the DNA damage-binding protein 1 (DDB1)-DDB2 complex, which mediates nucleosome displacement (Marteijn et al., 2014). XPC is a PAR reader and this feature is crucial for XPC relocation to UV lesions. DDB2 also associates with PARP1 boosting its catalytic activity (Pines et al., 2012; Robu et al., 2013), and, in this way, further contributing to chromatin decondensation, which facilitates the repair (Luijsterburg et al., 2012). Subsequent to recognition, PAR recruits XPA, which carries out the verification of the DNA lesion with the transcription and repair factor transcription factor IIH (TFIIH). This XPA-dependent step allows the engagement of the additional required factors XPB and XPD. Finally, the nucleases excision repair cross-complementing group 1 protein (ERCC1) and XPF,

and XPG excise the damaged nucleotides, leading to the formation of a gap that is subsequently filled by Pol δ, Pol ε and Pol κ, and the ligation is mediated by LIG1 or LIG3 (King et al., 2012).

2.11.4 Functions of PARP1 in the detection and repair of DNA Double Strand Breaks (DSBs)

DSBs can result from exogenous genotoxic insults, e.g., ionizing radiation, or endogenous events, such as replication fork collapse or genomic rearrangements (Mehta and Haber, 2014).

PARP1 is a sensor of DSBs, because of its direct binding to them. Once PARP1 recognition of the DSB occurs with consequent PARylation, the apical DDR kinase ATM is recruited through its PAR binding domains. This interaction has been shown to stimulate ATM activity *in vitro* (Aguilar-Quesada et al., 2007; Haince et al., 2007). PARs are also crucial for the recruitment of the DNA endonuclease meiotic recombination 11 (MRE11) and Nijmegen breakage syndrome protein 1 (NBS1) (Haince et al., 2008). However, PARP1 deficiency only delays DSB repair and does not completely abolish it, strongly suggesting the presence of redundant mechanisms. One of them could be PARP2 that is capable of PARylating the majority of PARP1 targets (Haince et al., 2007).

DSBs are repaired through two main pathways: the homologous recombination (HR) and the error-prone non-homologous end joining (NHEJ), which are used according to the cell cycle phase, the chromatin environment, and the structure of the DSB (Chapman et al., 2012; Price and D'Andrea, 2013). Additionally, the PAR-recruited MRE11 performs DNA-end processing, determining DNA-repair pathway choice (Hochegger et al., 2006). The MRE11-mediated conversion of DNA double strand breaks from double-ended to single-ended promotes HR. Therefore, PARP1 recruiting MRE11 ultimately supports HR. Additionally, PARP1supports HR by recruiting BRCA1 to the DSB. BRCA1 is a crucial component of the HR pathway because (i) it governs the initial end resection, (ii) it mediates the loading of RAD51, and (iii) it is required for RPA binding to ssDNA (Li and Yu, 2013; Schwertman et al., 2016). PARP1 contributes to BRCA1 engagement by different means: (i) BRCA1 can be recruited by PAR, in addition to ubiquitin (Li and Yu, 2013; Schwertman et al., 2016), (ii) PARP1 is indirectly recruiting BRCA1 through its interaction with BRCA1-associated RING domain protein 1 (BARD1) (Hu et al., 2014). Conversely, there are some reports that describe inhibitory effects of PARP1 toward HR; the loss of PARP1 enhances RAD51 foci formation and sister chromatid exchange (Morgan and Cleaver, 1982; Oikawa et al., 1980; Schultz et al., 2003; Yang et al., 2004). Secondly, PARylated BRCA1 is strongly bound by receptor-associated protein 80 (RAP80), limiting HR (Hu et al., 2014). These controversial evidences depict PARP1 as a factor that contributes to fine tune HR use. An alternative intriguing explanation to this controversy is that the enhanced sister chromatid exchanges, observed upon PARP1 loss, depends on

dysfunctional SSBR that gives rise to elevated levels of one-ended DSBs, promoting HR. According to this model, PARP1 would promote HR via the recruitment of BRCA1 as mentioned above, while preventing the accumulation of one-ended DSBs that induce HR (El-Khamisy et al., 2005; Fan et al., 2007).

Alternatively to HR, PARP1 is also involved in the classical and alternative sub-pathways of the NHEJ (Ray Chaudhuri and Nussenzweig, 2017). When the classical NHEJ (cNHEJ) is activated, DNA ends are bound by KU70–KU80 dimers, which act as another sensor of DSBs and induce DNA-dependent protein kinase catalytic subunit (DNA-PKcs). PARP1 PARylates DNA-PKcs, stimulating its kinase activity (Ruscetti et al., 1998; Spagnolo et al., 2012). In this context, PARP1 also favors chromatin remodeling by recruiting chromo domain helicase DNA-binding protein 2 (CHD2), which then engages X-ray repair cross-complementing protein 4 (XRCC4) and DNA ligase 4 (LIG4) (Luijsterburg et al., 2016). In this way, PARP1 activity enhances the efficiency of cNHEJ. PARP1 and KU proteins independently sense the breaks competing with each other to occupy DSBs, with KU acting predominantly in G1 and G1-S border, while PARP1 operating in S-G2 phases. During S phase PARP1 is even removing KU from DNA breaks (Yang et al., 2018).

When PARP1 acts at the DSB, instead of KU, alternative NHEJ (aNHEJ) takes place. Unlike cNHEJ, during aNHEJ MRE11, upon recruitment by PARP1, processes the DNA ends. Then the resected ends are joined though sequence microhomology, followed by DNA polymerase theta (Pol θ)-mediated gap filling, and LIG3 ligation (Truong et al., 2013).

2.12 PARP1 regulates DNA replication

A role of PARP1 in DNA replication is supported by its presence at moving and stalled DNA replication forks (Dungrawala et al., 2015). Additionally, PAR levels are enhanced in cells undergoing DNA replication, in particular behind DNA replication forks (Hanzlikova et al., 2018; Vaitsiankova et al., 2022). The exposure of ssDNA during replication triggers PARP1 activity with consequent SSBR (Figure 4, panel 1). Indeed, PARP1 inhibition or depletion reduces nascent DNA integrity, causing ssDNA gaps (Cong et al., 2021b). PARP1 was also reported by Prof. Caldecott's lab in 2018 to be involved in the processing of unligated Okazaki fragments, in a pathway that is acting in parallel to the canonical FEN1-LIG1 pathway (Hanzlikova et al., 2018) (Figure 4, panel 2). However, the role of PARP1 in the context of DNA replication goes beyond Okazaki fragments processing.

In 2012, PARP1 loss or inhibition was reported by Prof. Massimo Lopes laboratory to prevent fork reversal upon TOP1 inhibition, leading to genomic instability (Ray Chaudhuri et al., 2012). Replication fork reversal is a mechanism of DNA replication fork rearrangement, in which the canonical three-way junction is converted into a four-way junction by the annealing of the newly

synthesized strands, while the template strands re-anneal leading to fork regression (Neelsen and Lopes, 2015) (Figure 4, panel 3). Fork reversal was considered for decades as a mechanism present only in bacteria, with the function of lesion bypass during replication (Atkinson and McGlynn, 2009). However, reversed forks form in yeast, Xenopus and human cells, and in all these systems PARP1 is required for fork reversal. Later it was also reported that fork reversal is provoked by multiple sources of replication stress and requires the activity of RAD51, which mediates strand exchange (Neelsen and Lopes, 2015).

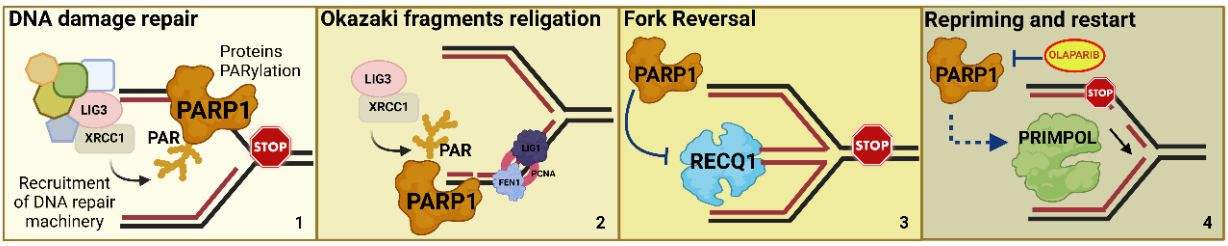

Figure 4. PARP1 functions at the DNA replication fork. 1) PARP1-mediated SSBR prevents the accumulation of ssDNA gaps. **2)** PARP1-dependent PARylation allows the recruitment of XRCC1, and the other components of SSBR to mediate religation of Okazaki fragments. **3)** PARP1 inhibits the activity of the helicase RECQ1, precluding fork restart upon reversal. **4)** Pharmacological inhibition of PARP1 enhances DNA replication fork progression and promotes the activity of the primase/polymerase PRIMPOL.

Reversed forks can be restarted by branch migration, which consists of the consecutive exchange of base pairings on homologous DNA strands, relocating the junction branch point in the DNA sequence (Neelsen and Lopes, 2015). This process is catalyzed by a helicase which is the ATP-dependent DNA helicase Q1 (RECQ1). Interestingly, RECQ1 activity is inhibited by PARP1, stabilizing reversed forks and pausing DNA synthesis, allowing the repair of lesions ahead of the fork (Berti et al., 2013). PARP1i activates RECQ1 with consequent fork restart, also in the presence of DNA damage, and in conditions of replication stress (Berti et al., 2013) (Figure 4, panel 3). This untimely restart of DNA synthesis by RECQ1 causes replication fork "run-off"' into unrepaired lesions ahead of the fork, resulting in fork collapse and subsequent DSBs accumulation (Berti et al., 2013; Ray Chaudhuri et al., 2012). This mechanism explains the enhancement of DNA replication fork progression observed upon PARPi (Maya-Mendoza et al., 2018) (Figure 4, panel 4).

Very recently, PARP1 inhibition has been shown to cause enhancement of DNA replication fork progression also by another mechanism, which is the primase/polymerase PRIMPOL-mediated restart of DNA synthesis. Whenever a roadblock to the progression of DNA polymerase epsilon is set on the leading strand, fork uncoupling occurs: the helicases continue translocating, while the DNA synthesis by the polymerase remains blocked. This leads to the formation of a short stretch of ssDNA, which is readily coated by RPA proteins (Berti et al., 2020). Upon fork uncoupling, PRIMPOL is recruited in an RPA-dependent manner (Berti et al.,

2020; Pouliot et al., 1999), and it re-primes DNA synthesis downstream the replication roadblock, leaving behind a ssDNA gap that is repaired by the so called post replicative gap filling, the mediators of which remains largely unknown (Berti et al., 2020) (Figure 4, panel 4).

PRIMPOL-dependent re-priming was found to promote the resistance of human cells to genotoxic treatments in a BRCA-deficient background (Quinet et al., 2020). In this context, PARP inhibition was also reported to enhance PRIMPOL activity (Quinet et al., 2020). Additionally, upon depletion of the PARP1 activator Coactivator Associated Arginine Methyltransferase 1 (CARM1), PRIMPOL re-priming becomes preponderant (Genois et al., 2021). In conclusion, PARP1 inactivation leads to an increase in DNA replication fork progression by enhancing RECQ1-mediated restart of reversed forks and PRIMPOL-dependent re-priming of DNA synthesis.

3. SCOPE OF THE THESIS

P53 regulates DNA replication as part of its tumor suppressive activity (Gottifredi and Wiesmuller, 2018). However, the mechanistic aspects of this regulation remain elusive. Despite some reports suggesting a direct role for p53 at the DNA replication fork (Gottifredi and Wiesmuller, 2018; Roy et al., 2018), the impact of p53-mediated transactivation on DNA replication remains to be defined. Interestingly, the p53 target gene product and antagonist MDM2 was found to promote DNA replication fork progression in a p53 deficient background (Klusmann et al., 2016; Klusmann et al., 2018; Wohlberedt et al., 2020). In this thesis work, we ask what is the impact of MDM2 on DNA replication fork progression in the context of the p53 response, and what is the mechanism leading to DNA elongation rate changes upon p53 induction. Recent advances in the study of DNA replication highlighted the need for a tight regulation of replication fork progression to ensure genome stability. In particular, the activity of Poly(ADP-Ribose) Polymerase 1 (PARP1) was shown to be necessary to regulate DNA synthesis rate (Maya-Mendoza et al., 2018). Based on that, we aim to characterize a potential functional interplay between PARP1 and MDM2. Namely, we aim to define weather MDM2 might directly or indirectly affect PARP1 enzymatic activity and stability, in turn perturbing DNA replication fork progression. Finally, we would like to delineate the impact of this interplay on genome stability and cellular fitness.

4. PUBLICATION

Contribution to the published manuscript:

Conceptualization of the project, figure arrangement, writing and revising of the manuscript.

Performed experiments and data analysis for all figures, except Figures 1A-E, 1G, 1I, 2B-E, 5G-I, 6, S1A-G, S2, S5I, S5J, S6C, S6D.

Cell Reports

Article

MDM2 binds and ubiquitinates PARP1 to enhance DNA replication fork progression

Graphical abstract

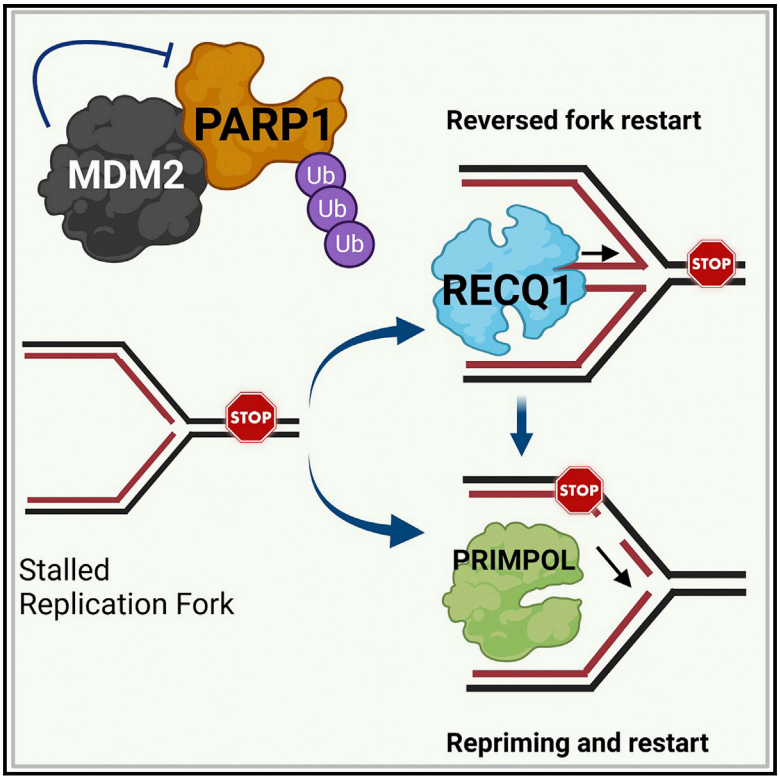

Authors

Celeste Giansanti, Valentina Manzini, Antje Dickmanns, ..., Martin Scheffner, Massimo Lopes, Matthias Dobbelstein

Correspondence

mdobbel@uni-goettingen.de

In brief

Giansanti et al. report that the MDM2 oncoprotein binds, ubiquitinates, and destabilizes poly(ADP-ribose) polymerase 1 (PARP1). As a result, they observe a far lower degree of DNA replication fork reversal, whereas DNA replication proceeds as a function of RECQ1 and PRIMPOL.

Highlights

- The MDM2 oncoprotein binds, ubiquitinates, and destabilizes poly(ADP-ribose) polymerase 1
- MDM2 suppresses formation of reversed DNA replication forks
- MDM2 enables RECQ1 and PRIMPOL to sustain replication fork progression
- This constitutes a functional interaction of two cancer-relevant biomolecules

Giansanti et al., 2022, Cell Reports *39*, 110879
May 31, 2022
https://doi.org/10.1016/j.celrep.2022.110879

CellPress

Cell Reports

CellPress
OPEN ACCESS

Article

MDM2 binds and ubiquitinates PARP1 to enhance DNA replication fork progression

Celeste Giansanti,[1,6] Valentina Manzini,[1,6] Antje Dickmanns,[1] Achim Dickmanns,[2] Maria Dilia Palumbieri,[3] Andrea Sanchi,[3] Simon Maria Kienle,[4] Sonja Rieth,[5] Martin Scheffner,[4] Massimo Lopes,[3] and Matthias Dobbelstein[1,7,*]

[1]Institute of Molecular Oncology, Göttingen Center of Molecular Biosciences (GZMB), University Medical Center Göttingen, Justus-von-Liebig-Weg 11, 37077 Göttingen, Germany

[2]Department of Molecular Structural Biology, Institute of Microbiology & Genetics, GZMB, Georg-August-University Göttingen, Justus-von-Liebig-Weg 11, 37077 Göttingen, Germany

[3]Institute of Molecular Cancer Research, University of Zurich, Winterthurerstrasse 190, 8057 Zurich, Switzerland

[4]Department of Biology, University of Konstanz, 78457 Konstanz, Germany

[5]Department of Chemistry, University of Konstanz, 78457 Konstanz, Germany

[6]These authors contributed equally

[7]Lead contact

*Correspondence: mdobbel@uni-goettingen.de

https://doi.org/10.1016/j.celrep.2022.110879

SUMMARY

The MDM2 oncoprotein antagonizes the tumor suppressor p53 by physical interaction and ubiquitination. However, it also sustains the progression of DNA replication forks, even in the absence of functional p53. Here, we show that MDM2 binds, inhibits, ubiquitinates, and destabilizes poly(ADP-ribose) polymerase 1 (PARP1). When cellular MDM2 levels are increased, this leads to accelerated progression of DNA replication forks, much like pharmacological inhibition of PARP1. Conversely, overexpressed PARP1 restores normal fork progression despite elevated MDM2. Strikingly, MDM2 profoundly reduces the frequency of fork reversal, revealed as four-way junctions through electron microscopy. Depletion of RECQ1 or the primase/polymerase (PRIMPOL) reverses the MDM2-mediated acceleration of the nascent DNA elongation rate. MDM2 also increases the occurrence of micronuclei, and it exacerbates camptothecin-induced cell death. In conclusion, high MDM2 levels phenocopy PARP inhibition in modulation of fork restart, representing a potential vulnerability of cancer cells.

INTRODUCTION

The tumor suppressor protein p53 is a stress-inducible transcription factor. It induces expression of genes that promote cell cycle arrest, DNA repair, or programmed cell death (Hafner et al., 2019; Kastenhuber and Lowe, 2017; Levine, 2020). One of the most strongly p53-responsive genes is the mouse double minute 2 homolog (MDM2). MDM2 is an E3 ubiquitin-protein ligase that targets p53 for proteasome-mediated degradation, giving rise to a regulatory feedback loop (Wade et al., 2013). MDM2 thus acts as an oncogene, and it is overexpressed in a variety of human tumors, most notably in sarcomas (Rayburn et al., 2005). In addition to its role in regulating p53, additional functions of MDM2 have been described, compatible with a role of MDM2 as an effector, not only a regulator, of tumor suppression by p53 (Levine, 2020). MDM2 interacts with the Polycomb repressor complex 2 and mediates histone modifications (Wienken et al., 2016, 2017). MDM2 binds and deactivates the Mre11-Rad50-Nbs1 (MRN) complex, delaying DNA repair (Alt et al., 2005). Finally, MDM2 can support the processivity of DNA replication forks in cooperation with its association partner MDM4 as well as another histone ubiquitin ligase, RNF2 (Klusmann et al., 2016, 2018; Wohlberedt et al., 2020). Because MDM2 relies on p53 for its full expression, this might also explain why the presence of p53 enhances DNA replication fork processivity (Klusmann et al., 2016). However, we still lack a clear mechanistic understanding of how MDM2 affects DNA replication forks upon p53 activation.

Poly(ADP-ribose) polymerase 1 (PARP1) is an emerging player in regulation of DNA replication. PARP1 binds to perturbed DNA replication forks and to damaged DNA, and this triggers its catalytic activity. It then covalently attaches ADP-ribose units to a number of target proteins, including PARP1 itself (Chambon et al., 1963; Kun et al., 2004; Langelier et al., 2011, 2014). PARP1 polymerizes these ADP-ribose units to form linear or branched poly(ADP-ribose) (PAR) chains in a reaction called PARylation. PARylation of proteins regulates their function, localization, and stability (Gibson and Kraus, 2012). In this way, PARP1 controls DNA repair and chromatin remodeling (Jungmichel et al., 2013; Ray Chaudhuri and Nussenzweig, 2017), and PARP inhibitors are established drugs for treating tumors with DNA repair deficiencies (Helleday, 2011). PARP1 controls DNA replication, and its inhibition leads to enhanced progression of replication forks (Maya-Mendoza et al., 2018). Correspondingly, most PARylation activity is detected during S phase at sites of

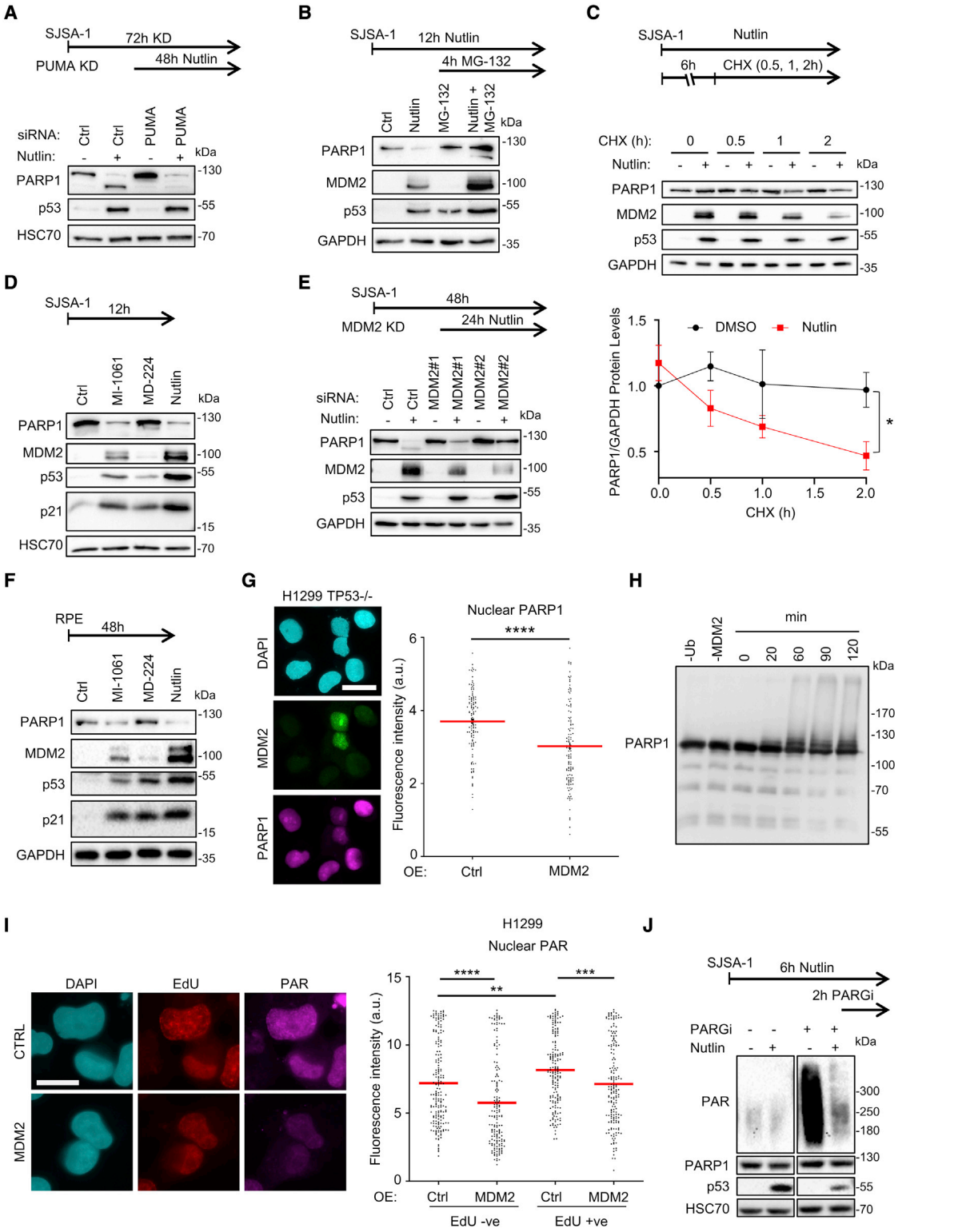

Figure 1. MDM2 ubiquitinates PARP1, triggering its proteasomal degradation

(A) Immunoblot analysis of SJSA-1 cells 72 h after transfection of siRNA against PUMA and upon treatment with Nutlin (20 μM, 48 h).

(B) SJSA-1 cells were treated with 20 μM Nutlin for 12 h. During the last 4 h, the proteasome inhibitor MG-132 (10 μM) was added, followed by immunoblot analysis. The efficacy of proteasome inhibition is demonstrated by accumulation of p53, MDM2, and PARP1.

(legend continued on next page)

DNA replication. This is at least partially triggered by processing of Okazaki fragments, which can be carried out by a PARP1- and XRCC1-dependent pathway as an alternative to the canonical FEN1- and LIG1-driven pathway (Hanzlikova et al., 2018). PARP1 delays restarting of reversed DNA replication forks. Fork reversal is a replication fork remodeling process by which a canonical three-way replication fork is converted to a four-way junction by reannealing of parental DNA strands and coordinated annealing of newly synthesized strands (Betous et al., 2012; Higgins et al., 1976). This happens during replication in response to genotoxic agents but also when replication forks hit endogenous obstacles; e.g., repetitive DNA forming secondary structures (Follonier et al., 2013; Schmid et al., 2018; Zellweger et al., 2015). Fork reversal contributes to temporal arrest of replication, allowing repair or bypass of DNA damage (Berti et al., 2020; Neelsen and Lopes, 2015; Quinet et al., 2017).

When active, PARP1 stabilizes DNA replication forks in the regressed state and limits fork restarting by inhibiting the activity of the helicase RECQ1 (Berti et al., 2013). Conversely, PARP1 inhibition accelerates replication forks and antagonizes fork reversal (Berti et al., 2013; Maya-Mendoza et al., 2018; Ray Chaudhuri et al., 2012). When PARP1 activity is diminished, alternative DNA damage tolerance (DDT) mechanisms become prominent. These include translesion synthesis (TLS) and repriming of DNA synthesis downstream of the replication block by the action of the primase and DNA polymerase (PRIMPOL) (Genois et al., 2021; Quinet et al., 2020). Thus, PARP1 activity determines how replication forks cope with obstacles. It remains largely unknown how PARP1 activity itself is regulated during replication. Recently, the methyl transferase CARM1 has been found to support PARP1 activity at replication forks (Genois et al., 2021), but additional factors might well be involved in regulation of PARP1 activity in this context.

In addition to its role in DNA synthesis and repair, PARP1 is widely known for its cleavage during apoptosis. In this context, caspases cleave PARP1 into fragments that are readily detectable by immunoblot analysis (Kaufmann et al., 1993; Soldani et al., 2001). This study was initiated by the surprising observation that p53 activity not only induced cleavage of PARP1 into fragments but also led to degradation of PARP1 altogether, even when apoptosis was blocked. This raised the questions of whether the most prominent p53-inducible ubiquitin ligase, MDM2, might mediate PARP1 degradation and how this would affect the DNA replication process.

We observed that MDM2 inhibits and destabilizes PARP1 by physically binding and ubiquitinating it. Consequently, MDM2 promotes progression of DNA replication forks. This increase in the DNA elongation rate requires RECQ1 as well as PRIMPOL, and it coincides with suppression of fork reversal. Thus, MDM2 not only counteracts p53 activity but also antagonizes PARP1. It therefore promotes DNA replication fork progression via RECQ1-driven resumption of reversed replication forks and PRIMPOL-mediated re-priming of DNA synthesis.

RESULTS

MDM2 ubiquitinates PARP1, triggering its proteasomal degradation

We were initially studying p53-induced apoptosis, using an inhibitor of MDM2. The pharmacological MDM2 antagonist Nutlin-3a (Vassilev et al., 2004), referred to as Nutlin from here on, binds to a hydrophobic pocket domain of MDM2, disrupting its interaction with p53. This impairs MDM2-driven ubiquitination of p53, leading to accumulation of p53 and enhanced expression of its target genes, including the pro-apoptotic effector BBC3/PUMA, but also MDM2 itself. We had studied apoptosis in the osteosarcoma cell line SJSA-1, characterized by wild type TP53 and MDM2 amplification (Bi et al., 2016). When treating SJSA-1 cells with Nutlin, PARP1 cleavage by caspases resulted in the characteristic fragment visualized by immunoblot analysis (Kaufmann et al., 1993; Soldani et al., 2001; Figure 1A). Surprisingly, Nutlin also reduced the levels of full-length PARP1 (Figures 1A and 1B), not only in SJSA-1 cells but also in the non-transformed retinal pigment epithelium (RPE) cells (Figure S1A).

(C) Cycloheximide (CHX) chase analysis of PARP1 degradation. SJSA-1 cells were pre-treated with Nutlin (20 μM) for 6 h. CHX (40 μg/mL) was added to Nutlin for 0.5, 1, and 2 h. Top panel: treatment scheme. Center panel: representative immunoblot. Bottom panel: quantification of PARP1 band intensity normalized to GAPDH in three independent experiments. PARP1 protein levels started dropping after 6.5 h of Nutlin treatment and further at 7 and 8 h.

(D) SJSA-1 cells were treated with 1 μM MDM2 PROTAC (MD-224), 1 μM MI-1061 (ligand control), or 20 μM Nutlin for 12 h, followed by immunoblot analysis. Treatment with MD-224 induced a p53 response comparable with MI-1061, as shown by p21 levels, leading to MDM2 degradation.

(E) Immunoblot analysis of SJSA-1 cells transfected with two different siRNAs to knock down MDM2 or control siRNA for 48 h and treated with Nutlin (20 μM, 24 h). PARP1 full-length protein levels were restored to different degrees, depending on the efficacy of MDM2 knockdown.

(F) RPE cells were treated with 1 μM MDM2 PROTAC (MD-224), 1 μM MI-1061 (ligand control), or 10 μM Nutlin for 48 h to reveal MDM2-dependent loss of PARP1.

(G) PARP1 and MDM2 immunofluorescence staining. H1299 cells were transfected with a control empty vector (pCMV) or with an MDM2 overexpressing plasmid (pCMV-MDM2) for 48 h. Left panel: representative images; scale bar, 50 μm. Right panel: quantification of nuclear fluorescence intensity of PARP1 staining. This was quantified specifically in cells expressing medium/high levels of MDM2. The same number of cells was randomly selected for quantification from the Ctrl sample (n = 122). The mean of the fluorescence intensity values is represented by the red line. Unpaired Student's t test was used for statistical analysis: ***$p \leq 0.001$, ****$p < 0.0001$.

(H) Ubiquitination of PARP1 by MDM2 *in vitro*. Purified recombinant MDM2 was incubated with PARP1 for up to 120 min. Additional negative controls without ubiquitin (−Ub) or without MDM2 (−MDM2) were included. At the indicated time points, the samples were subjected to immunoblot analysis. PARP1 was ubiquitinated by MDM2, as shown by accumulation of high-molecular-weight bands with increasing intensities at increasing incubation times.

(I) PAR immunofluorescence staining. H1299 cells were transfected with empty vector (pCMV) or the pCMV-MDM2 plasmid for 48 h, and nuclear levels of PAR were quantified in EdU-positive cells (i.e., cells undergoing S phase) and EdU-negative cells. Cells were treated for 2 h with PARG inhibitor (PARGi) (20 μM) to stabilize the PAR chains. Left panel: representative images; scale bar, 20 μm. Right panel: quantification of single nuclear intensities; red lines represent the mean of fluorescence intensity values. A minimum of 150 cells were quantified for each condition.

(J) Western blot analysis of SJSA-1 cells treated with 20 μM Nutlin for 6 h and/or 10 μM PARGi for 2 h. PAR became visible upon PARG inhibition but was found to be reduced upon p53 induction. Bands relative to different conditions were cropped.

Previous studies reported that Nutlin induces PARP1 degradation in the human breast cancer cell line MCF-7 in an MDM2- and proteasome-dependent fashion (Kobayashi et al., 2020; Matsushima et al., 2011; Nagai et al., 2012), which was confirmed in our experiments (Figures S1B and S1C). However, the underlying molecular mechanisms have remained elusive. To assess whether the suppression of PARP1 levels results from apoptosis-associated caspase activity, we depleted the pro-apoptotic p53 target gene product PUMA using small interfering RNAs (siRNAs) (Figure S1D). As expected, PUMA knockdown prevented formation of the caspase-dependent PARP1 fragment in response to Nutlin. However, overall PARP1 levels were still suppressed in SJSA-1 cells upon depletion of PUMA (Figure 1A) and in MCF-7 cells that were co-treated with a caspase inhibitor (Figure S1E). In contrast, a proteasome inhibitor restored PARP1 levels in Nutlin-treated SJSA-1 cells (Figure 1B), indicating that PARP1 degradation in response to p53 requires the proteasome rather than caspases. Cycloheximide chase experiments revealed that PARP1 is destabilized upon Nutlin treatment, and its levels drop to half 2 h after stalling protein synthesis (Figure 1C). MDM2 is by far the most well-characterized ubiquitin ligase that can be induced by p53 (Sane and Rezvani, 2017). We therefore tested whether MDM2 degrades PARP1 in the context of p53 activation. We used a proteolysis-targeting chimera (PROTAC), MD-224, composed of two active domains connected by a linker. One domain, MI-1061, binds MDM2 like Nutlin and displaces p53. The other domain binds the Cereblon-associated E3 ubiquitin ligase (Figure S1F). Thus, MD-224 recruits Cereblon to ubiquitinate and degrade MDM2, whereas p53 remains active (Li et al., 2019). MI-1061 alone was also included in the experiment as a control. As expected, MD-224 and MI-1061 induced accumulation of p53 and its target gene product p21, whereas MDM2 levels increased with MI-1061 but not with MD-224 (Figure 1D). Importantly, the MDM2-antagonist MI-1061 decreased PARP1 levels similarly as Nutlin but the MDM2 PROTAC MD-224 did not (Figure 1D). Far less pronounced PARP1 degradation in response to Nutlin was also observed when MDM2 was depleted by two independent siRNAs, and the degree of PARP1 level rescue correlated with knockdown efficiency (Figure 1E). Similar results were obtained when treating the non-transformed RPE cells with the MDM2-directed PROTAC in comparison with Nutlin or MI-1061 (Figure 1F). This indicates that MDM2 is necessary for PARP1 degradation upon p53 activation. To test whether MDM2 is also sufficient to diminish PARP1 levels even in the absence of p53, we transiently overexpressed MDM2 in the *TP53*$^{-/-}$ lung cancer cell line H1299 and detected PARP1 by immunofluorescence analysis. Here again, PARP1 levels were significantly reduced upon MDM2 overexpression, indicating that enhanced MDM2 levels are sufficient for PARP1 degradation (Figure 1G).

Correspondingly, purified MDM2 was sufficient for PARP1 ubiquitination *in vitro*. In this assay, ubiquitination of p53 by MDM2 served as a positive control (Figure S1G). When PARP1 was exposed to MDM2 *in vitro*, along with the E2 ubiquitin-conjugating enzyme UbcH5b and ubiquitin, a smear was observed ranging from mono-ubiquitinated forms to presumably poly-ubiquitinated forms of PARP1 (Figures 1H and S1G). These higher-molecular-weight forms of PARP1 could not be caused by auto-PARylation because the reaction was carried out in the absence of the essential PARP1 substrate NAD^+. Our result demonstrates that MDM2 is capable of transferring ubiquitin onto PARP1, as it does on p53.

Because PARP1 accounts for most of the cellular PARylation (Chen et al., 2018), we investigated whether the drop in PARP1 levels in response to MDM2 was affecting the cellular PAR content. In this experiment, PAR was stabilized by inhibiting PAR glycohydrolase (PARG) using the small molecule PDD 00017273, facilitating its detection. Accumulation of MDM2 correlated with reduced PAR levels, as shown by immunofluorescence analysis of H1299 cells (Figure 1I). This included cells displaying ongoing DNA synthesis, as visualized by 5-ethynyl-2′-deoxyuridine (EdU) incorporation, meaning that the MDM2-mediated decrease of PAR was also visible during S phase (Figure 1I), when PARP1-mediated PARylation is most active (Hanzlikova et al., 2018). Nutlin reduced PAR levels in SJSA-1 cells (Figure 1J), arguing that p53-induced MDM2 diminishes poly(ADP-ribosyl)ation. The reduction of PAR upon Nutlin treatment became visible at time points where PARP1 was not yet found to be degraded (Figures 1J). Along the same line, when SJSA-1 cells were co-treated with Nutlin and the proteasome inhibitor MG-132, we still observed a reduced PAR signal (Figure S1H). This suggests that MDM2 suppresses PARP1 activity, in addition to its stability. To further test this hypothesis, we transfected H1299 cells to overexpress MDM2 and its mutant C464A, carrying a point mutation that eliminates its RING-finger-associated E3 ubiquitin ligase activity (Itahana et al., 2007). The MDM2 C464A mutant caused a significant decrease in nuclear PARylation, similarly to MDM2 wild type (Figure S1I), strongly suggesting that MDM2-mediated ubiquitination is not required for diminishing PARP1 activity by MDM2.

These results indicate that MDM2 directly ubiquitinates PARP1 and thereby mediates its degradation via the proteasome. MDM2 also reduces cellular PAR levels independently of PARP1 ubiquitination and degradation.

MDM2 forms a complex with PARP1 *in vitro* and *in vivo*

Given the ubiquitination of PARP1 by MDM2, we tested whether the two proteins physically interact. Co-immunoprecipitation (coIP) of purified MDM2 and PARP1 demonstrated that PARP1 directly binds MDM2 (Figure 2A). Bacterially expressed MDM2 was fused to glutathione S-transferase (GST) and coupled to glutathione-Sepharose beads, followed by incubation with purified PARP1. In these assays, PARP1 associated with GST-MDM2 but not with GST alone, confirming that MDM2 is indeed capable of physically binding PARP1 (Figure S2A). The interaction was recapitulated in cells by coIP and by proximity ligation assay (PLA). First, we transiently overexpressed MDM2 and PARP1 in H1299 cells. When PARP1 was captured by an antibody for IP, we observed co-precipitation of MDM2 as well (Figure 2B). The association was also observed between endogenous PARP1 and MDM2 in Nutlin-treated SJSA-1 cells (Figure 2C), also when using an antibody to MDM2 for precipitation (Figure S2B). PLA confirmed that PARP1 and MDM2 are in a complex upon overexpression in H1299 cells (Figure 2D) and when detecting endogenous proteins in Nutlin-treated SJSA-1 cells (Figure 2E). The PLA signal was also observed when

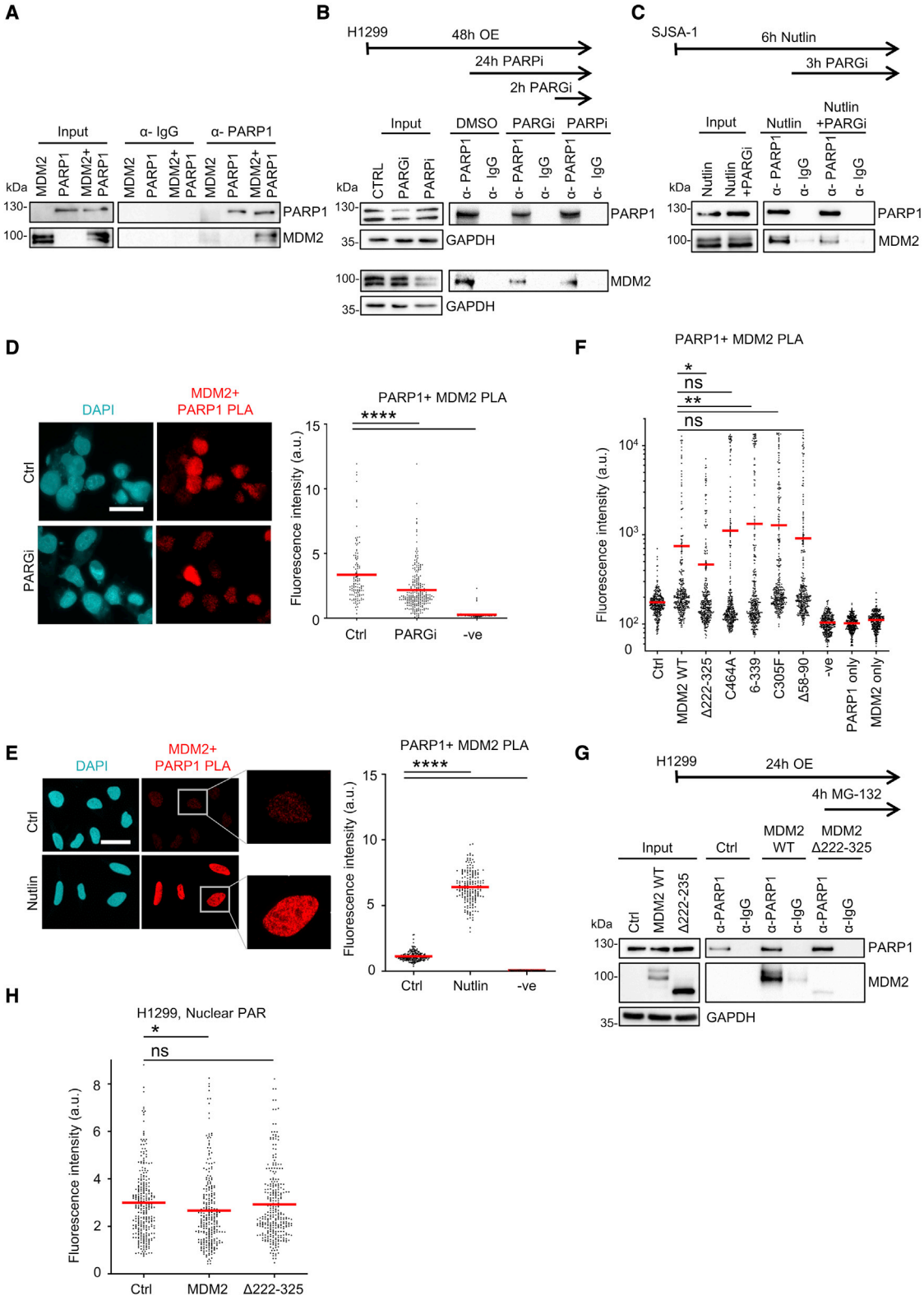

(legend on next page)

overexpressing MDM2 alone in H1299 cells, in agreement with its binding to endogenous PARP1 (Figure S2C). Controls omitting one of the two antibodies ensured signal specificity from the interacting MDM2 and PARP1 proteins (Figures S2C–S2E).

We next tested whether the interaction of MDM2 and PARP1 is influenced by the presence of PAR. We inhibited PARylation through a 24-h pre-treatment with the PARP1/2 inhibitor olaparib (Figure S2F). This did not impair co-precipitation of MDM2 with PARP1 (Figure 2B). Conversely, inducing accumulation of PARylated PARP1 by treatment with a PARG inhibitor (PDD 00017273) did not increase co-precipitation and co-localization of PARP1 and MDM2 but reduced them (Figures 2B–2D, S2F, and S2G). We concluded that the interaction of MDM2 with PARP1 is not mediated but, in fact, partially compromised by PAR accumulation.

To map the PARP1-interacting domain(s) on MDM2, we tested the capability of five different MDM2-derived mutants and fragments to co-localize with PARP1, as revealed by PLA (Figures S2H and S2I). Removing the central domain of MDM2 (mutant Δ222–325) significantly decreased the PLA signal arising from co-localization of MDM2 and PARP1, indicating that this domain contributes to the association (Figure 2F). Likewise, the central domain mutant Δ222–325 co-precipitated with PARP1 to a much lower extent than wild-type MDM2 (Figure 2G), and PARylation was not affected by this MDM2 mutant (Figure 2H).

These findings indicate that PARP1 is a direct interaction partner of MDM2 *in vitro* and *in vivo*. Binding of PARP1 to MDM2 does not require PARylation and does not involve the p53 binding site of MDM2 but, rather, the acidic/central domain, which is also crucial for MDM2 suppression of PARP1 activity.

MDM2 enhances the elongation rate of DNA synthesis, which is abolished by PARP1 overexpression

We and others have previously reported an increase in replication fork processivity upon p53 activation (Klusmann et al., 2016; Yeo et al., 2016). Conversely, MDM2 depletion in a p53-deficient background reduces replication fork progression (Klusmann et al., 2016, 2018). Now we wanted to determine whether the increased levels of MDM2 in the context of p53 activation are actually responsible for enhanced fork progression. To assess this, we took advantage of the MDM2-targeting PROTAC MD-224 and the corresponding MDM2 antagonist MI-1061 as a control. Upon treatment of SJSA-1 cells with these compounds, the lengths of labelled tracks representing newly synthetized DNA were determined by DNA fiber assays (Figure 3A), as described earlier (Köpper et al., 2013). When treating SJSA-1 cells with Nutlin or MI-1061, the levels of p53 and the p53-target gene products p21 and MDM2 were increased as expected (Figure 3B; Nutlin was used at higher concentrations and induced higher p53 levels), and the tracks of newly synthetized DNA were elongated by 50% (Figures 3C and 3D; Table S1). Strikingly, despite activating p53 comparably with MI-1061, the PROTAC MD-224 had much less potency than Nutlin or MI-1061 to increase DNA track lengths (Figures 3B–3D).In the non-transformed RPE cells, Nutlin and MI-1061 still enhanced progression of replication forks whereas the PROTAC MD-224 did not (Figures S3A–S3D). This demonstrates that MDM2, rather than p53 itself or other p53-target gene products, directly causes the observed increase in replication fork progression upon activation of p53.

Next we wanted to determine whether the interaction of MDM2 and PARP1 might form the mechanistic basis for MDM2-dependent enhancement of DNA replication fork progression. This was motivated by previous reports describing enhanced fork progression upon PARP1 inhibition (Maya-Mendoza et al., 2018). As a first step to address this, we tested how simultaneous MDM2 induction and PARP1 inhibition affect DNA replication. We combined a PARP1 inhibitor, olaparib, with Nutlin in SJSA-1 cells (Figure 3A). We confirmed enhanced fork progression with the PARP inhibitor (Maya-Mendoza et al., 2018) as well as Nutlin individually (Figures 3C and 3D). Bidirectional replication forks displayed a symmetric increase in replication rate by Nutlin (Figure S3E), resembling what was already observed in cells treated with PARP1 inhibitors (Maya-Mendoza et al., 2018; Paes Dias et al., 2021). Simultaneous addition of Nutlin and olaparib did not

Figure 2. MDM2 forms a complex with PARP1 *in vitro* and *in vivo*

(A) Co-immunoprecipitation (coIP) of purified MDM2-PARP1. IP using an anti-rabbit immunoglobulin G (IgG) antibody was used as a negative control.

(B) Physical association between MDM2 and PARP1 in H1299 cells, shown by coIP upon overexpression of both proteins for 48 h. Because this cell line is *TP53*$^{-/-}$ and, thus, cannot express MDM2, the MDM2 construct was overexpressed 9-fold in excess compared with PARP1. IP was performed with an anti-PARP1 antibody, followed by detection of both proteins by immunoblot analysis. Where indicated, the cells were treated with 20 μM of PARGi 2 h prior to harvest or 10 μM PARP inhibitor (PARPi) for 24 h. IP using an anti-rabbit IgG antibody was used as a negative control.

(C) CoIP revealed physical interaction between endogenous MDM2 and PARP1 in SJSA-1 cells upon Nutlin treatment for 6 h (20 μM). Where indicated, cells were co-treated with 10 μM PARGi for 3 h prior to harvest.

(D) Left panel: representative images from the proximity ligation assay (PLA) that was used to test the interaction of PARP1 and MDM2 in H1299 cells upon overexpression of both proteins for 48 h. Scale bar, 20 μm. Right panel: quantification of nuclear fluorescence intensity of the PLA signal. DAPI was used to identify nuclei. A negative control (-ve) was obtained by omitting the primary antibodies. The red line represents the mean for each sample.

(E) Left panel: representative images of the PLA to determine the interaction of PARP1 and MDM2 in SJSA-1 cells upon treatment with DMSO (Ctrl) or 20 μM Nutlin for 6 h. Scale bar, 30 μm. Right panel: quantification of the nuclear PLA signal.

(F) H1299 cells were transfected for 48 h with empty vector (pCMV) or expression plasmids for MDM2 wild-type (WT) or MDM2 mutants. Negative controls included only one of the two antibodies ("PARP1 only" and "MDM2 only") or neither of them (-ve).

(G) CoIP of MDM2 WT and the MDM2 central domain mutant (Δ222–325) with PARP1. H1299 cells were transfected to overexpress MDM2 WT or mutant MDM2 together with PARP1. MDM2 was overexpressed in excess compared with PARP1 (9:1) to ensure sufficient expression levels. After 24 h, cells were treated for 4 h with the proteasome inhibitor (MG-132, 20 μM) to stabilize MDM2 prior to harvesting. IP was performed with an anti-PARP1 antibody, followed by detection of both proteins by immunoblot analysis.

(H) PAR immunofluorescence staining. H1299 cells were transfected with empty vector Ctrl (pCMV) or plasmids expressing WT or mutant MDM2 (Δ222–325) for 48 h. PARGi (2 h, 20 μM) was added to all samples to stabilize PAR. Nuclear levels of PAR were quantified in MDM2-positive cells. The same number of cells was randomly selected for quantification from the control sample (n = 259).

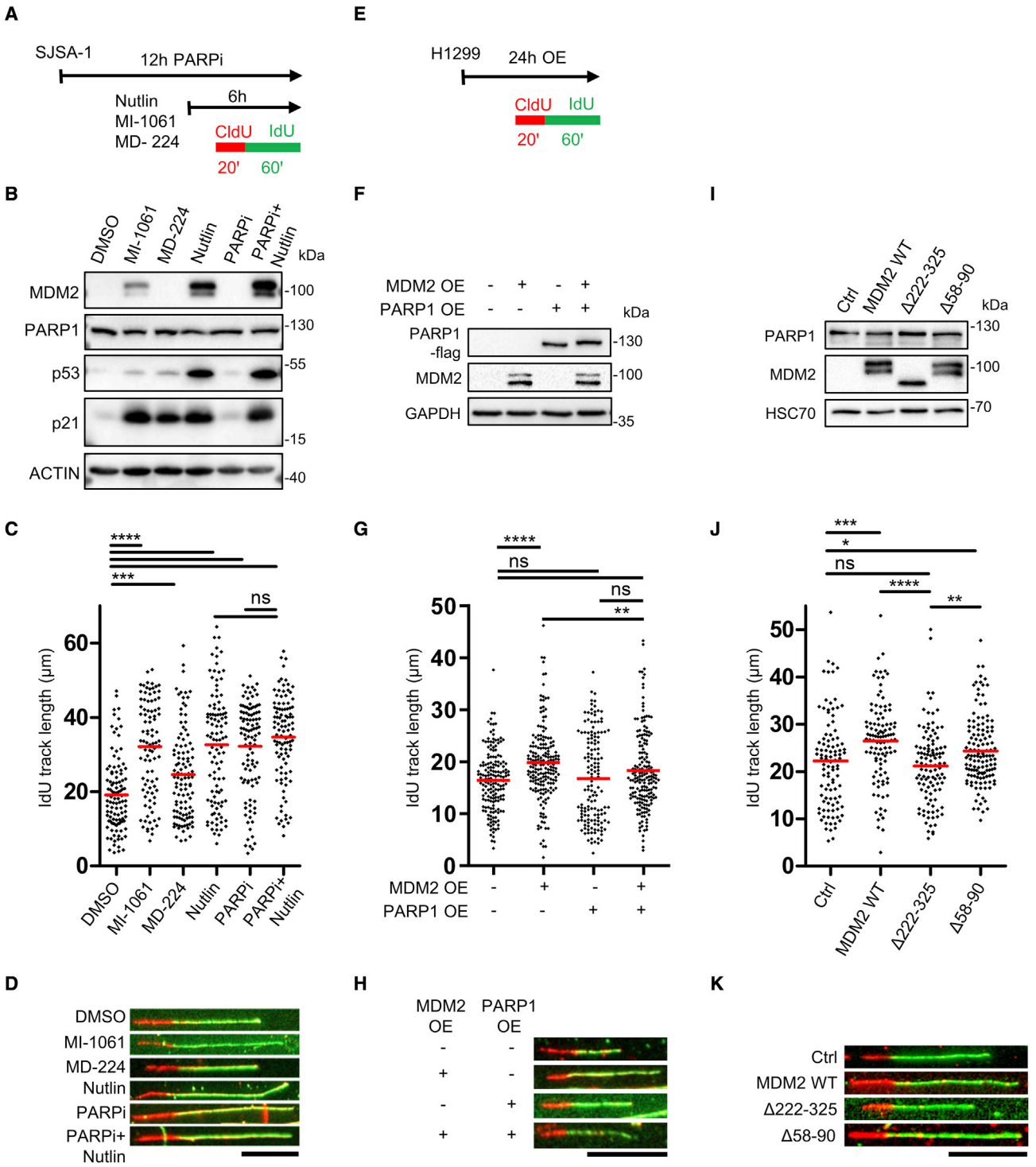

Figure 3. MDM2 enhances the elongation rate of DNA synthesis, which is abolished by PARP1 overexpression

(A) Treatment scheme. SJSA-1 cells were treated with Nutlin (20 μM, 6 h), MI-1061 (1 μM, 6 h), MD-224 (1 μM, 6 h), and the PARPi olaparib (10 μM, 12 h). DNA fiber assays were performed, sequentially labeling newly synthetized DNA with 5-chloro-2-deoxyuridine (CldU; 25 μM, 20 min) and 5-iodo-2-deoxyuridine (IdU) (25 μM, 60 min).

(B) Immunoblot analysis of SJSA-1 cells treated as delineated in (A), confirming comparable p53 activation by MI-1061, MD-224, and Nutlin, as shown by p21 accumulation, whereas MD-224 specifically depleted MDM2.

(legend continued on next page)

further increase the lengths of the tracks compared with the single drugs (Figures 3C and 3D). This suggests an epistatic relation between enhanced MDM2 expression and PARP inhibition. Because MDM2 antagonizes PARP1 in response to Nutlin, it is conceivable that PARP1 inhibition does not increase fork progression above the level seen with Nutlin. PARP1 inhibition alone still accelerated fork progression as much as the drug combination, suggesting that targeting PARP1 is the predominant mechanism by which MDM2 increases fork speed.

A similar increase in nascent DNA elongation was found in the *TP53*$^{-/-}$ H1299 cells upon plasmid-based overexpression of MDM2. This effect of MDM2 was also observed upon topoisomerase I inhibition by camptothecin (CPT) (Figures 3E–3H and S3F–S3I). Again, the symmetry of bidirectional replication forks was not detectably changed by MDM2 (Figure S3J). Fork asymmetry was increased upon CPT-mediated topoisomerase I inactivation, as reported previously (Chappidi et al., 2020; Tuduri et al., 2009), but this was not exacerbated by MDM2 (Figure S3J).

Simultaneous overexpression of PARP1 along with MDM2 significantly attenuated the increase in DNA track lengths (Figures 3E–3H), also in the presence of CPT (Figures S3K–S3M). Overexpression of MDM2 with deletion of the central domain (Δ222–325), which diminishes the interaction with PARP1 (Figures 2F and 2G), had no effect on nascent DNA elongation, unlike wild-type MDM2 or a mutant of MDM2 that fails to bind p53 (Δ58–90) (Figures 3I–3K).

These observations strongly suggest that antagonizing PARP1 by MDM2 is the predominant mechanism by which MDM2 accelerates progression of DNA replication forks.

MDM2-mediated PARP1 inactivation induces nascent DNA elongation through RECQ1

We next investigated the mechanisms by which MDM2-mediated inactivation of PARP1 increases progression of DNA replication forks. PARP1 has been found previously to inhibit the DNA helicase RECQ1, avoiding premature restarting of reversed replication forks (Berti et al., 2013). We thus hypothesized that RECQ1 might become active and favor replication fork progression when MDM2 accumulates to antagonize PARP1. To test this, we depleted RECQ1 from SJSA-1 cells (Figures 4A, 4B, S4A, and S4B). Although treatment with Nutlin or the PARP inhibitor olaparib enhanced the lengths of newly synthesized DNA tracks, this was reversed by depletion of RECQ1 (Figures 4C and S4C). Upon plasmid-driven overexpression of MDM2 in H1299 cells, depleting RECQ1 prevented the MDM2-induced increase in the elongation rate of nascent DNA (Figures 4D–4F and S4D–S4F). This was still observed when treating the cells with CPT (Figures S4G–S4I), which is known to promote replication fork reversal (Ray Chaudhuri et al., 2012). MDM2 overexpression did not affect RECQ1 protein levels (Figure S4J).

This strongly suggests that RECQ1 mediates unrestrained fork progression in response to MDM2 accumulation.

MDM2 accumulation favors PRIMPOL-mediated fork progression and accumulation of DNA damage

We then investigated whether DDT pathways are supported by MDM2 via degradation of PARP1, explaining enhanced DNA elongation. As one emerging DDT pathway, repriming of DNA synthesis by PRIMPOL resumes DNA elongation at stalled replication forks (Berti et al., 2020; Mouron et al., 2013).

We thus investigated whether accelerated progression of replication forks upon MDM2 accumulation might require PRIMPOL. Depletion of PRIMPOL counteracted the enhancement of fork progression in Nutlin-treated SJSA-1 cells (Figures 5A–5C and S5A–S5E) and upon MDM2 overexpression in H1299 cells (Figures 5D–5F). This was still seen when replication fork stalling was induced by CPT treatment (Figures S5F–S5H). PRIMPOL knockdown also attenuated the increase in replication fork progression caused by treatment of SJSA-1 cells with the PARP inhibitor olaparib (Figure 5B), further corroborating the induction of PRIMPOL repriming activity by PARP1 inhibition (Genois et al., 2021; Quinet et al., 2020).

RECQ1-mediated fork restarting can overcome the pausing of replication in the presence of a damaged leading-strand template (Berti et al., 2013). Repriming through PRIMPOL leaves behind gaps of single-stranded DNA (Mouron et al., 2013). We thus expected MDM2-mediated enhancement of fork progression to induce a DNA damage response. We observed an MDM2-driven increase in the DNA damage marker γH2AX in H1299 and SJSA-1 cells (Figures 5G and 5H). In contrast, depletion of MDM2 via the PROTAC MD-224 failed to induce γH2AX in SJSA-1 cells despite p53 activation (Figure 5H). The MDM2-driven increase in γH2AX was only visible in H1299 cells that had incorporated the label EdU (Figures 5G and S5I) (i.e., in cells undergoing S phase), indicating that MDM2 specifically causes DNA damage accumulation in the context of DNA replication. To test to which extent PRIMPOL and RECQ1 contribute to DNA damage accumulation, we depleted each of them upon MDM2 accumulation. The Nutlin-induced increase in γH2AX levels was attenuated upon depletion of PRIMPOL but not RECQ1 (Figures 5I and S5J), suggesting that PRIMPOL-induced gaps in the newly synthesized DNA strand are the predominant

(C) DNA fiber assay following the treatment shown in (A). Only fibers containing both labels were considered for quantification. The mean track length of the second label (IdU) is shown as a red line for each condition. A minimum of 100 fibers was quantified from each sample in three independent experiments with similar results. Mann-Whitney U test, two sided, was used for statistical analysis: ns, not significant; *p ≤ 0.05, **p ≤ 0.01, ***p ≤ 0.001, ****p < 0.0001.
(D) Representative images of DNA fibers obtained upon treatment as depicted in (A). Scale bar, 20 μm.
(E) Protocol used for DNA fiber assays. H1299 cells were subjected to plasmid transfection for overexpression (OE) of Ctrl (pCMV), MDM2 WT (pCMV-MDM2) and/or PARP1 (pCMV-PARP1), MDM2 central domain mutant (pCMV-Δ222–325), and p53-binding defective mutant (pCMV-Δ58–90).
(F) Immunoblot analysis of H1299 cells transfected as shown in (E), confirming MDM2 as well as PARP1 OE.
(G) DNA fiber assay performed upon MDM2 and/or PARP1 OE in H1299 cells.
(H) Representative images of DNA fibers analyzed after transfection according to (E). Scale bar, 20 μm.
(I) Immunoblot analysis of H1299 cells transfected as shown in E, to overexpress WT and mutant versions of MDM2.
(J) DNA fiber assay upon WT MDM2 and mutant OE in H1299 cells.
(K) Representative images of the DNA fiber assay quantified in (J). Scale bar, 20 μm.

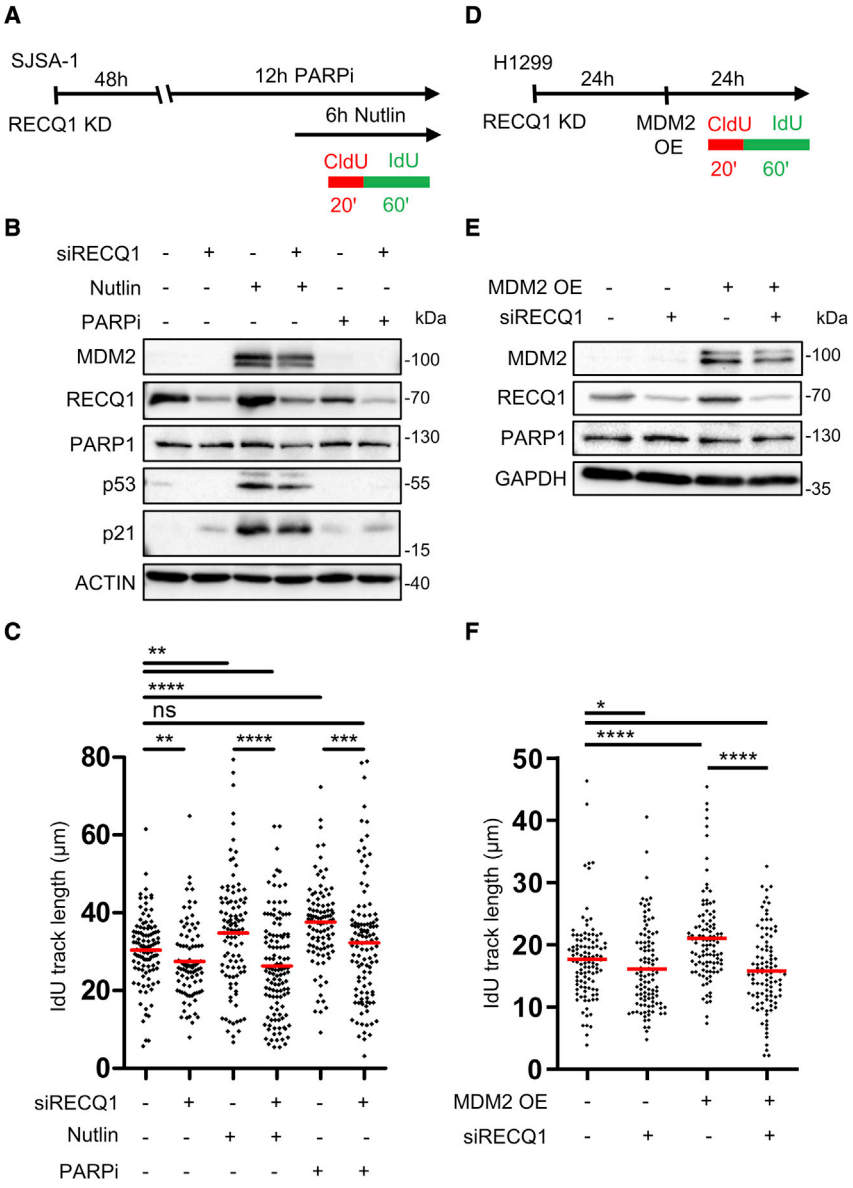

Figure 4. MDM2-mediated PARP1 inactivation induces nascent DNA elongation through RECQ1

(A) Transfection and treatment protocol. SJSA-1 cells were transfected with siRNAs against RECQ1 (siRECQ1 #1) and treated with Nutlin (20 μM, 6 h) or the PARPi olaparib (10 μM, 12 h). For DNA fiber assays, sequential labeling of newly synthetized DNA with CldU (25 μM, 20 min) and IdU (25 μM, 60 min) was performed.

(B) Immunoblot analysis after transfection and treatment described in (A), confirming the depletion of RECQ1 by siRNA and accumulation of p53, p21, and MDM2 upon Nutlin treatment.

(C) DNA fiber assay using SJSA-1 cells treated as shown in (A). The mean track lengths of the second label (IdU), within bicolored fibers, are shown as red lines. For each condition, a minimum of 100 fibers was quantified in two independent experiments with similar results. Mann-Whitney U test, two sided, was used for statistical analysis: *p ≤ 0.05, **p ≤ 0.01, ***p ≤ 0.001, ****p < 0.0001.

(D) Transfection scheme. H1299 cells were transfected with siRECQ1 #1 and subjected to plasmid transfection (control plasmid, pCMV; expression plasmid, pCMV-MDM2) 24 h later.

(E) Immunoblot analysis upon treatment as indicated in (D), confirming MDM2 OE and RECQ1 knockdown.

(F) DNA fiber assay of H1299 cells upon transfection as shown in (D).

cause of DNA damage accumulation upon MDM2 induction. Thus, in addition to RECQ1, PRIMPOL is an essential mediator of increased fork progression upon MDM2 induction, and PRIMPOL activity causes DNA damage in this context.

MDM2 accumulation antagonizes replication fork reversal

PRIMPOL-mediated fork repriming and fork reversal are two alternative mechanisms by which cells ensure replication when hitting obstacles on the parental DNA (Bai et al., 2020; Quinet et al., 2020; Vallerga et al., 2015). We therefore wanted to determine whether MDM2, promoting RECQ1-mediated fork restart and PRIMPOL-dependent repriming of DNA synthesis, might repress fork reversal. Specifically, we tested whether MDM2 accumulation reduces the proportion of reversed replication forks, visualized as four-way junctions using electron microscopy (EM) (Zellweger and Lopes, 2018; Figure 6A). MDM2 accumulation was achieved by treating SJSA-1 cells with Nutlin or by overexpression of MDM2 in H1299 cells. The topoisomerase inhibitor CPT was used at concentrations that reduced fork progression and induced replicative stress (Figures S6A–S6D), enhancing fork reversal to detectable levels. The proportion of reversed forks was strongly reduced by Nutlin in SJSA-1 cells and even diminished to a quarter of its original frequency by MDM2 overexpression (Figure 6B). Thus, MDM2 strongly represses DNA replication fork reversal while enhancing fork restarting and repriming.

MDM2 enhances accumulation of micronuclei and CPT-induced cytotoxicity

Finally, we investigated the effect of MDM2-mediated PARP1 inactivation on cell fate. Perturbed DNA replication can leave behind acentric chromosome fragments and give rise to extranuclear bodies known as micronuclei, which serve as biomarkers of genomic instability (Fenech et al., 2020; Luzhna et al., 2013). In H1299 cells, plasmid-based overexpression of MDM2 significantly increased the number of micronuclei (Figures 7A–7C). This was even further enhanced upon genotoxic stress; i.e., CPT treatment. Co-overexpression of PARP1 reversed this

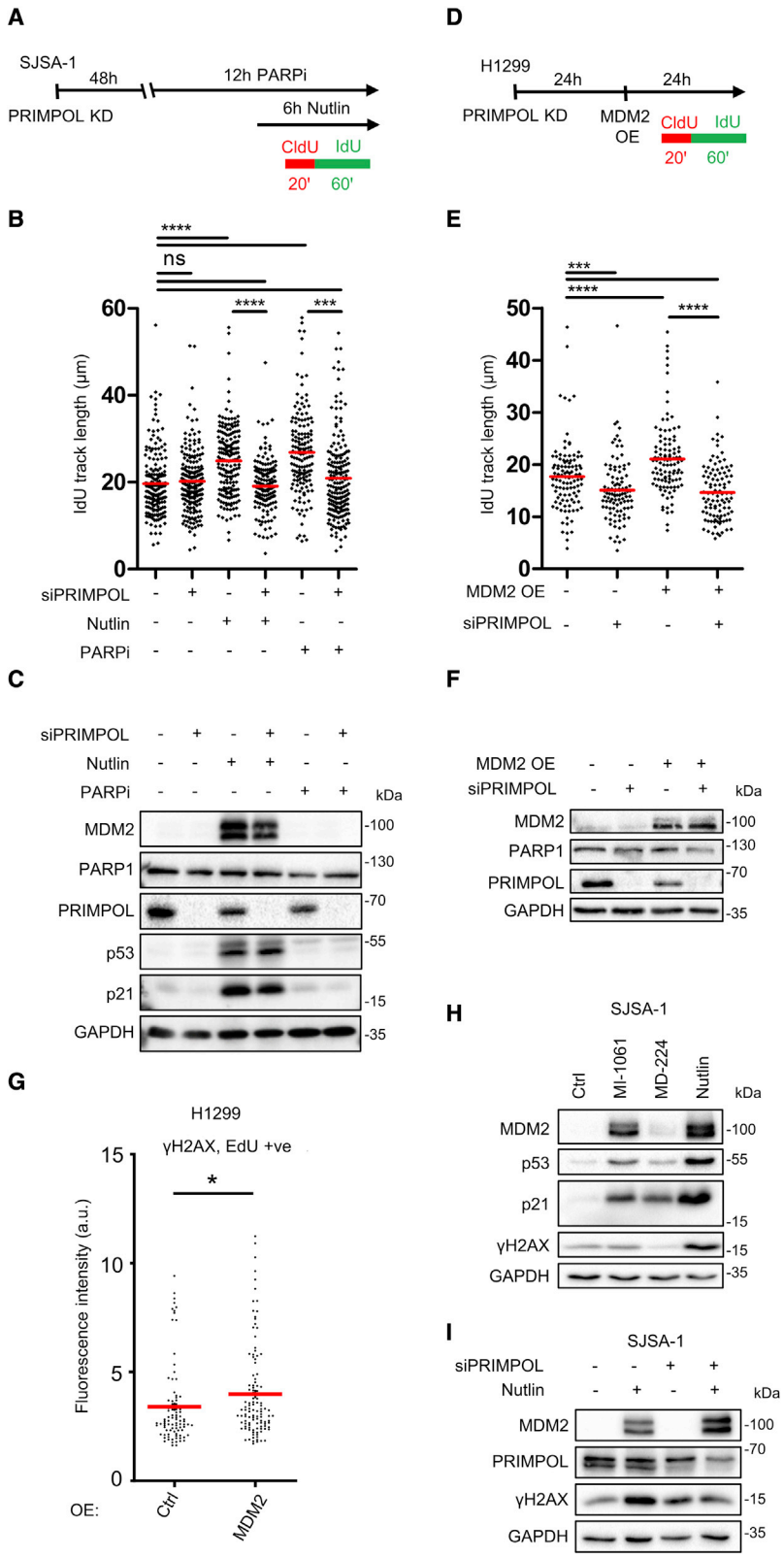

Figure 5. MDM2 accumulation favors PRIMPOL-mediated fork progression and accumulation of DNA damage

(A) Transfection and treatment schedule. SJSA-1 cells were transfected with siRNAs against PRIMPOL (siPRIMPOL #2) and treated with Nutlin (20 μM, 6 h) or the PARPi olaparib (10 μM, 12 h). For fiber assays, newly synthetized DNA was labeled with CldU (25 μM, 20 min) and IdU (25 μM, 60 min) as indicated.

(B) DNA fiber assay following transfection and treatment as depicted in (A). Mean track lengths of the second label (IdU) in bicolored fibers are indicated as red lines. A minimum of 100 fibers per sample was quantified in two independent experiments with similar results. Mann-Whitney U test, two sided, was used for statistical analysis: ***$p \leq 0.001$, ****$p < 0.0001$.

(C) Immunoblot analysis after transfection and treatment as described in (A), indicating depletion of PRIMPOL and regulation of p53 and MDM2 by Nutlin.

(D) Transfection scheme. H1299 cells were transfected with siPRIMPOL #2 and, after 24 h, subjected to plasmid OE (control plasmid, pCMV; expression plasmid, pCMV-MDM2).

(E) DNA fiber assay following treatment as shown in (D).

(F) Immunoblot analysis upon treatment as indicated in (D), confirming MDM2 OE and PRIMPOL knockdown.

(G) Quantitative immunofluorescence analysis of phosphorylated histone 2AX (γH2AX) in H1299 cells upon OE of MDM2 (48 h). The analysis was restricted to cells in S phase, identified by EdU incorporation. Red lines represent the mean values. Number of quantified cells: Ctrl, n = 92; MDM2, n = 116.

(H) Immunoblot analysis of SJSA-1 cells treated with MDM2-binding compounds (Nutlin, 20 μM; MI-1061, 1 μM) or the MDM2 PROTAC (MD-224, 1 μM) for 12 h. MD-224 induced p53-activation comparable with MI-1061, as shown by p21 accumulation but depleted MDM2.

(I) Immunoblot analysis upon 12-h treatment with 20 μM Nutlin, with or without PRIMPOL depletion via siRNA (siPRIMPOL #2), revealing the drop in DNA damage response in the absence of PRIMPOL.

A

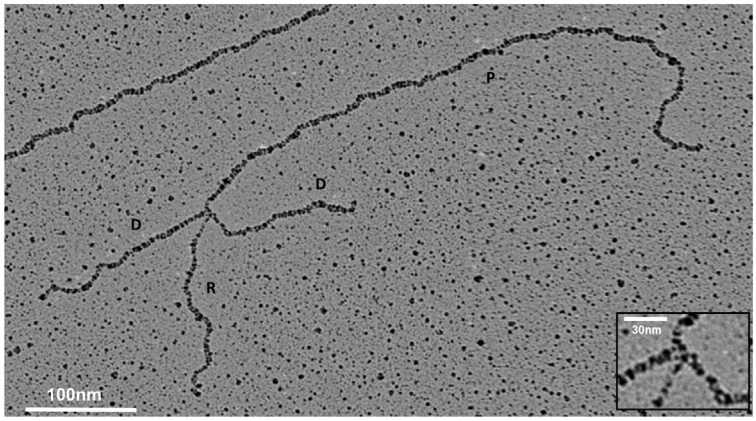

B

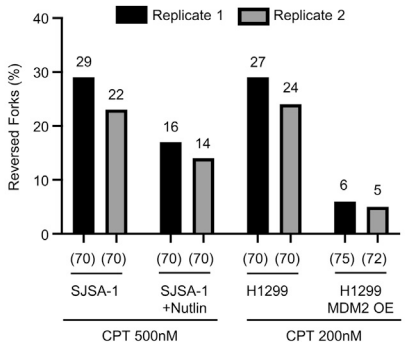

Figure 6. MDM2 accumulation antagonizes replication fork reversal

(A) Representative EM image of a reversed replication fork (four-ways). D, daughter strand; P, parental strand; R, reversed arm. The relevant portions of the molecules are magnified in the inset.

(B) Frequency of fork reversal in SJSA-1 cells subjected to Nutlin treatment (20 μM, 6 h) and H1299 cells that were transfected with plasmids (control plasmid, pCMV; expression plasmid, pCMV-MDM2), each treated with CPT as indicated. Two distinct biological replicates are displayed.

MDM2-dependent increase in micronuclei (Figure 7B), and deletion of the central, PARP1-binding domain of MDM2 (Δ222–325) prevented augmentation of micronuclei (Figure 7C). Nutlin treatment promoted micronuclei in SJSA-1 cells (Figure 7D). These observations strongly suggest that MDM2 not only increases replication fork progression but also micronucleus formation and genomic instability through PARP1 inactivation.

To study whether MDM2-mediated PARP1 inactivation also affects cell survival upon genotoxic stress, we monitored phosphatidylserine externalization and membrane integrity via staining with Annexin V and propidium iodide. We treated synchronized SJSA-1 cells with pharmacological MDM2 antagonists prior to release into S phase. At the time of release, CPT was added to induce genotoxic stress (Figure 7E). MI-1061, but not the PROTAC MD-224, significantly enhanced CPT-induced cell death, similar to PARP1 inhibition (Figures 7F and S7A). Correspondingly, MI-1061 but not MD-224, reduced cellular proliferation in the presence of CPT (Figures 7G and S7B). Thus, enhancing MDM2 levels not only leads to chromosomal instability but also diminishes survival when cells undergo genotoxic stress.

DISCUSSION

Our results reveal a functional interaction of MDM2 with PARP1, resulting in PARP1 inactivation and enhanced replication fork progression. When MDM2 antagonizes PARP1, the activity of the helicase RECQ1 and the primase/polymerase PRIMPOL becomes preponderant, with suppression of fork reversal and consequent acceleration of fork progression (Figure 7H).

We found RECQ1 and PRIMPOL to be necessary for replication fork acceleration in the context of elevated MDM2. However, these factors perform different functions. RECQ1 is a helicase that acts mainly by resolving reversed replication forks (Berti et al., 2013; Debnath and Sharma, 2020). In contrast, PRIMPOL acts by re-priming DNA synthesis on uncoupled forks to continue replication. This leaves behind gaps of single-stranded DNA that then need to be repaired by post-replicative gap filling (Guilliam and Doherty, 2017; Mouron et al., 2013; Tirman et al., 2021). Because PARP1 PARylates and antagonizes RECQ1 (Berti et al., 2013; Larsen et al., 2018), and because the increase in fork progression upon PARP inhibition requires RECQ1 (Figure 4) and PRIMPOL (Figure 5; Simoneau et al., 2021), we propose that PARP1 opposes each way of fork restarting, whereas MDM2 promotes both by counteracting PARP1. We observed that MDM2 confers enhanced vulnerability towards the topoisomerase I inhibitor CPT (Figure 7), which might be clinically relevant when MDM2 levels are increased in tumors; e.g., through gene amplification in sarcomas.

p53 induces the lncRNA SPARCLE, which promotes PARP1 cleavage by caspases (Meza-Sosa et al., 2022). This might be a way for p53 to eliminate PARP1 in addition to the MDM2-mediated inactivation and ubiquitination that we are reporting here.

PARP1 and p53 each form part of the fork speed regulatory network (FSRN), an integrated molecular machinery that regulates the velocity of DNA replication forks, as proposed previously (Merchut-Maya et al., 2019) based on the observation of PARP1 as a regulator of replication forks (Maya-Mendoza et al., 2018). Our results expand and corroborate this model by the mechanism of PARP1 degradation through p53-induced MDM2.

Antagonizing p53 was the first function of MDM2 that was discovered (Chen et al., 1993; Oliner et al., 1993). Targeted disruption of TP53 and/or MDM2 in mice revealed the

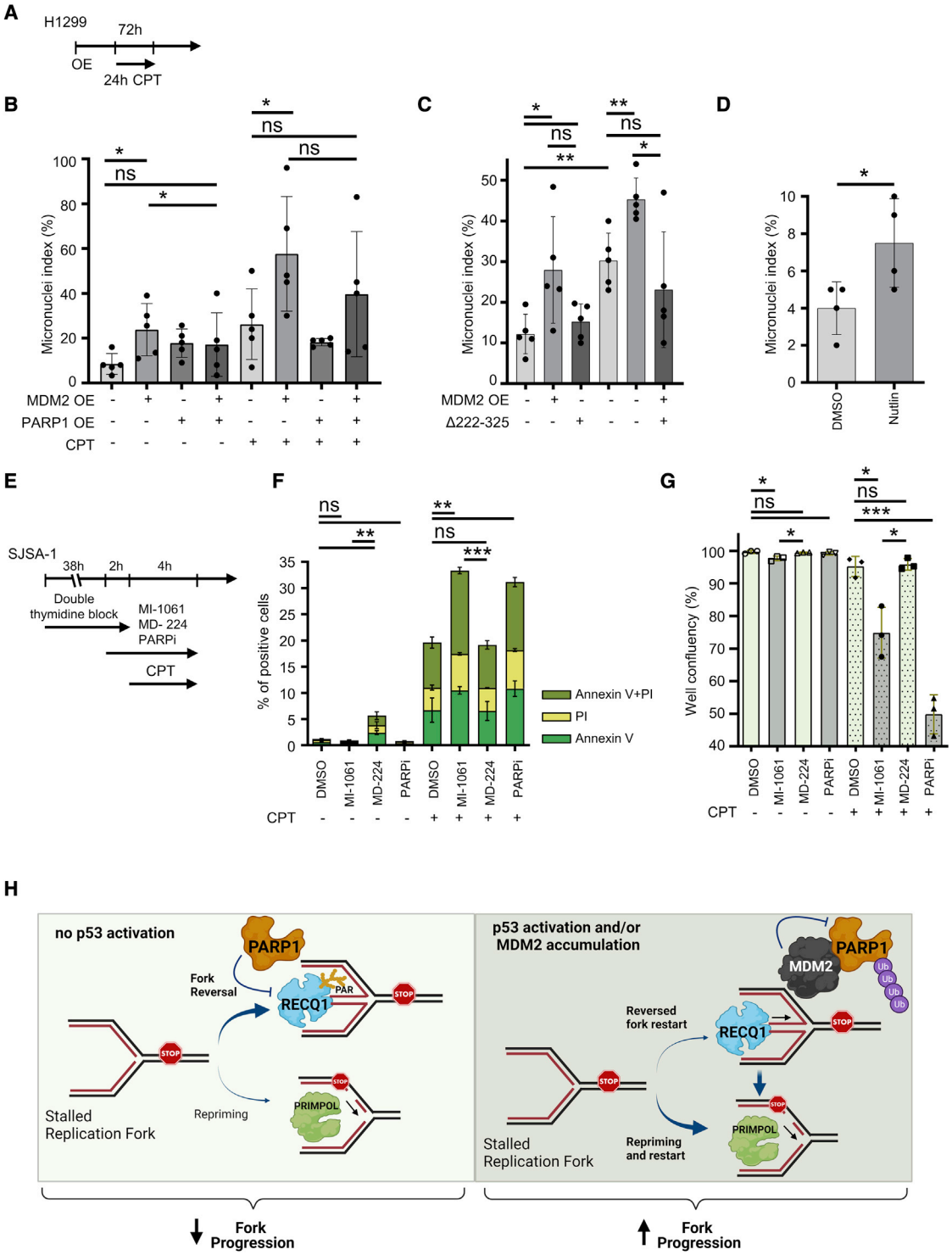

Figure 7. MDM2 enhances accumulation of micronuclei and CPT-induced cytotoxicity

(A) Transfection and treatment scheme. 24 h after plasmid-based OE, CPT (5 nM) was administered for 24 h, followed by 24 h of treatment washout.

(B) Quantification of micronucleus formation in H1299 cells. Cells were transfected to overexpress Ctrl plasmid (pCMV), MDM2 (pCMV-MDM2), and/or PARP1 (pCMV-PARP1) as described in (A). All plasmids were co-transfected with a GFP overexpressing plasmid (pCMV-GFP). The number of micronuclei (MNs) over the number of cells was quantified, considering only transfected cells (GFP/MDM2/flag-PARP1-positive cells). The results of five independent experiments are shown. Unpaired Student's t test was used for statistical analysis: *p $\leq$ 0.05, **p $\leq$ 0.01.

(legend continued on next page)

essentiality of MDM2, but only in the presence of p53 (Montes de Oca Luna et al., 1995). This might lead to the assumption that antagonizing p53 is the only relevant function of MDM2, despite many p53-independent functions of MDM2 reported previously (Alt et al., 2005; Fåhraeus and Olivares-Illana, 2014; Wienken et al., 2016, 2017). However, animals lacking p53 cannot upregulate MDM2 in response to stress. This may obscure any functions of MDM2 as an effector rather than a negative regulator of p53 (Dobbelstein and Levine, 2020). We propose that MDM2 supports DNA replication as part of a p53 response, in agreement with our earlier finding that p53 as well as MDM2 can support DNA replication (Klusmann et al., 2016, 2018).

Previous reports have suggested a role of p53 in DNA synthesis upon replication stress (Hampp et al., 2016; Klusmann et al., 2016; Roy et al., 2018; Yeo et al., 2016). Some of them describe a direct role of p53 in DNA replication independent of its function as a transcription factor. For instance, p53 interacts with the DNA polymerase iota (POLI), inducing idling cycles that slow down replication and induce fork reversal (Hampp et al., 2016; Khare and Eckert, 2002). On the other hand, p53 enhances fork progression and facilitates TLS by formation of p21-POLI complexes (Ihle et al., 2021). The choice between these opposing phenotypes depends on the differentiation status of the cell (Ihle et al., 2021). Such a scenario is entirely compatible with our findings that indicate a transcriptional function of p53 in DNA replication; i.e., enhancing the levels of MDM2 and thereby antagonizing PARP1. We propose that p53 can exert its effect on DNA replication in multiple ways, involving mechanisms that do or do not depend on its function as a transcription factor, possibly in a cell-type-specific manner.

On top of its interaction with MDM2, PARP1 can associate with additional regulatory factors. These include histone PARylation factor 1 (HPF1) (Gibbs-Seymour et al., 2016; Palazzo et al., 2018) and the methyltransferase CARM1 (Genois et al., 2021). Both of them are activators of PARP1, whereas MDM2 acts as a negative regulator according to our results. Because MDM2 reduces cellular PAR levels independent of PARP1 ubiquitination and degradation (Figures 1J, S1H, and S1I), we conclude that MDM2 inactivates PARP1 independent of PARP1 degradation. Such a scenario has also been found for p53, which is also inactivated but not destabilized by MDM2 mutants lacking E3 ligase activity (Dobbelstein et al., 1999).

The E3 ubiquitin ligases CHFR (Kashima et al., 2012), RNF146/Iduna (Kang et al., 2011), and TRIP12 (Gatti et al., 2020) act on PARP1. Unlike these E3 ligases, the interaction of MDM2 with PARP1 does not require PAR. MDM2 binds PARP1 directly, as demonstrated by co-IP of the purified proteins (Figures 2A and S2A), and the interaction is counteracted by increased PAR levels rather than depending on them (Figures 2B–2D). Conceivably, PARylation upon replication fork stalling might first delay the interaction of PARP1 and MDM2, allowing stabilization of PARP1 and reversed forks. Conversely, when PAR is degraded upon DNA damage repair or resolution of replication obstacles, this might trigger MDM2-mediated PARP1 degradation and replication restarting.

PARP inhibitors, a major class of cancer therapeutic agents, often exert their effect by trapping PARP1 on chromatin, as exemplified by olaparib (Pettitt et al., 2018). Wild-type p53 renders cancer cells resistant to PARP inhibitors (Ireno et al., 2014). This protective effect of p53 to PARP inhibitors might at least be partially due to MDM2-mediated PARP1 degradation, which would prevent cytotoxic PARP1 trapping on the chromatin.

Fork reversal and PRIMPOL-mediated repriming are two alternative mechanisms by which cells cope with obstacles to leading DNA strand synthesis. Our results strongly suggest that MDM2 accumulation tilts the balance toward repriming. In the context of repeated genotoxic stress, in a BRCA-deficient background, PRIMPOL activity protects replication forks against DNA degradation (Quinet et al., 2020), and MDM2 might then support this protective function. PRIMPOL expression is induced by the kinase ATR (Quinet et al., 2020), a principal transducer of the replication stress signal (Saldivar et al., 2017). ATR might promote repriming via p53 phosphorylation and consequent MDM2 induction (Tibbetts et al., 1999). PRIMPOL activation by p53 and MDM2 could thus explain the lengthening of labeled DNA tracks in TP53 wild-type cells compared with their TP53-null counterparts upon DNA damage (Yeo et al., 2016).

In addition to providing negative feedback on p53, MDM2 emerges as a determinant of genome dynamics. By antagonizing the predominant PARP, it tips the balance between fork reversal and progression toward the latter, acting as a central switch to govern the DNA replication machinery.

Limitations of the study

Two intrinsic limitations apply to the interpretation of our data. First, RECQ1 and PRIMPOL are required for upregulated fork progression upon enhancing MDM2 levels; however, we do not know whether both factors act on the same replication fork or

(C) MN formation in H1299 cells subjected to OE of Ctrl plasmid (pCMV), MDM2 (pCMV-MDM2), and MDM2 central domain mutant (pCMV-Δ222–325) as described in (A). MNs were quantified as described above in five independent experiments.
(D) Quantification of MNs in SJSA-1 cells treated with Nutlin (20 μM) for 24 h. Statistical analysis and quantification were performed, considering four independent experiments and as indicated above.
(E) Treatment protocol. SJSA-1 cells were synchronized by double thymidine block. 2 h prior to release, cells were treated with MI-1061 (1 μM), MD-224 (1 μM), or the PARPi olaparib (10 μM). At release from the second thymidine block, cells were also treated with CPT (50 nM, 4 h).
(F) Annexin V-PI staining after treatment as described in (E) and 24 h of drug washout. One of four independent experiments with similar outcome is shown. Unpaired Student's t test was used for statistical analysis: $^{**}p \leq 0.01$, $^{***}p < 0.001$.
(G) Well confluency (percent) upon treatment as shown in (E) and after 7 days of drug washout. One of three independent experiments with three technical replicates with similar outcome is shown. Unpaired Student's t test was used for statistical analysis: $^{*}p \leq 0.05$, $^{**}p \leq 0.01$, $^{***}p < 0.001$.
(H) Model of PARP1 regulation by MDM2 at stalled DNA replication forks. Obstacles to replication can lead to fork reversal. When MDM2 levels are low, PARP1 antagonizes RECQ1 by PARylation, delaying re-initiation of replication (left panel). When MDM2 is induced (e.g., by p53 activation), PARP1 is inactivated, allowing RECQ1 to resolve reversed forks and PRIMPOL to reprime DNA synthesis downstream of the replication obstacle (right panel). The model was created using BioRender.com.

whether we are observing two distinct fork populations that proceed with enhanced efficiency by two different mechanisms. Second, we are mostly studying p53-induced MDM2. This has the advantage of observing MDM2 in a physiological context, but it makes it more difficult to distinguish the activities of p53 and MDM2. Because of a negative regulatory feedback loop, both gene products are intimately linked in their levels and activity. Therefore, we cannot easily exclude that p53 or some of its target gene products other than MDM2 may also contribute to progression of replication forks. Still, use of a PROTAC to eliminate MDM2 strongly suggests that MDM2 plays a major role in regulation of fork reversal in the context of a p53 response.

STAR★METHODS

Detailed methods are provided in the online version of this paper and include the following:

- KEY RESOURCES TABLE
- RESOURCE AVAILABILITY
  - Lead contact
  - Materials availability
  - Data and code availability
- EXPERIMENTAL MODEL AND SUBJECT DETAILS
  - Cell culture
- METHOD DETAILS
  - DNA fiber assay
  - Immunoblot analysis
  - Co-immunoprecipitation (Co-IP)
  - RNA extraction, reverse transcription, and real time quantitative PCR
  - Immunofluorescence staining
  - Proximity ligation assay
  - EdU incorporation and staining for identification of cells in S-phase
  - Cell death and cell proliferation assays
  - Electron microscopy
  - GST pull-down assay
  - *In vitro* ubiquitination assay
- QUANTIFICATION AND STATISTICAL ANALYSIS
  - Statistics
  - Immunofluorescence staining quantification
  - Quantification of micronuclei
  - DNA fibers and fork symmetry quantification
  - Western blot quantification

SUPPLEMENTAL INFORMATION

Supplemental information can be found online at https://doi.org/10.1016/j.celrep.2022.110879.

ACKNOWLEDGMENTS

We thank Juan Méndez for kindly sharing the PRIMPOL antibody with us. We thank Martin Standley for editing the manuscript, Evangelos Prokakis for PLA protocol establishment, and Lorenzo Dezi for data analysis automation. V.M. and C.G. were supported by the Göttingen Graduate School for Neurosciences, Biophysics, and Molecular Biosciences (GGNB). V.M. was a member of the IMPRS/MSc./PhD program Molecular Biology at Göttingen during this work. This work was kindly supported by Deutsche Krebshilfe, Deutsche Forschungsgemeinschaft, the Wilhelm Sander-Stiftung, and the Else Kröner-Fresenius-Stiftung. Work in the Lopes lab was supported by SNF grant 310030_189206. M.D.P. was supported by an AIRC Fellowship for Abroad.

AUTHOR CONTRIBUTIONS

Conceptualization, C.G., V.M., and M.D.; methodology, C.G., V.M., and Achim Dickmanns; validation, Antje Dickmanns; investigation, C.G., V.M., M.D.P., A.S., and S.M.K.; writing – original draft, M.D. and C.G.; writing – review & editing, V.M., M.D.P., A.S., and M.L.; supervision M.D., M.S., and M.L.

DECLARATION OF INTERESTS

The authors declare no competing interests.

Received: November 29, 2021
Revised: April 15, 2022
Accepted: May 5, 2022
Published: May 31, 2022

REFERENCES

Alt, J.R., Bouska, A., Fernandez, M.R., Cerny, R.L., Xiao, H., and Eischen, C.M. (2005). Mdm2 binds to Nbs1 at sites of DNA damage and regulates double strand break repair. J. Biol. Chem. *280*, 18771–18781. https://doi.org/10.1074/jbc.m413387200.

Bai, G., Kermi, C., Stoy, H., Schiltz, C.J., Bacal, J., Zaino, A.M., Hadden, M.K., Eichman, B.F., Lopes, M., and Cimprich, K.A. (2020). HLTF promotes fork reversal, limiting replication stress resistance and preventing multiple mechanisms of unrestrained DNA synthesis. Mol. Cell *78*, 1237–1251.e7. https://doi.org/10.1016/j.molcel.2020.04.031.

Berti, M., Cortez, D., and Lopes, M. (2020). The plasticity of DNA replication forks in response to clinically relevant genotoxic stress. Nat. Rev. Mol. Cell Biol. *21*, 633–651. https://doi.org/10.1038/s41580-020-0257-5.

Berti, M., Ray Chaudhuri, A., Thangavel, S., Gomathinayagam, S., Kenig, S., Vujanovic, M., Odreman, F., Glatter, T., Graziano, S., Mendoza-Maldonado, R., et al. (2013). Human RECQ1 promotes restart of replication forks reversed by DNA topoisomerase I inhibition. Nat. Struct. Mol. Biol. *20*, 347–354. https://doi.org/10.1038/nsmb.2501.

Betous, R., Mason, A.C., Rambo, R.P., Bansbach, C.E., Badu-Nkansah, A., Sirbu, B.M., Eichman, B.F., and Cortez, D. (2012). SMARCAL1 catalyzes fork regression and Holliday junction migration to maintain genome stability during DNA replication. Genes Dev. *26*, 151–162. https://doi.org/10.1101/gad.178459.111.

Bi, H., Tian, T., Zhu, L., Zhou, H., Hu, H., Liu, Y., Li, X., Hu, F., Zhao, Y., and Wang, G. (2016). Copy number variation of E3 ubiquitin ligase genes in peripheral blood leukocyte and colorectal cancer. Sci. Rep. *6*, 29869. https://doi.org/10.1038/srep29869.

Chambon, P., Weill, J.D., and Mandel, P. (1963). Nicotinamide mononucleotide activation of a new DNA-dependent polyadenylic acid synthesizing nuclear enzyme. Biochem. Biophys. Res. Commun. *11*, 39–43. https://doi.org/10.1016/0006-291x(63)90024-x.

Chappidi, N., Nascakova, Z., Boleslavska, B., Zellweger, R., Isik, E., Andrs, M., Menon, S., Dobrovolna, J., Balbo Pogliano, C., Matos, J., et al. (2020). Fork cleavage-religation cycle and active transcription mediate replication restart after fork stalling at co-transcriptional R-loops. Mol. Cell *77*, 528–541.e8. https://doi.org/10.1016/j.molcel.2019.10.026.

Chen, J., Marechal, V., and Levine, A.J. (1993). Mapping of the p53 and mdm-2 interaction domains. Mol. Cell Biol. *13*, 4107–4114. https://doi.org/10.1128/mcb.13.7.4107-4114.1993.

Chen, Q., Kassab, M.A., Dantzer, F., and Yu, X. (2018). PARP2 mediates branched poly ADP-ribosylation in response to DNA damage. Nat. Commun. *9*, 3233. https://doi.org/10.1038/s41467-018-05588-5.

Debnath, S., and Sharma, S. (2020). RECQ1 helicase in genomic stability and cancer. Genes (Basel) *11*, 622.

Dobbelstein, M., and Levine, A.J. (2020). Mdm2: open questions. Cancer Sci. *111*, 2203–2211. https://doi.org/10.1111/cas.14433.

Dobbelstein, M., Wienzek, S., Konig, C., and Roth, J. (1999). Inactivation of the p53-homologue p73 by the mdm2-oncoprotein. Oncogene *18*, 2101–2106. https://doi.org/10.1038/sj.onc.1202512.

Fåhraeus, R., and Olivares-Illana, V. (2014). MDM2's social network. Oncogene *33*, 4365–4376. https://doi.org/10.1038/onc.2013.410.

Fenech, M., Knasmueller, S., Bolognesi, C., Holland, N., Bonassi, S., and Kirsch-Volders, M. (2020). Micronuclei as biomarkers of DNA damage, aneuploidy, inducers of chromosomal hypermutation and as sources of pro-inflammatory DNA in humans. Mutat. Res. Rev. Mutat. Res. *786*, 108342. https://doi.org/10.1016/j.mrrev.2020.108342.

Follonier, C., Oehler, J., Herrador, R., and Lopes, M. (2013). Friedreich's ataxia-associated GAA repeats induce replication-fork reversal and unusual molecular junctions. Nat. Struct. Mol. Biol. *20*, 486–494. https://doi.org/10.1038/nsmb.2520.

Gatti, M., Imhof, R., Huang, Q., Baudis, M., and Altmeyer, M. (2020). The ubiquitin ligase TRIP12 limits PARP1 trapping and constrains PARP inhibitor efficiency. Cell Rep. *32*, 107985. https://doi.org/10.1016/j.celrep.2020.107985.

Genois, M.M., Gagne, J.P., Yasuhara, T., Jackson, J., Saxena, S., Langelier, M.F., Ahel, I., Bedford, M.T., Pascal, J.M., Vindigni, A., et al. (2021). CARM1 regulates replication fork speed and stress response by stimulating PARP1. Mol. Cell *81*, 784–800.e8. https://doi.org/10.1016/j.molcel.2020.12.010.

Gibbs-Seymour, I., Fontana, P., Rack, J.G.M., and Ahel, I. (2016). HPF1/C4orf27 is a PARP-1-interacting protein that regulates PARP-1 ADP-ribosylation activity. Mol. Cell *62*, 432–442. https://doi.org/10.1016/j.molcel.2016.03.008.

Gibson, B.A., and Kraus, W.L. (2012). New insights into the molecular and cellular functions of poly(ADP-ribose) and PARPs. Nat. Rev. Mol. Cell Biol. *13*, 411–424. https://doi.org/10.1038/nrm3376.

Guilliam, T.A., and Doherty, A.J. (2017). PrimPol-prime time to reprime. Genes (Basel) *8*, 20.

Hafner, A., Bulyk, M.L., Jambhekar, A., and Lahav, G. (2019). The multiple mechanisms that regulate p53 activity and cell fate. Nat. Rev. Mol. Cell Biol. *20*, 199–210. https://doi.org/10.1038/s41580-019-0110-x.

Hampp, S., Kiessling, T., Buechle, K., Mansilla, S.F., Thomale, J., Rall, M., Ahn, J., Pospiech, H., Gottifredi, V., and Wiesmuller, L. (2016). DNA damage tolerance pathway involving DNA polymerase iota and the tumor suppressor p53 regulates DNA replication fork progression. Proc. Natl. Acad. Sci. U S A *113*, E4311–E4319. https://doi.org/10.1073/pnas.1605828113.

Hanzlikova, H., Kalasova, I., Demin, A.A., Pennicott, L.E., Cihlarova, Z., and Caldecott, K.W. (2018). The importance of poly(ADP-ribose) polymerase as a sensor of unligated Okazaki fragments during DNA replication. Mol. Cell *71*, 319–331.e3. https://doi.org/10.1016/j.molcel.2018.06.004.

Helleday, T. (2011). The underlying mechanism for the PARP and BRCA synthetic lethality: clearing up the misunderstandings. Mol. Oncol. *5*, 387–393. https://doi.org/10.1016/j.molonc.2011.07.001.

Henry-Mowatt, J., Jackson, D., Masson, J.Y., Johnson, P.A., Clements, P.M., Benson, F.E., Thompson, L.H., Takeda, S., West, S.C., and Caldecott, K.W. (2003). XRCC3 and Rad51 modulate replication fork progression on damaged vertebrate chromosomes. Mol. Cell *11*, 1109–1117. https://doi.org/10.1016/s1097-2765(03)00132-1.

Higgins, N.P., Kato, K., and Strauss, B. (1976). A model for replication repair in mammalian cells. J. Mol. Biol. *101*, 417–425. https://doi.org/10.1016/0022-2836(76)90156-x.

Ihle, M., Biber, S., Schroeder, I.S., Blattner, C., Deniz, M., Damia, G., Gottifredi, V., and Wiesmuller, L. (2021). Impact of the interplay between stemness features, p53 and pol iota on replication pathway choices. Nucleic Acids Res. *49*, 7457–7475. https://doi.org/10.1093/nar/gkab526.

Ireno, I.C., Wiehe, R.S., Stahl, A.I., Hampp, S., Aydin, S., Troester, M.A., Selivanova, G., and Wiesmuller, L. (2014). Modulation of the poly (ADP-ribose) polymerase inhibitor response and DNA recombination in breast cancer cells by drugs affecting endogenous wild-type p53. Carcinogenesis *35*, 2273–2282. https://doi.org/10.1093/carcin/bgu160.

Itahana, K., Mao, H., Jin, A., Itahana, Y., Clegg, H.V., Lindstrom, M.S., Bhat, K.P., Godfrey, V.L., Evan, G.I., and Zhang, Y. (2007). Targeted inactivation of Mdm2 RING finger E3 ubiquitin ligase activity in the mouse reveals mechanistic insights into p53 regulation. Cancer Cell *12*, 355–366. https://doi.org/10.1016/j.ccr.2007.09.007.

Jungmichel, S., Rosenthal, F., Altmeyer, M., Lukas, J., Hottiger, M.O., and Nielsen, M.L. (2013). Proteome-wide identification of poly(ADP-Ribosyl)ation targets in different genotoxic stress responses. Mol. Cell *52*, 272–285. https://doi.org/10.1016/j.molcel.2013.08.026.

Kang, H.C., Lee, Y.I., Shin, J.H., Andrabi, S.A., Chi, Z., Gagne, J.P., Lee, Y., Ko, H.S., Lee, B.D., Poirier, G.G., et al. (2011). Iduna is a poly(ADP-ribose) (PAR)-dependent E3 ubiquitin ligase that regulates DNA damage. Proc. Natl. Acad. Sci. U S A *108*, 14103–14108. https://doi.org/10.1073/pnas.1108799108.

Kashima, L., Idogawa, M., Mita, H., Shitashige, M., Yamada, T., Ogi, K., Suzuki, H., Toyota, M., Ariga, H., Sasaki, Y., and Tokino, T. (2012). CHFR protein regulates mitotic checkpoint by targeting PARP-1 protein for ubiquitination and degradation. J. Biol. Chem. *287*, 12975–12984. https://doi.org/10.1074/jbc.m111.321828.

Kastenhuber, E.R., and Lowe, S.W. (2017). Putting p53 in context. Cell *170*, 1062–1078. https://doi.org/10.1016/j.cell.2017.08.028.

Kaufmann, S.H., Desnoyers, S., Ottaviano, Y., Davidson, N.E., and Poirier, G.G. (1993). Specific proteolytic cleavage of poly(ADP-ribose) polymerase: an early marker of chemotherapy-induced apoptosis. Cancer Res. *53*, 3976–3985.

Khare, V., and Eckert, K.A. (2002). The proofreading 3′–>5′ exonuclease activity of DNA polymerases: a kinetic barrier to translesion DNA synthesis. Mutat. Res. *510*, 45–54. https://doi.org/10.1016/s0027-5107(02)00251-8.

Klusmann, I., Rodewald, S., Muller, L., Friedrich, M., Wienken, M., Li, Y., Schulz-Heddergott, R., and Dobbelstein, M. (2016). p53 activity results in DNA replication fork processivity. Cell Rep. *17*, 1845–1857. https://doi.org/10.1016/j.celrep.2016.10.036.

Klusmann, I., Wohlberedt, K., Magerhans, A., Teloni, F., Korbel, J.O., Altmeyer, M., and Dobbelstein, M. (2018). Chromatin modifiers Mdm2 and RNF2 prevent RNA: DNA hybrids that impair DNA replication. Proc. Natl. Acad. Sci. U S A *115*, E11311–E11320. https://doi.org/10.1073/pnas.1809592115.

Kobayashi, M., Ishizaki, Y., Owaki, M., Matsumoto, Y., Kakiyama, Y., Hoshino, S., Tagawa, R., Sudo, Y., Okita, N., Akimoto, K., and Higami, Y. (2020). Nutlin-3a suppresses poly (ADP-ribose) polymerase 1 by mechanisms different from conventional PARP1 suppressors in a human breast cancer cell line. Oncotarget *11*, 1653–1665. https://doi.org/10.18632/oncotarget.27581.

Köpper, F., Bierwirth, C., Schön, M., Kunze, M., Elvers, I., Kranz, D., Saini, P., Menon, M.B., Walter, D., Sørensen, C.S., et al. (2013). Damage-induced DNA replication stalling relies on MAPK-activated protein kinase 2 activity. Proc. Natl. Acad. Sci. U S A *110*, 16856–16861. https://doi.org/10.1073/pnas.1304355110.

Kruger, A., Burkle, A., Hauser, K., and Mangerich, A. (2020). Real-time monitoring of PARP1-dependent PARylation by ATR-FTIR spectroscopy. Nat. Commun. *11*, 2174. https://doi.org/10.1038/s41467-020-15858-w.

Kun, E., Kirsten, E., Mendeleyev, J., and Ordahl, C.P. (2004). Regulation of the enzymatic catalysis of poly(ADP-ribose) polymerase by dsDNA, polyamines, Mg^{2+}, Ca^{2+}, histones H1 and H3, and ATP. Biochemistry *43*, 210–216. https://doi.org/10.1021/bi0301791.

Langelier, M.F., Planck, J.L., Roy, S., and Pascal, J.M. (2011). Crystal structures of poly(ADP-ribose) polymerase-1 (PARP-1) zinc fingers bound to DNA. J. Biol. Chem. *286*, 10690–10701. https://doi.org/10.1074/jbc.m110.202507.

Langelier, M.F., Riccio, A.A., and Pascal, J.M. (2014). PARP-2 and PARP-3 are selectively activated by 5′ phosphorylated DNA breaks through an allosteric regulatory mechanism shared with PARP-1. Nucleic Acids Res. *42*, 7762–7775. https://doi.org/10.1093/nar/gku474.

Larsen, S.C., Hendriks, I.A., Lyon, D., Jensen, L.J., and Nielsen, M.L. (2018). Systems-wide analysis of serine ADP-ribosylation reveals widespread occurrence and site-specific overlap with phosphorylation. Cell Rep. *24*, 2493–2505.e4. https://doi.org/10.1016/j.celrep.2018.07.083.

Levine, A.J. (2020). p53: 800 million years of evolution and 40 years of discovery. Cancer *20*, 471–480. https://doi.org/10.1038/s41568-020-0262-1.

Li, Y., Yang, J., Aguilar, A., McEachern, D., Przybranowski, S., Liu, L., Yang, C.Y., Wang, M., Han, X., and Wang, S. (2019). Discovery of MD-224 as a first-in-class, highly potent, and efficacious proteolysis targeting chimera murine double minute 2 degrader capable of achieving complete and durable tumor regression. J. Med. Chem. *62*, 448–466. https://doi.org/10.1021/acs.jmedchem.8b00909.

Liszczak, G., Diehl, K.L., Dann, G.P., and Muir, T.W. (2018). Acetylation blocks DNA damage-induced chromatin ADP-ribosylation. Nat. Chem. Biol. *14*, 837–840. https://doi.org/10.1038/s41589-018-0097-1.

Luzhna, L., Kathiria, P., and Kovalchuk, O. (2013). Micronuclei in genotoxicity assessment: from genetics to epigenetics and beyond. Front. Genet. *4*, 131. https://doi.org/10.3389/fgene.2013.00131.

Matsuda, T., and Cepko, C.L. (2004). Electroporation and RNA interference in the rodent retina *in vivo* and *in vitro*. Proc. Natl. Acad. Sci. U S A *101*, 16–22. https://doi.org/10.1073/pnas.2235688100.

Matsushima, S., Okita, N., Oku, M., Nagai, W., Kobayashi, M., and Higami, Y. (2011). An Mdm2 antagonist, Nutlin-3a, induces p53-dependent and proteasome-mediated poly(ADP-ribose) polymerase1 degradation in mouse fibroblasts. Biochem. Biophys. Res. Commun. *407*, 557–561. https://doi.org/10.1016/j.bbrc.2011.03.061.

Maya-Mendoza, A., Moudry, P., Merchut-Maya, J.M., Lee, M., Strauss, R., and Bartek, J. (2018). High speed of fork progression induces DNA replication stress and genomic instability. Nature *559*, 279–284. https://doi.org/10.1038/s41586-018-0261-5.

Meng, X., Carlson, N.R., Dong, J., and Zhang, Y. (2015). Oncogenic c-Myc-induced lymphomagenesis is inhibited non-redundantly by the p19Arf-Mdm2-p53 and RP-Mdm2-p53 pathways. Oncogene *34*, 5709–5717. https://doi.org/10.1038/onc.2015.39.

Merchut-Maya, J.M., Bartek, J., and Maya-Mendoza, A. (2019). Regulation of replication fork speed: mechanisms and impact on genomic stability. DNA Repair (Amst) *81*, 102654. https://doi.org/10.1016/j.dnarep.2019.102654.

Meza-Sosa, K.F., Miao, R., Navarro, F., Zhang, Z., Zhang, Y., Hu, J.J., Hartford, C.C.R., Li, X.L., Pedraza-Alva, G., Perez-Martinez, L., et al. (2022). SPARCLE, a p53-induced lncRNA, controls apoptosis after genotoxic stress by promoting PARP-1 cleavage. Mol. Cell *82*, 785–802.e10. https://doi.org/10.1016/j.molcel.2022.01.001.

Montes de Oca Luna, M., Wagner, D.S., Lozano, G.R., Wagner, D.S., and Lozano, G. (1995). Rescue of early embryonic lethality in mdm2-deficient mice by deletion of p53. Nature *378*, 203–206. https://doi.org/10.1038/378203a0.

Mouron, S., Rodriguez-Acebes, S., Martinez-Jimenez, M.I., Garcia-Gomez, S., Chocron, S., Blanco, L., and Mendez, J. (2013). Repriming of DNA synthesis at stalled replication forks by human PrimPol. Nat. Struct. Mol. Biol. *20*, 1383–1389. https://doi.org/10.1038/nsmb.2719.

Nagai, W., Okita, N., Matsumoto, H., Okado, H., Oku, M., and Higami, Y. (2012). Reversible induction of PARP1 degradation by p53-inducible cis-imidazoline compounds. Biochem. Biophys. Res. Commun. *421*, 15–19. https://doi.org/10.1016/j.bbrc.2012.03.091.

Neelsen, K.J., and Lopes, M. (2015). Replication fork reversal in eukaryotes: from dead end to dynamic response. Nat. Rev. Mol. Cell Biol. *16*, 207–220. https://doi.org/10.1038/nrm3935.

Oliner, J.D., Pietenpol, J.A., Thiagalingam, S., Gyuris, J., Kinzler, K.W., and Vogelstein, B. (1993). Oncoprotein MDM2 conceals the activation domain of tumour suppressor p53. Nature *362*, 857–860. https://doi.org/10.1038/362857a0.

Paes Dias, M., Tripathi, V., van der Heijden, I., Cong, K., Manolika, E.M., Bhin, J., Gogola, E., Galanos, P., Annunziato, S., Lieftink, C., et al. (2021). Loss of nuclear DNA ligase III reverts PARP inhibitor resistance in BRCA1/53BP1 double-deficient cells by exposing ssDNA gaps. Mol. Cell *81*, 4692–4708.e9. https://doi.org/10.1016/j.molcel.2021.09.005.

Palazzo, L., Leidecker, O., Prokhorova, E., Dauben, H., Matic, I., and Ahel, I. (2018). Serine is the major residue for ADP-ribosylation upon DNA damage. Elife *7*, e34334.

Pettitt, S.J., Krastev, D.B., Brandsma, I., Drean, A., Song, F., Aleksandrov, R., Harrell, M.I., Menon, M., Brough, R., Campbell, J., et al. (2018). Genome-wide and high-density CRISPR-Cas9 screens identify point mutations in PARP1 causing PARP inhibitor resistance. Nat. Commun. *9*, 1849. https://doi.org/10.1038/s41467-018-03917-2.

Quinet, A., Lemacon, D., and Vindigni, A. (2017). Replication fork reversal: players and guardians. Mol. Cell *68*, 830–833. https://doi.org/10.1016/j.molcel.2017.11.022.

Quinet, A., Tirman, S., Jackson, J., Svikovic, S., Lemacon, D., Carvajal-Maldonado, D., Gonzalez-Acosta, D., Vessoni, A.T., Cybulla, E., Wood, M., et al. (2020). PRIMPOL-mediated adaptive response suppresses replication fork reversal in BRCA-deficient cells. Mol. Cell *77*, 461–474.e9. https://doi.org/10.1016/j.molcel.2019.10.008.

Ray Chaudhuri, A., Hashimoto, Y., Herrador, R., Neelsen, K.J., Fachinetti, D., Bermejo, R., Cocito, A., Costanzo, V., and Lopes, M. (2012). Topoisomerase I poisoning results in PARP-mediated replication fork reversal. Nat. Struct. Mol. Biol. *19*, 417–423. https://doi.org/10.1038/nsmb.2258.

Ray Chaudhuri, A., and Nussenzweig, A. (2017). The multifaceted roles of PARP1 in DNA repair and chromatin remodelling. Nat. Rev. Mol. Cell Biol. *18*, 610–621. https://doi.org/10.1038/nrm.2017.53.

Rayburn, E., Zhang, R., He, J., and Wang, H. (2005). MDM2 and human malignancies: expression, clinical pathology, prognostic markers, and implications for chemotherapy. Curr. Cancer Drug Targets *5*, 27–41. https://doi.org/10.2174/1568009053332636.

Roth, J., Dobbelstein, M., Freedman, D.A., Shenk, T., and Levine, A.J. (1998). Nucleo-cytoplasmic shuttling of the hdm2 oncoprotein regulates the levels of the p53 protein via a pathway used by the human immunodeficiency virus rev protein. EMBO J. *17*, 554–564. https://doi.org/10.1093/emboj/17.2.554.

Roy, S., Tomaszowski, K.H., Luzwick, J.W., Park, S., Li, J., Murphy, M., and Schlacher, K. (2018). p53 orchestrates DNA replication restart homeostasis by suppressing mutagenic RAD_{52} and POLtheta pathways. Elife *7*, e31723.

Saldivar, J.C., Cortez, D., and Cimprich, K.A. (2017). The essential kinase ATR: ensuring faithful duplication of a challenging genome. Nat. Rev. Mol. Cell Biol. *18*, 622–636. https://doi.org/10.1038/nrm.2017.67.

Sane, S., and Rezvani, K. (2017). Essential roles of E3 ubiquitin ligases in p53 regulation. Int. J. Mol. Sci. *18*, 442.

Schmid, J.A., Berti, M., Walser, F., Raso, M.C., Schmid, F., Krietsch, J., Stoy, H., Zwicky, K., Ursich, S., Freire, R., et al. (2018). Histone ubiquitination by the DNA damage response is required for efficient DNA replication in unperturbed S phase. Mol. Cell *71*, 897–910.e8. https://doi.org/10.1016/j.molcel.2018.07.011.

Simoneau, A., Xiong, R., and Zou, L. (2021). The trans cell cycle effects of PARP inhibitors underlie their selectivity toward BRCA1/2-deficient cells. Genes Dev. *35*, 1271–1289. https://doi.org/10.1101/gad.348479.121.

Soldani, C., Lazze, M.C., Bottone, M.G., Tognon, G., Biggiogera, M., Pellicciari, C.E., and Scovassi, A.I. (2001). Poly(ADP-ribose) polymerase cleavage during apoptosis: when and where? Exp. Cell Res. *269*, 193–201. https://doi.org/10.1006/excr.2001.5293.

Tibbetts, R.S., Brumbaugh, K.M., Williams, J.M., Sarkaria, J.N., Cliby, W.A., Shieh, S.Y., Taya, Y., Prives, C., and Abraham, R.T. (1999). A role for ATR in the DNA damage-induced phosphorylation of p53. Genes Dev. *13*, 152–157. https://doi.org/10.1101/gad.13.2.152.

Tirman, S., Quinet, A., Wood, M., Meroni, A., Cybulla, E., Jackson, J., Pegoraro, S., Simoneau, A., Zou, L., and Vindigni, A. (2021). Temporally distinct post-replicative repair mechanisms fill PRIMPOL-dependent ssDNA gaps in human cells. Mol. Cell *81*, 4026–4040.e8. https://doi.org/10.1016/j.molcel.2021.09.013.

Tuduri, S., Crabbe, L., Conti, C., Tourriere, H., Holtgreve-Grez, H., Jauch, A., Pantesco, V., De Vos, J., Thomas, A., Theillet, C., et al. (2009). Topoisomerase I suppresses genomic instability by preventing interference between replication and transcription. Nat. Cell Biol. *11*, 1315–1324. https://doi.org/10.1038/ncb1984.

Vallerga, M.B., Mansilla, S.F., Federico, M.B., Bertolin, A.P., and Gottifredi, V. (2015). Rad51 recombinase prevents Mre11 nuclease-dependent degradation and excessive PrimPol-mediated elongation of nascent DNA after UV irradiation. Proc. Natl. Acad. Sci. U S A *112*, E6624–E6633. https://doi.org/10.1073/pnas.1508543112.

Vassilev, L.T., Vu, B.T., Graves, B., Carvajal, D., Podlaski, F., Filipovic, Z., Kong, N., Kammlott, U., Lukacs, C., Klein, C., et al. (2004). In vivo activation of the p53 pathway by small-molecule antagonists of MDM2. Science *303*, 844–848. https://doi.org/10.1126/science.1092472.

Wade, M., Li, Y.C., and Wahl, G.M. (2013). MDM2, MDMX and p53 in oncogenesis and cancer therapy. Cancer *13*, 83–96. https://doi.org/10.1038/nrc3430.

Wienken, M., Dickmanns, A., Nemajerova, A., Kramer, D., Najafova, Z., Weiss, M., Karpiuk, O., Kassem, M., Zhang, Y., Lozano, G., et al. (2016). MDM2 associates with Polycomb repressor complex 2 and enhances stemness-promoting chromatin modifications independent of p53. Mol. Cell *61*, 68–83. https://doi.org/10.1016/j.molcel.2015.12.008.

Wienken, M., Moll, U.M., and Dobbelstein, M. (2017). Mdm2 as a chromatin modifier. J. Mol. Cell Biol. *9*, 74–80. https://doi.org/10.1093/jmcb/mjw046.

Wohlberedt, K., Klusmann, I., Derevyanko, P.K., Henningsen, K., Choo, J.A.M.Y., Manzini, V., Magerhans, A., Giansanti, C., Eischen, C.M., Jochemsen, A.G., and Dobbelstein, M. (2020). Mdm4 supports DNA replication in a p53-independent fashion. Oncogene *39*, 4828–4843. https://doi.org/10.1038/s41388-020-1325-1.

Yeo, C.Q.X., Alexander, I., Lin, Z., Lim, S., Aning, O.A., Kumar, R., Sangthongpitag, K., Pendharkar, V., Ho, V.H.B., and Cheok, C.F. (2016). p53 maintains genomic stability by preventing interference between transcription and replication. Cell Rep. *15*, 132–146. https://doi.org/10.1016/j.celrep.2016.03.011.

Zellweger, R., Dalcher, D., Mutreja, K., Berti, M., Schmid, J.A., Herrador, R., Vindigni, A., and Lopes, M. (2015). Rad51-mediated replication fork reversal is a global response to genotoxic treatments in human cells. J. Cell Biol. *208*, 563–579. https://doi.org/10.1083/jcb.201406099.

Zellweger, R., and Lopes, M. (2018). Dynamic architecture of eukaryotic DNA replication forks *in vivo*, visualized by electron microscopy. Methods Mol. Biol. *1672*, 261–294. https://doi.org/10.1007/978-1-4939-7306-4_19.

STAR★METHODS

KEY RESOURCES TABLE

REAGENT or RESOURCE	SOURCE	IDENTIFIER
Antibodies		
FLAG M2-Peroxidase (HRP) (WB)	Sigma-Aldrich	Cat# A8592; RRID:AB_439702
DYKDDDDK Tag (IF)	Thermo Fisher Scientific	Cat# 740001; RRID:AB_2610628
MDM2 IF2 (WB, IF, PLA, coIP)	Millipore	Cat# OP46-100UG; RRID:AB_564803
p53 DO-1 (WB)	Santa Cruz Biotechnology	Cat# sc-126; RRID:AB_628082
p53 DO-1 (WB)	Millipore	Cat# OP43-20UG; RRID:AB_564968
GST (WB)	Sigma-Aldrich	Cat# SAB5300159
PARP1 (co-IP)	Enzo Life Sciences	Cat# ALX-210-302-R100; RRID:AB_2052175
PARP1 (WB, IF)	Abcam	Cat# ab227244
Phopho-Chk1 (Ser317) (WB)	Cell Signaling Technology	Cat# 2344; RRID:AB_331488
Chk1 (WB)	Cell Signaling Technology	Cat# 2360; RRID:AB_2080320
Phopho-Chk1 (Ser345) (WB)	Cell Signaling Technology	Cat# 2348; RRID:AB_331212
phospho-histone H2A.x (ser139) (WB, IF)	Cell Signaling Technology	Cat# 9718, RRID:AB_2118009
p21 (WB)	Cell Signaling Technology	Cat# 2947; RRID:AB_823586
Beta-Actin (WB)	Abcam	Cat# ab6276; RRID:AB_2223210
GAPDH (WB)	Abcam	Cat# ab8245; RRID:AB_2107448
HSC70 (WB)	Santa Cruz Biotechnology	Cat# sc-7298; RRID:AB_627761
RECQ1 (WB)	Bethyl	Cat# A300-761A-T; RRID:AB_2632119
PRIMPOL (WB)	J. Mendez (Mouron et al., 2013)	N/A
Poly/Mono-ADP Ribose (WB, IF)	Cell Signaling Technology	Cat# 83732; RRID:AB_2749858
Poly(ADP-Ribose)Polymer (IF)	Abcam	Cat# ab14459, RRID:AB_301239
Mouse IgG (co-IP)	Abcam	Cat# ab37355; RRID:AB_2665484
Rabbit IgG (co-IP)	Abcam	Cat# ab171870; RRID:AB_2687657
B-Galactosidase (co-IP)	Promega	Cat# Z3781; RRID:AB_430877
IdU/BrdU (fiber assay)	BD Biosciences	Cat# 347580; RRID:AB_10015219
CldU/BrdU (fiber assay)	Abcam	Cat# ab6326; RRID:AB_305426
Alexa Fluor 488 goat anti-mouse	Thermo Fisher Scientific	Cat# A-11029; RRID:AB_2534088
Alexa Fluor 555 goat Anti-rat	Thermo Fisher Scientific	Cat# A-21434; RRID:AB_2535855
Alexa Flour 647 anti-mouse	Thermo Fisher Scientific	Cat# A-21235; RRID:AB_2535804
Alexa Flour 546 anti-rabbit	Thermo Fisher Scientific	Cat# A10040; RRID:AB_2534016
Donkey anti-mouse IgG, HRP conj.	Jackson ImmunoResearch Labs	Cat# 715-036-150; RRID:AB_2340773
Donkey anti-rabbit IgG, HRP conj.	Jackson ImmunoResearch Labs	Cat# 711-036-152; RRID:AB_2340590
Goat anti-rat IgG, HRP conjugated	Jackson ImmunoResearch Labs	Cat# 112-035-003; RRID:AB_2338128
Chemicals, peptides, and recombinant proteins		
Nutlin-3a	BOC Sciences	Cat# B0084-425358
Camptothecin	Sigma-Aldrich	Cat# C9911
PDD 00017273, PARGi	Tocris	Cat# 5952
MI-1061	Hoelzel	Cat# HY-125858
MD-224	Hoelzel	Cat# HY-114312
Olaparib, PARPi	Selleckchem	Cat# S1060
MG-132	Millipore	Cat# 474791
ABT-737	Selleckchem	Cat# ABT-737
Z-VAD-FMK (zVAD)	Enzo Life Sciences	Cat# ALX-260-020-M005
5-Chloro-2′-deoxyuridine	Sigma-Aldrich	Cat# C6891
5-Iodo-2′-deoxyuridine	Sigma-Aldrich	Cat# I7125

(*Continued on next page*)

Continued

REAGENT or RESOURCE	SOURCE	IDENTIFIER
5-ethynyl-2′-deoxyuridine	Thermo Fisher Scientific	Cat# A10044
Hygromycin B	Thermo Fisher Scientific	Cat# 10687010
Trizol	Life Technologies	Cat# 15596018
Protein G Sepharose	GE Healthcare Life Science	Cat# 17061805
5-ethynyl-2′-deoxyuridine	Thermo Fisher Scientific	Cat# A10044
AlexaFlour594 picolyl-azide	Jena Biosciences	Cat# CLK-1296-1
CuSO4	Jena Biosciences	Cat# CLK-MI004
Tris(3-hydroxypropyltriazolylmethyl)amine	Jena Biosciences	Cat# 762342
Na-Ascorbate	Jena Biosciences	Cat# CLK-MI005
Propidium Iodide (PI)	Thermo Fisher Scientific	Cat# P3566
Hoechst 33342	Thermo Fisher Scientific	Cat# H3570
DAPI	Thermo Fisher Scientific	Cat# 62248
Cycloheximide	Sigma-Aldrich	Cat# C7698
Thymidine	Sigma-Aldrich	Cat# 855006
PARP1 (human recombinant protein)	Enzo Life Sciences	Cat# ALX-201-063-C020
MDM2 (human recombinant protein)	Abcam	Cat# ab82080
Critical commercial assays		
Duolink In Situ Detection Reagents	Sigma-Aldrich	Cat# DUO92007
Lipofectamine 3000 transfection reagent	Thermo Fisher Scientific	Cat# L3000015
Annexin V-FITC Apoptosis Detection Kit	Thermo Fisher Scientific	Cat# ICT-9124
Experimental models: Cell lines		
Human: H1299	ATCC	Cat# CRL-5803; RRID:CVCL_0060
Human: RPE	ATCC	Cat# CRL-4000; RRID:CVCL_4388
Human: MCF7	ATCC	Cat# HTB-22; RRID:CVCL_0031
Human: SJSA-1	ATCC	Cat# CRL-2098; RRID:CVCL_1697
Oligonucleotides		
siRNA PRIMPOL#1	Thermo Fisher Scientific	Cat# s47416
siRNA PRIMPOL#2	Thermo Fisher Scientific	Cat# s47417
siRNA PRIMPOL#3	Thermo Fisher Scientific	Cat# s47418
siRNA RECQ1#1	Thermo Fisher Scientific	Cat# s11903
siRNA RECQ1#2	Thermo Fisher Scientific	Cat# s11904
siRNA MDM2 #1	Thermo Fisher Scientific	Cat# s8629
siRNA MDM2 #2	Thermo Fisher Scientific	Cat# s224037
siRNA MDM2 #3	Thermo Fisher Scientific	Cat# s4390828
siRNA PUMA	Thermo Fisher Scientific	Cat# s25841
siRNA Scrambled #1	Thermo Fisher Scientific	Cat# s4390844
siRNA Scrambled #2	Thermo Fisher Scientific	Cat# s4390847
36B4 forward primer 5′-GATTGGCTACCCAACTGTTG-3′	This study	N/A
36B4 reverse primer 5′-CAGGGGCAGCAGCCACAAA-3′	This study	N/A
PUMA forward primer 5′-GCCAGATTTGTGAGACAAGAGG-3′	This study	N/A
PUMA reverse primer 5′-CAGGCACCTAATTGGGCTC-3′	This study	N/A
Recombinant DNA		
pCMV6-XL5 empty control (plasmid)	Origene	Cat# PCMV6XL5
pCMV MDM2 (plasmid)	B. Vogelstein (Oliner et al., 1993)	N/A
pCMV-PARP1-3xFlag-WT (plasmid)	T.W. Muir (Liszczak et al., 2018)	Addgene Cat# 111575

(*Continued on next page*)

Continued

REAGENT or RESOURCE	SOURCE	IDENTIFIER
pcHDM Δ222-325 (plasmid)	J. Chen (Chen et al., 1993)	N/A
pcHDM Δ58-90 (plasmid)	J. Chen (Chen et al., 1993)	N/A
pCMV MDM2 mtRING (plasmid)	B. Vogelstein (Roth et al., 1998)	N/A
pCMV MDM2 C305F (plasmid)	Y. Zhang (Meng et al., 2015)	N/A
pCMV MDM2 6-339	J. Chen (Chen et al., 1993)	N/A
pCMV-GFP	L. Cepko (Matsuda and Cepko, 2004)	Addgene Cat# 11153
Software and algorithms		
Prism v. 5.04	GraphPad	N/A
Prism v. 9.00	GraphPad	N/A
ImageJ	NIH	N/A
Fiji v2.0.0	NIH	N/A
Image Lab v. 5.2.1	Bio Rad	N/A

RESOURCE AVAILABILITY

Lead contact

Further information and requests for resources and reagents should be directed to and will be fulfilled by the lead contact, Matthias Dobbelstein (mdobbel@uni-goettingen.de).

Materials availability

This study did not generate new unique reagents.

Data and code availability

- All data reported in this paper will be shared by the lead contact upon request.
- This paper does not report original code.
- Any additional information required to reanalyze the data reported in this paper is available from the lead contact upon request.

EXPERIMENTAL MODEL AND SUBJECT DETAILS

Cell culture

The human non-small cell lung cancer cell line H1299, the human osteosarcoma cell line SJSA-1, and the human breast cancer cell line MCF-7 were maintained in Dulbecco's modified Eagle's medium (DMEM, 31600091, Thermo Fisher Scientific) supplemented with 10% Fetal Bovine Serum (ACSM0190, Anprotec), 50 U/mL Penicillin, 50 μg/mL Streptomycin (15140122, GIBCO) and 2 mM Glutamine (25030024, GIBCO). The non-tumorigenic human retinal pigment epithelial RPE cells were cultured in DMEM as above, supplemented with 10 μg/mL Hygromycin (10687010, Thermo Fisher Scientific) for hTERT activation. Hygromycin was removed from culturing medium 24 h prior to experiments. All cell lines were cultured at 37°C with 5% CO2 and routinely tested for mycoplasma contamination.

Cells were treated with Nutlin-3a (B0084-425358, BOC Sciences), Camptothecin (C9911, Sigma-Aldrich), PDD 00017273 (5952, Tocris), MI-1061 (HY-125858, Hölzel), MD-224 (HY-114312, Hölzel), Olaparib (S1060, Selleckchem), MG-132 (474791, Millipore), ABT-737 (S1002, Selleckchem), zVAD (ALX-260-020-M005, Enzo Life Sciences), cycloheximide (62248, Thermo Fisher Scientific). Double thymidine block for cell cycle synchronization was performed adding 2 mM of thymidine (855006, Sigma-Aldrich) for 16 h, followed by thymidine wash out. After 8 h a second thymidine treatment (2 mM, 16 h) was applied.

Transfections were performed using Lipofectamine 3000 transfection reagent (Thermo Fisher Scientific) according to manufacturer instructions. Cells were reverse transfected with final siRNA concentration of 10 nM siRNA against PRIMPOL (#1 s47416, #2 s47417, #3 s47418, Thermo Fisher Scientific), RECQ1 (#1 s11903, #2 s11904, Thermo Fisher Scientific), MDM2 (#1 s8629, #2 s224037, #3 4390828, Thermo Fisher Scientific), PUMA (s25841, Thermo Fisher Scientific) or scrambled siRNA controls (s4390844, s4390847, Thermo Fisher Scientific). Cells were transfected to overexpress the following plasmids: pCMV6-XL5 empty control (Origene, #PCMV6XL5), pCMV MDM2 (Oliner et al., 1993), pCMV-PARP1-3xFlag-WT (Addgene, #111575) (Liszczak et al., 2018), pcHDM Δ222-325 (Chen et al., 1993), pcHDM Δ58-90 (Chen et al., 1993), pCMV MDM2 mtRING (Roth et al., 1998), pCMV MDM2 C305F (Meng et al., 2015), pCMV MDM2 6-339 (Chen et al., 1993), pCMV GFP (Addgene, #11153) (Matsuda and Cepko, 2004). Medium was refreshed after 6 h, and cells were harvested for experiments 24 and 48 h post-transfection.

METHOD DETAILS

DNA fiber assay

DNA fiber assays were carried out as previously described (Köpper et al., 2013). Newly synthetized DNA was labeled with 5-chloro-2-deoxyuridine (CldU, 25 μM, Sigma-Aldrich) for 20 min, followed by 5-iodo-2-deoxyuridine (IdU, 25 μM, Sigma-Aldrich) for 1 h. Cells were lysed by spreading buffer (200 mM Tris pH 7.4, 50 mM EDTA, 0.5% SDS), and DNA fibers were spread on glass slides prior to fixation in a solution of methanol and acetic acid (Roth). After DNA denaturation by 2.5 M HCl (Sigma-Aldrich), CldU- and IdU-labelled tracts were detected by immunostaining, using antibodies that were originally developed against BrdU. These were mouse anti-BrdU (B44, BD Biosciences) and rat anti-BrdU (BU1/75, ICR1, Abcam). Then, Alexa Fluor 488-conjugated goat anti-mouse IgG and Alexa Fluor 555-conjugated goat anti-rat IgG (Thermo Fisher Scientific) were used as secondary antibodies. DNA fibers were visualized by fluorescence microscopy (Axio Scope A1 microscope, Zeiss) and analyzed with ImageJ.

Immunoblot analysis

Cells were harvested in protein lysis buffer, i.e. 20 mM Tris-HCl pH 7.5, 10 mM NaCl, 1 mM NaCl, 10 mM EDTA, 1% Triton-X 100, 1% deoxycholate salt, 0.1% SDS, 2 M urea, and protease inhibitors (pepstatin, leupeptin hemisulfate, aprotinin, AppliChem). The samples were briefly sonicated to disrupt DNA-protein complexes. Total protein concentration was measured using a BCA protein assay kit (Thermo Fisher Scientific). The samples were boiled in Laemmli buffer at 95°C for 5 min, and equal amounts of proteins were separated by SDS-PAGE. Subsequently, proteins were transferred onto a nitrocellulose membrane, blocked in 5% (w/v) non-fat milk (Roth) in TBS containing 0.1% Tween-20 (AppliChem) for 1 h and incubated with the primary antibodies at 4°C overnight.

Membranes were then incubated with peroxidase (HRP)-conjugated secondary antibodies (Jackson ImmunoResearch Labs) and the proteins were detected using either Super Signal West Femto Maximum Sensitivity Substrate (Thermo Fisher Scientific) or Immobilion Western Substrate (Millipore).

Co-immunoprecipitation (Co-IP)

For *in vitro* co-IP, purified proteins were incubated at 4°C overnight on a rotator in co-IP buffer (50 mM Tris, pH 7.5, 300 mM NaCl, 1% NP-40), followed by overnight incubation with 2 μg anti-PARP1 antibody and 30 min incubation with Protein G Sepharose (GE Healthcare) (4°C). Beads were washed 5 times with co-IP buffer.

For *in vivo* Co-IP, cells were washed with cold PBS followed by lysis in Co-IP Buffer (50 mM Tris, pH 7.5, 300 mM NaCl, 1% NP-40), supplemented with protease inhibitors (11836153001, Roche). Homogenized cell lysate was precleared with Protein G Sepharose (GE Healthcare), followed by overnight incubation with 2 μg of the precipitating antibody. Samples were then incubated with Protein G Sepharose for coupling with the primary antibody for 2 h (4°C) and then washed 8 times with Co-IP Buffer.

For both *in vitro* and *in vivo* co-IP, beads were re-suspended in 3x Laemmli Buffer and boiled for 10 min at 95°C to release precipitated protein. Immunoprecipitates were subjected to SDS-PAGE and immunoblot analysis. The following antibodies were used for all precipitations: PARP1 (ALX-210-302-R100, Enzo Life Sciences), MDM2 (IF2 OP46, Millipore), IgG rabbit (ab171870, Abcam), β-galactosidase mouse (Z378B, Promega).

RNA extraction, reverse transcription, and real time quantitative PCR

Total RNA was extracted from cells using TRIzol® (Invitrogen). mRNA was reverse-transcribed using oligo-dT and random nonamers as primers, followed by qRT-PCR analysis using SYBR Green (Invitrogen). Gene expression levels were normalized to the mRNA from the gene 36B4, and the analysis was conducted using the ΔΔCt method.

Immunofluorescence staining

Cells were grown in 8-well permanox slides (177445, Nunc) fixed with 3.7% PFA in PBS for 30 min before being permeabilized with 0.5% Triton-X-100 (AppliChem) in PBS for 30 min. Cells were treated with blocking buffer (10% FCS in 0.1% Tween-PBS) for 10 min at room temperature, followed by incubation with primary antibodies at 4°C, overnight. After washing with PBS (3 × 10 min), slides were incubated with secondary antibody and 4′,6-diamidino-2-phenylindole (DAPI, Sigma-Aldrich) for 1 h at room temperature. Following washes in PBS (3 × 10 min), the chambers were removed, and slides were mounted onto coverslips using fluorescent mounting medium (S302380-2, DakoCytomation). Images were acquired using a Zeiss Axio Scope.A1 fluorescence microscope equipped with an Axio Cam MRc/503 camera using a 40x magnification, and further analyzed with ImageJ. The DAPI signal was used to create binary images (segmentation) to define the nuclear area as region of interest (ROI). These ROIs were then used to quantify the nuclear signal of the other channels. Single nuclei mean gray values are represented on dot plots.

Proximity ligation assay

Cells were grown in 12-well slides (81201, Ibidi) and following treatment or transfection, cells were fixed and permeabilized as described above, and subjected to the PLA assay using the Duolink In Situ Detection Reagents Orange (DUO92007, Sigma-Aldrich) in a humid chamber. Briefly, after blocking samples were incubated with primary antibodies anti-MDM2 antibody (IF2 OP46, Millipore), anti-PARP1 antibody (ab22724, Abcam) overnight at 4°C. This was followed by incubation with PLA probes (Duolink™ In Situ PLA® Probe Anti-Mouse PLUS DUO92001, Duolink™ In Situ PLA® Probe Anti-Rabbit MINUS DUO92005) for 1 h, at 37°C while

shaking. Ligase was then added to hybridized PLA probes to generate a closed circle (60 min at 37°C), before DNA amplification for 100 min at 37°C while shaking. After performing the PLA protocol, cells were counterstained with DAPI, the plastic chambers were removed and the slides were mounted onto coverslips using fluorescent mounting medium (S302380-2, DakoCytomation). Images were acquired and analyzed as described for immunofluorescence staining.

EdU incorporation and staining for identification of cells in S-phase

EdU (5-ethynyl-2′-deoxyuridine, Thermo Fisher Scientific) was diluted in DMSO to a final concentration of 10 mM. Cells were grown and transfected in 8-well permanox slides (177445, Nunc) and EdU was added to growing cultures to a final concentration of 10 μM for 30 min. Following fixation with 3.7% PFA in PBS (30 min, at room temperature) and permeabilization with 0.5% Triton-X-100 in PBS (30 min, at room temperature), the following reagents were added to 100 mM Na-phosphate buffer (pH 7) in order to perform the click chemistry reaction: 5 μM AlexaFlour594 picolyl-azide (Jena Biosciences, #CLK-1296-1), 100 μM CuSO4 (Jena Biosciences, #CLK-MI004) in 500 μM Tris(3-hydroxypropyltriazolylmethyl)amine (THPTA; Sigma-Aldrich, #762342), 5 mM Na-Ascorbate (Jena Biosciences, #CLK-MI005). Click chemistry was performed at RT, for 1 h, followed by 3 × 10 min washes in PBS. Immunofluorescence was consecutively carried on as described above.

Cell death and cell proliferation assays

Cell death was studied by performing Annexin V-Propidium Iodide (PI) staining. Annexin V-FITC Apoptosis Detection Kit (ICT-9124, Biozol) was used according to manufacturer instructions, with the addition of PI (10 μg/mL, Thermo Fisher Scientific), Hoechst 33342 (100 μg/mL, Thermo Fisher Scientific). For cellular proliferation analysis cells were plated at low density (2000 cells/well) in 96-well plates (CLS3603, Merck). Cellular proliferation was measured by bright field microscopy at the indicated time points quantifying the percentage of surface occupied by adherent cells over the total surface. For imaging and analysis Celigo Adherent Cell Cytometer (Nexcelom Bioscience) was used.

Electron microscopy

Asynchronous and subconfluent H1299 cells were transfected with the empty vector pCMV-XL5 (control) or the expression plasmid pCMV-MDM2 WT. After 24 h, the cells were treated with 200 nM of CPT (Sigma-Aldrich) for 1 h. Asynchronous and subconfluent SJSA-1 cells were treated with Nutlin (20uM, BOC Sciences) or DMSO for 6 h. CPT was then added at the concentration of 500 nM for 1 h. Cells were collected, resuspended in ice-cold PBS and crosslinked with 4,5′,8-trimethylpsoralen (10 μg/mL final concentration), followed by irradiation pulses with 365 nm monochromatic UV light (UV Stratalinker 1800; Agilent Technologies). For DNA extraction, cells were lysed (1.28 M sucrose, 40 mM Tris-HCl [pH 7.5], 20 mM MgCl2, and 4% Triton X-100; Qiagen) and digested (800 mM guanidine–HCl, 30 mM Tris-HCl [pH 8.0], 30 mM EDTA [pH 8.0], 5% Tween-20, and 0.5% Triton X-100) at 50°C for 2 h in the presence of 1 mg/mL proteinase K. The DNA was purified using chloroform/isoamyl alcohol (24:1) and precipitated in 0.7 volume of isopropanol. Finally, the DNA was washed with 70% EtOH and resuspended in 200 μL TE (Tris-EDTA) buffer. 100 U of restriction enzyme (PvuII high fidelity, New England Biolabs) were used to digest 6 μg of mammalian genomic DNA for 5 h. RNase A (R5503, Sigma–Aldrich) to a final concentration of 250 ug/mL was added for the last 2 h of this incubation. The digested DNA was purified using the Silica Bead DNA Gel Extraction Kit (Thermo Fisher Scientific). The Benzyldimethylalkylammonium chloride (BAC) method was used to spread the DNA on the water surface and then load it on carbon-coated 400-mesh nickel grids (G2400 N, Plano Gmbh). Subsequently, DNA was coated with platinum using a High Vacuum Evaporator BAF060 (Leica). The grids were scanned using a transmission electron microscope (Tecnai G2 Spirit; FEI; LaB6 filament; high tension $\leq$120 kV) and images were acquired with a side mount charge-coupled device camera (2600 × 4000 pixels; Orius 1000; Gatan, Inc.) and processed with DigitalMicrograph Version 1.83.842 (Gatan, Inc.). For each experimental condition at least 70 DNA replication fork molecules were analyzed in two different biological replicates by using ImageJ.

GST pull-down assay

For *in vitro* MDM2-PARP1 binding assays, 1.5 μM of GST-SUMO tagged HA-MDM2 or GST (as control) were incubated 10 min on ice in binding buffer (2 mM $MgCl_2$ and 1 mM DTT) with 2 μM of recombinant PARP1 prior to the addition of 10 μL Glutathion-Sepharose® 4B (17-0756-01, Cytiva) pre-equilibrated in binding buffer. The mixtures were incubated for 3 h at room temperature in an overhead shaker, followed by 4 washing steps with 200 μL washing buffer (1x PBS, 1 mM DTT). Bound proteins were eluted twice by incubating beads with 25 μL elution buffer (1x PBS and 40 mM GSH pH 7.6). Eluates were combined and electrophoresed on 10% SDS gels followed by Western blot analysis against p53 (DO-I Calbiochem Cat: OP43-20UG (ASK07) Lot: 489202-25), GST (SAB5300159, Sigma-Aldrich) or PARP1 (ALX-804-211-R050, F1-23 Enzo Life Sciences). For generation of recombinant PARP1, His-tagged PARP1 was expressed and purified as previously described (Kruger et al., 2020; Langelier et al., 2011).

In vitro ubiquitination assay

0.25 μM p53 or PARP1 were incubated with 100 nM UBA1, 0.5 μM UbcH5b, 0.35 μM MDM2 in 25 mM Tris- HCl pH 7.5, 50 mM NaCl, 1 mM DTT, 2 mM ATP, 2 mM $MgCl_2$ at 37°C for the times indicated. Reactions were started by the addition of 39 μM Ub and stopped by the addition of 5x Laemmli stop buffer. Reaction mixtures were subjected to SDS-PAGE followed by Western blot analysis against p53 (DO-I Millipore, OP43-20UG (ASK07) Lot: 489202-25) or PARP1 (ALX-804-211-R050, F1-23 Enzo Life Sciences).

QUANTIFICATION AND STATISTICAL ANALYSIS

Statistics

Statistical testing was performed using GraphPad Prism Software. Unpaired Student's t-test was used for statistical analysis of immunofluorescence staining, PLA, Cycloheximide (CHX) chase analysis, cell death, cell proliferation analysis. For DNA fiber assays and fork symmetry analysis, Mann–Whitney U test was used. Ns, not significant; *p-value $\leq$ 0.05; **p-value $\leq$ 0.01; ***p-value $\leq$ 0.001; ****p-value < 0.0001. All of the statistical details can be found in the figure legends.

Immunofluorescence staining quantification

Fluorescence intensity quantification was performed in an automated fashion using the following macro on Fiji:

```
#prior running the macro, open all RAW files (.czi) and use command "Images to Stack".
open("Stack of all images from same experiment, DAPI + POI IF");
run("Subtract Background…", "rolling=500 stack");
run("Split Channels");
selectWindow("Stack with DAPI");
//run("Threshold…");
setAutoThreshold("Otsu dark");
setOption("BlackBackground", true);
run("Convert to Mask", "method=Otsu background=Dark black");
run("Analyze Particles…", "size=80-Infinity exclude include add stack");
roiManager("Select", newArray(#select ROIs));
selectWindow("Stack with POIs IF");
roiManager("Measure");
```

Quantification of micronuclei

Micronuclei were stained with DAPI and identified using the Fiji Cell Counter plug-in according to the following criteria: the micronucleus has a diameter of less than 1/3 of the corresponding nucleus; it is contained in the same cytoplasm as the corresponding nucleus; it presents circular or oval shape (circularity $\sim$1.0); and its intensity is comparable to the corresponding nucleus. In overexpression experiments, exclusively GFP/MDM2/flag-PARP1 positive cells were considered for quantification. The index of micronuclei was obtained by dividing all micronuclei by the number of cells per sample.

DNA fibers and fork symmetry quantification

Newly synthetized DNA track length in micrometers was calculated measuring the fiber length in pixel and converting it to micrometers using the conversion factor: 1 pixel = 5.7 μm, as previously described (Köpper et al., 2013). Fiber length in micrometers can be converted to kb using the conversion factor 1 μm = 2.59 kb (Henry-Mowatt et al., 2003).

Symmetry of bidirectional forks was analyzed considering only fibers containing three labels, i.e. fibers showing the first label (CldU) in the middle and the second label (IdU) at both sides. We measured the length of the two IdU-labeled tracks and calculated the ratio by dividing the length of the longer track by that of the shorter one.

Western blot quantification

Western blot analysis and quantification was performed using Image Lab (Bio Rad). The total amount of signal for pixels within each band was quantified, normalized to the housekeeping gene GAPDH, and then plotted in graphs using GraphPad Prism Software.

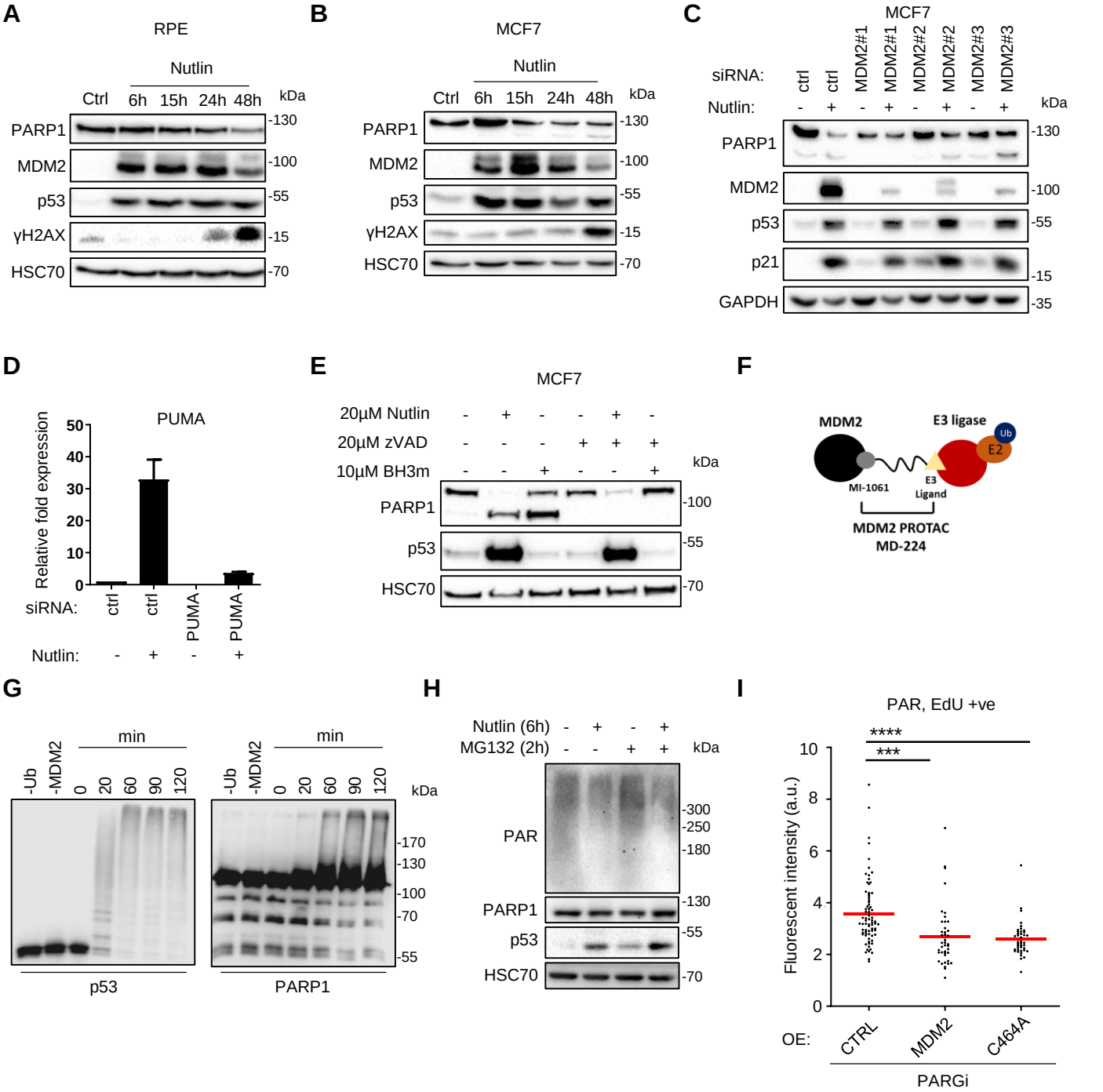

Figure S1. MDM2 ubiquitinates PARP1, triggering its proteasomal degradation. Related to Figure 1.

A) RPE cells were treated with 10μM Nutlin and harvested at the indicated time points for immunoblot analysis. Reduction of PARP1 levels was observed starting at 24 h and became more prominent at 48 h.

B) MCF7 cells were treated with 20μM Nutlin for the indicated periods, and immunoblot analysis was performed. PARP1 levels started to be reduced at 15 h.

C) MCF7 cells were treated with three separate siRNAs against MDM2 for 48 h. Prior to harvest and immunoblot analysis, cells were treated with 20μM Nutlin for 24 h.

D) RT-qPCR analysis of PUMA mRNA levels in SJSA-1 cells. P53 activation by Nutlin induced PUMA gene expression, as expected, while siRNA transfection led to depletion of PUMA mRNA, confirming the efficacy of the knock down. Two independent experiments with similar outcomes were performed. *(legend continued on next page)*

E) MCF7 cells were treated with either 20µM Nutlin, 20µM of the caspase inhibitor zVAD, or 10µM of the BH3 mimetic (BH3m) ABT-737. ABT-737 induces caspase activation independent of p53 and was used as control. PARP1 was degraded specifically in the presence of Nutlin but not ABT-737. In both cases, the caspase inhibitor zVAD prevented PARP1 cleavage; however, a loss of full length PARP1 was observed in the presence of Nutlin, but not ABT-737, and this loss could not be rescued by zVAD.

F) Mechanism of targeted protein degradation via proteolysis-targeting chimeras (PROTACs). MD-224 is composed of two active domains connected by a linker. One domain is a MDM2 ligand (MI-1061) that disrupts the MDM2-p53 interaction. A second domain recruits an E3 ubiquitin ligase machinery (Cereblon). This leads to the ubiquitination and proteasomal degradation of MDM2, while p53 remains active.

G) Ubiquitination of PARP1 by MDM2 *in vitro*. Purified recombinant MDM2 was incubated either with PARP1 (right side) or with p53 (positive control, left side). Additional negative controls without ubiquitin (-Ub) or without MDM2 (-MDM2) were included. MDM2 was incubated with the target protein for up to 120 min. At indicated time points, the samples were subjected to immunoblot analysis. Both p53 and PARP1 were ubiquitinated by MDM2, as shown by accumulation of proteins at high molecular weight with increasing intensities at increasing incubation time. A shorter exposure for PARP1 is shown in Figure 1H.

H) Immunoblot analysis of PAR. SJSA-1 cells have been treated with Nutlin (20µM) for 6 h. In the last 2h MG-132 (10µM) was added. PARGi (10µM, 2h) was administered to increase PAR to a detectable level. Reduction of PAR upon Nutlin was confirmed, also in the presence of MG-132.

I) H1299 cells were transfected with either empty vector (pCMV), MDM2 wild type (pCMV-MDM2), MDM2 RING finger mutant (pCMV-C464A) plasmids for 48 h, and nuclear levels of PAR were quantified. Cells were treated for 2 h with PARGi (20µM) to stabilize the PAR chains. EdU positive cells (i.e. undergoing S-phase were considered for quantification). One of two independent experiments with similar outcomes is shown. Unpaired Student's t-test was used for statistical analysis: ***p-value≤0.001; ****p-value < 0.0001.

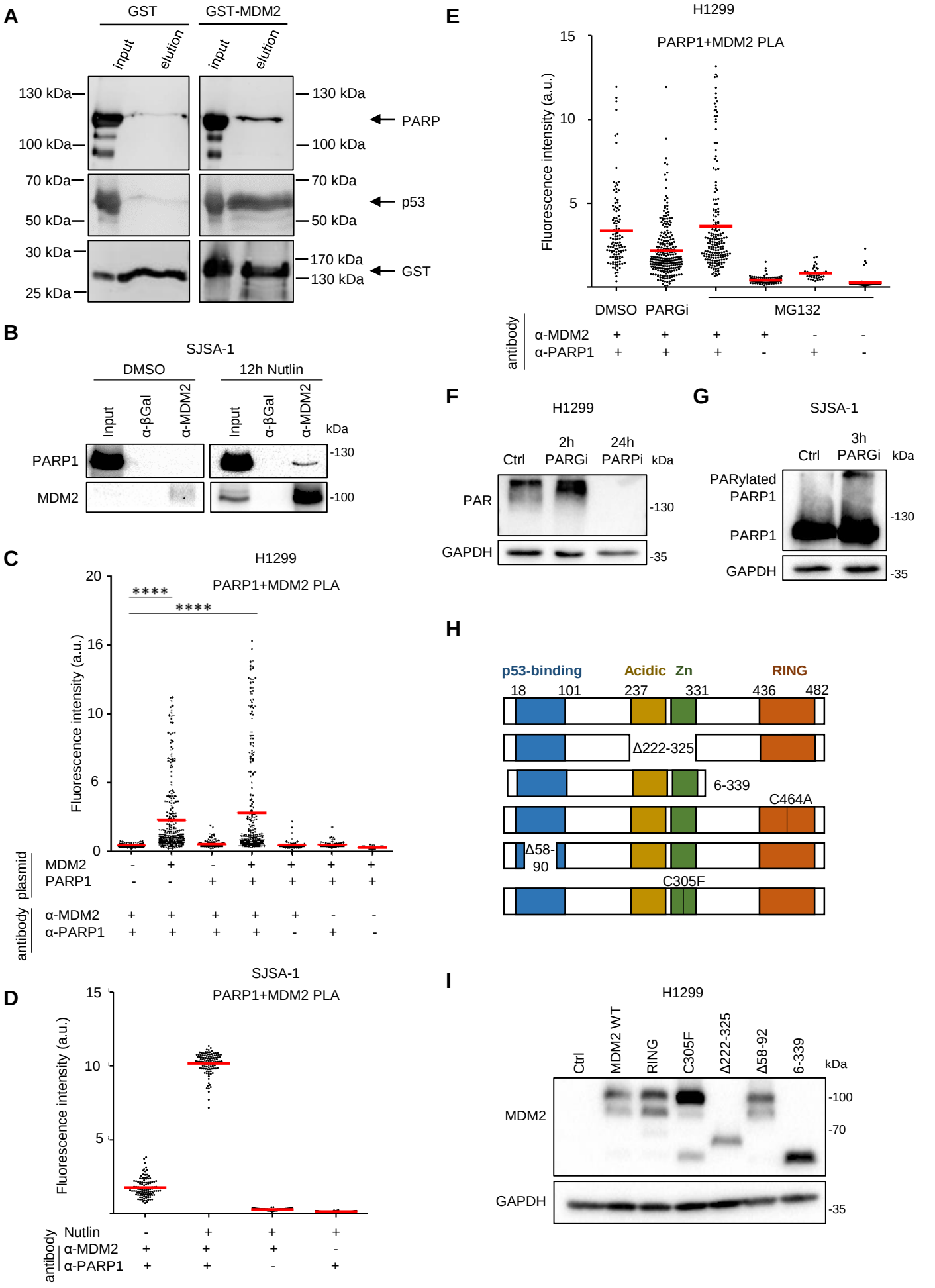
A
GST
GST-MDM2
input
elution
input
elution
130 kDa
100 kDa
70 kDa
50 kDa
30 kDa
25 kDa
130 kDa
100 kDa
70 kDa
50 kDa
170 kDa
130 kDa
PARP
p53
GST
B
SJSA-1
DMSO
12h Nutlin
Input
α-βGal
α-MDM2
Input
α-βGal
α-MDM2
kDa
PARP1
MDM2
-130
-100
C
H1299
PARP1+MDM2 PLA
****
****
Fluorescence intensity (a.u.)
20
16
10
6
0
MDM2 plasmid
PARP1
antibody
α-MDM2
α-PARP1
D
SJSA-1
PARP1+MDM2 PLA
Fluorescence intensity (a.u.)
15
10
5
Nutlin
antibody
α-MDM2
α-PARP1
E
H1299
PARP1+MDM2 PLA
Fluorescence intensity (a.u.)
15
10
5
DMSO
PARGi
MG132
antibody
α-MDM2
α-PARP1
F
H1299
Ctrl
2h PARGi
24h PARPi
kDa
PAR
GAPDH
-130
-35
G
SJSA-1
Ctrl
3h PARGi
kDa
PARylated PARP1
PARP1
GAPDH
-130
-35
H
p53-binding
Acidic
Zn
RING
18
101
237
331
436
482
Δ222-325
6-339
C464A
Δ58-90
C305F
I
H1299
Ctrl
MDM2 WT
RING
C305F
Δ222-325
Δ58-92
6-339
kDa
MDM2
GAPDH
-100
-70
-35

Figure S2. MDM2 forms a complex with PARP1 *in vitro* and *in vivo*. Related to Figure 2.

A) GST pull-down assay indicating PARP1 association with GST-MDM2. GST or GST-MDM2 fusion protein were coupled to glutathione beads and incubated with purified PARP1 or p53, followed by washes and elution. Immunoblots were probed to detect PARP1, p53, and GST. The images to the left (GST) and right (GST-MDM2) were each taken from the same blot with the same exposure time.

B) Immunoblot analysis following immunoprecipitation (IP) of MDM2, upon treatment with 20μM Nutlin for 12 h. The IP was performed using an antibody against MDM2 to confirm a physical interaction between MDM2 and PARP1 in SJSA-1 cells. An antibody targeting β-Galactosidase (β-Gal) was used as a negative control.

C) Technical controls of the PLA shown in Figure 2D for H1299 cells. Each antibody was tested individually to assess the background signal of the assay. Note that negative controls were performed under conditions where high levels of both proteins are expected (e.g. when overexpressing both MDM2 and PARP1). Additionally, single over-expressions of either MDM2 or PARP1 were performed by plasmid transfection, to reveal that overexpressed MDM2 associates with endogenous PARP1 as well.

D) Technical controls of the PLA shown in Figure 2E for SJSA-1 cells. Negative controls were performed in cells treated with Nutlin for 6 h to enhance MDM2 levels.

E) Technical controls of the PLA shown in Figure 2D. H1299 cells were either treated with PARGi (2 h, 20μM), or with the proteasome inhibitor MG-132 (10μM, 4 h) to increase protein levels.

F) Immunoblot analysis of input samples used for Co-IP (Figure 2B). The PAR signal becomes stronger upon PARGi (20μM, 2 h) treatment. PARP1i treatment (Olaparib, 10μM, 24 h) completely abolished PARylation.

G) Immunoblot analysis of input samples used for Co-IP (Figure 2C). Auto-PARylated PARP1 becomes visible upon PARGi treatment (10μM, 3 h).

H) Schematic representation of the MDM2 mutants used in this study. Five different MDM2 mutants were overexpressed in H1299 cells together with PARP1. These MDM2 mutants contain deletions in either the central domain (Δ222-325), the RING domain (6-339) or the hydrophobic pocket that binds p53 (Δ58-90). We also included two point mutants, either in the RING domain (C464A) or in the zinc finger (Zn) domain (C305F).

I) Immunoblot analysis of MDM2 mutants (related to Figure 2F).

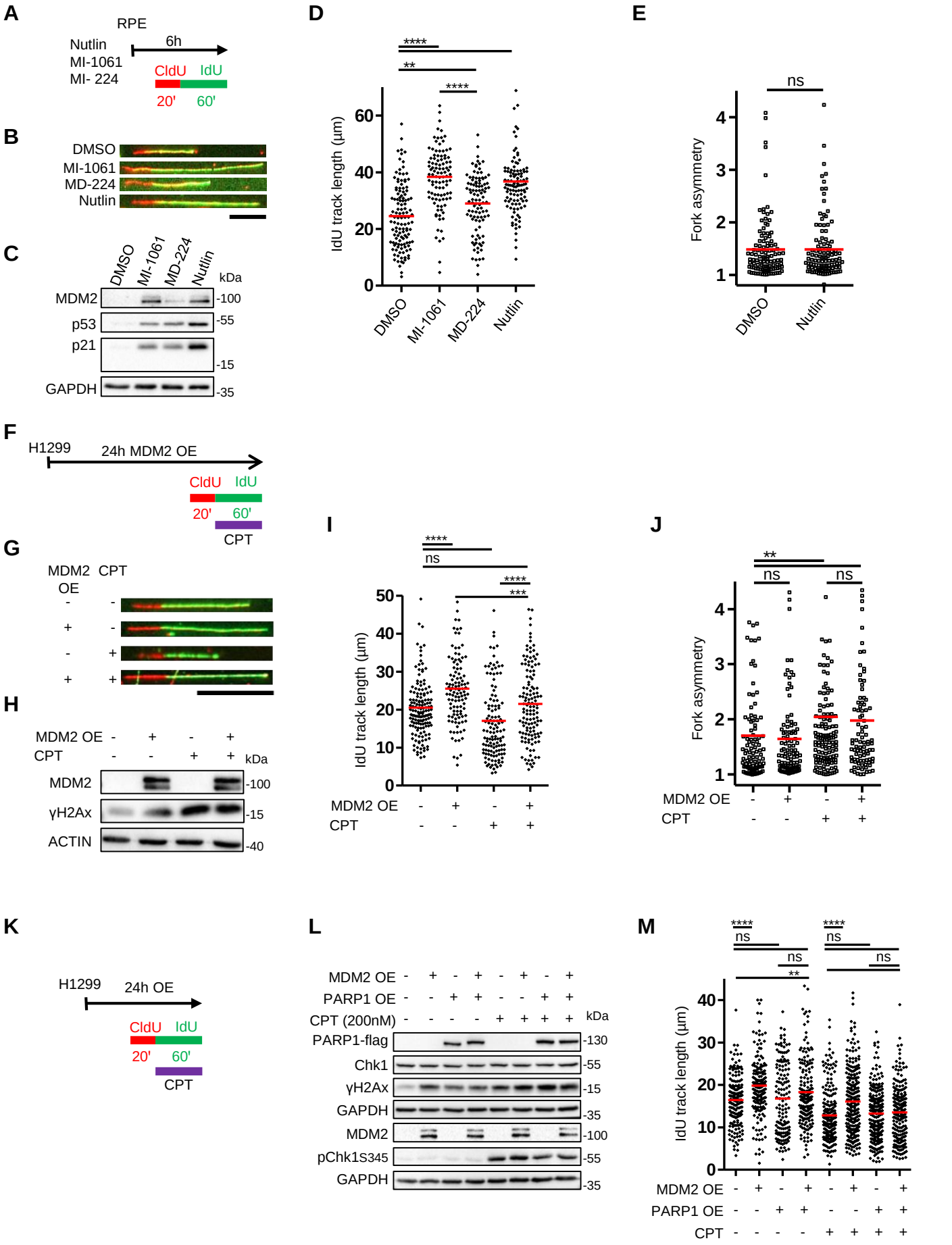
A
RPE
Nutlin
MI-1061
MI- 224
6h
CldU
IdU
20'
60'
B
DMSO
MI-1061
MD-224
Nutlin
C
DMSO
MI-1061
MD-224
Nutlin
kDa
MDM2
p53
p21
GAPDH
-100
-55
-15
-35
D
IdU track length (µm)
****
**
****
DMSO
MI-1061
MD-224
Nutlin
E
Fork asymmetry
ns
DMSO
Nutlin
F
H1299
24h MDM2 OE
CldU
IdU
20'
60'
CPT
G
MDM2 OE
CPT
H
MDM2 OE
CPT
kDa
MDM2
γH2Ax
ACTIN
-100
-15
-40
I
IdU track length (µm)
****
ns
****
***
MDM2 OE
CPT
J
Fork asymmetry
**
ns
ns
MDM2 OE
CPT
K
H1299
24h OE
CldU
IdU
20'
60'
CPT
L
MDM2 OE
PARP1 OE
CPT (200nM)
kDa
PARP1-flag
Chk1
γH2Ax
GAPDH
MDM2
pChk1S345
GAPDH
-130
-55
-15
-35
-100
-55
-35
M
IdU track length (µm)
****
ns
ns
**
****
ns
ns
MDM2 OE
PARP1 OE
CPT

Figure S3. MDM2 enhances the elongation rate of DNA synthesis, which is abolished by PARP1 overexpression. Related to Figure 3.

A) Treatment protocol. RPE cells were treated with Nutlin (20μM, 6 h), MI-1061 (1μM, 6 h), or MD-224 (1μM, 6 h). DNA fiber assays were performed by sequential labeling of newly synthetized DNA with CldU (25μM, 20 min) and IdU (25μM, 60 min).

B) Representative images of DNA fibers detected upon treatment shown in A. Scale bar=20μm.

C) Immunoblot analysis of RPE cells treated following the protocol shown in A.

D) DNA fiber assay following treatment shown in A. Mean IdU track lengths, within bicolored fibers, are indicated by red lines. A minimum of 100 fibers was quantified in three independent experiments with similar results. Mann-Whitney U test, two sided, was used for statistical analysis: **p-value≤0.01, ****p-value < 0.0001.

E) Bidirectional forks symmetry analysis of SJSA-1 cells treated with Nutlin (20μM, 6h). Only fibers containing three labels, i.e. fibers showing the first label (CldU) in the middle and the second label (IdU) at both sides were considered for quantification. The ratio between the longer and the shorter IdU-labeled track is represented. Mean of the ratios is shown by the red line. ns, not significant (Mann-Whitney U test).

F) Transfection and treatment schedule. H1299 cells were subjected to plasmid transfection (control plasmid pCMV, expression plasmid pCMV-MDM2). Treatment with CPT (200nM) was performed 1h prior to harvest. For DNA fiber assays, the newly synthetized DNA was labeled as indicated above.

G) Representative images of DNA fibers upon transfection and treatment depicted in F. Scale bar=20μm.

H) Immunoblot analysis upon treatment indicated in F, confirming MDM2 overexpression and DNA damage (γH2AX) induced by CPT treatment.

I) DNA fiber assay following transfection and treatment indicated in F.

J) Bidirectional forks symmetry analysis of H1299 cells upon CPT treatment and plasmid transfection (control plasmid pCMV, expression plasmid pCMV-MDM2), as shown in F. Fork asymmetry quantification and analysis was performed as described above.

K) Protocol used for DNA fiber assays. H1299 cells were subjected to plasmid transfection (control plasmid pCMV, expression plasmid pCMV-MDM2 and/or pCMV-PARP1), followed by CPT treatment and fiber assays.

L) Immunoblot analysis upon transfection and treatment as indicated in K.

M) DNA fiber assay following transfection and treatment described in K.

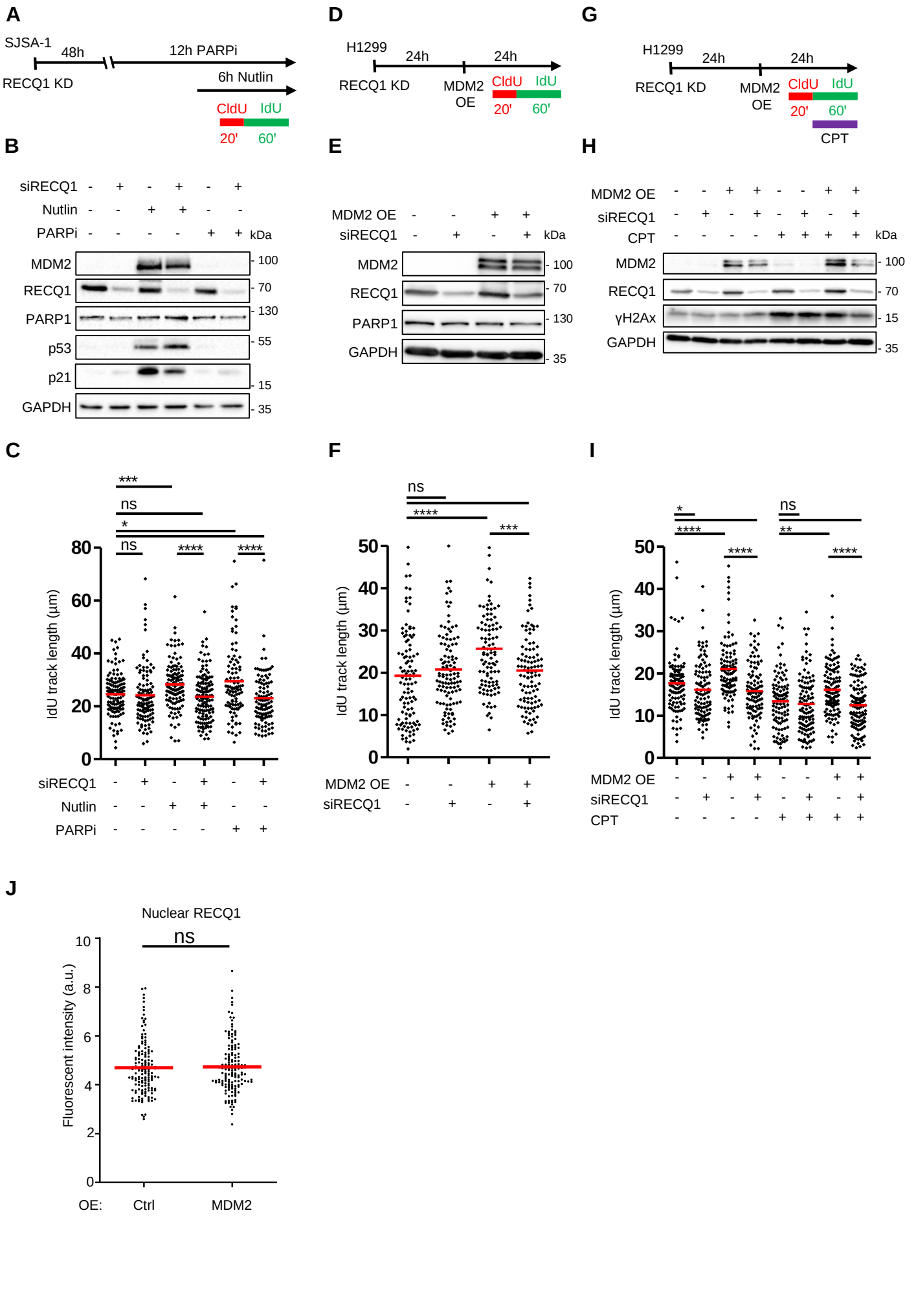
A
SJSA-1
48h
12h PARPi
RECQ1 KD
6h Nutlin
CldU
IdU
20'
60'
D
H1299
24h
24h
RECQ1 KD
MDM2 OE
CldU
IdU
20'
60'
G
H1299
24h
24h
RECQ1 KD
MDM2 OE
CldU
IdU
20'
60'
CPT
B
siRECQ1
Nutlin
PARPi
kDa
MDM2
RECQ1
PARP1
p53
p21
GAPDH
100
70
130
55
15
35
E
MDM2 OE
siRECQ1
kDa
MDM2
RECQ1
PARP1
GAPDH
100
70
130
35
H
MDM2 OE
siRECQ1
CPT
kDa
MDM2
RECQ1
γH2Ax
GAPDH
100
70
15
35
C
IdU track length (μm)
***
ns
*
ns
****
****
siRECQ1
Nutlin
PARPi
F
IdU track length (μm)
ns
****
***
MDM2 OE
siRECQ1
I
IdU track length (μm)
*
****
ns
**
****
****
MDM2 OE
siRECQ1
CPT
J
Nuclear RECQ1
ns
Fluorescent intensity (a.u.)
OE:
Ctrl
MDM2

Figure S4. MDM2-mediated PARP1 inactivation induces nascent DNA elongation through RECQ1. Related to Figure 4.

A) Transfection and treatment schedule. SJSA-1 cells were transfected with siRNA against RECQ1 (siRECQ1 #2) and treated with Nutlin (20μM, 6 h) or the PARPi Olaparib (10μM, 12 h). Newly synthetized DNA was marked with CldU (25μM, 20 min) and IdU (25μM, 60 min) to perform DNA fiber assay.

B) Immunoblot analysis upon treatment as indicated in A.

C) DNA fiber assay using SJSA-1 cells after treatment shown in A. For each condition, a minimum of 100 fibers was quantified. One of three independent experiments with similar results is shown. Mann-Whitney U test, two sided, was used for statistical analysis: ns, not significant; *p-value≤0.05, **p-value≤0.01, ***p-value≤0.001, ****p-value < 0.0001.

D) Transfection and treatment scheme. H1299 cells were subjected to plasmid transfection (control plasmid pCMV, expression plasmid pCMV-MDM2) and RECQ1 depletion via siRNA (siRECQ1 #2). For DNA fiber assay the cells were labeled with CldU (25μM, 20 min) and then IdU (25μM, 60 min).

E) Immunoblot analysis upon treatment shown in D.

F) DNA fiber assay following transfection of H1299 cells described in D. A minimum of 100 fibers was quantified in three independent experiments with similar outcome.

G) Transfection and treatment scheme. H1299 cells were subjected to plasmid transfection and RECQ1 depletion via siRNA (siRECQ1 #1). For DNA fiber assay the cells were labeled as indicated above. CPT (200nM) was added 1h prior harvest.

H) Immunoblot analysis upon treatment indicated in G.

I) DNA fiber assay following transfection of H1299 cells depicted in G. A minimum of 100 fibers was quantified in two independent experiments with similar outcomes.

J) RECQ1 immunofluorescence staining. H1299 cells were transfected either with a control empty vector (pCMV) or with a MDM2 overexpressing plasmid (pCMV-MDM2) and all co-transfected with a GFP overexpressing plasmid (pCMV-GFP) for 24 h. GFP/MDM2 immunofluorescence signal was used to identify transfected cells. Nuclear fluorescence intensity was quantified for more than 150 cells per condition. Red lines represent mean values for each plot. Unpaired Student's t-test was used for statistical analysis: ns, not significant.

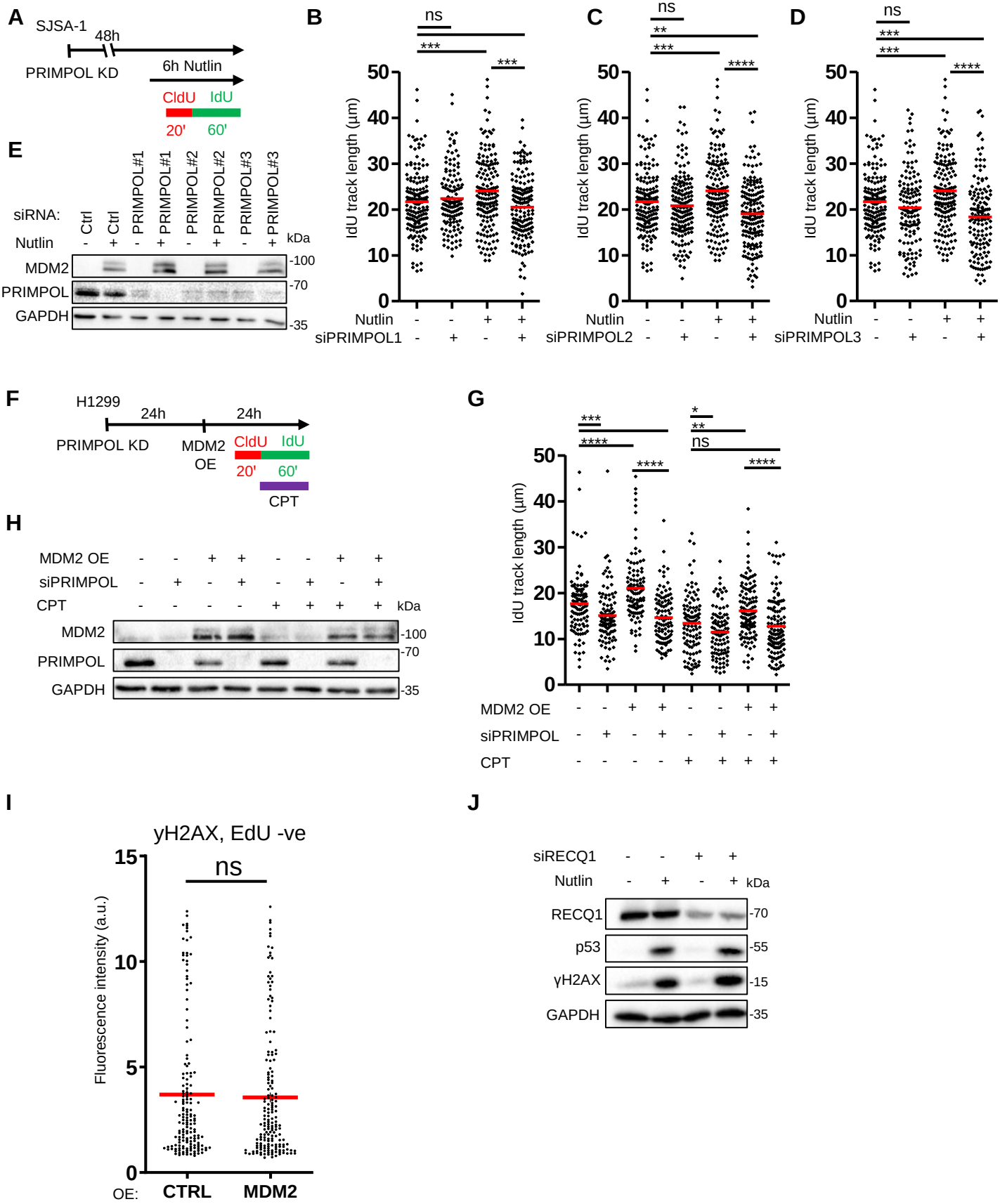

Figure S5. MDM2 accumulation favors PRIMPOL-mediated fork progression and accumulation of DNA damage. Related to Figure 5.

A) Transfection and treatment scheme. SJSA-1 cells were transfected with three different siRNAs to deplete PRIMPOL (siPRIMPOL #1 siPRIMPOL #2, siPRIMPOL #3). For DNA fiber assays, the nascent DNA was labeled with CldU (25µM, 20 min) and then IdU (25µM, 60 min). *(legend continued on next page)*

B-D) DNA fiber assay following transfection and treatment described in A. A minimum of 100 fibers for each sample was quantified in two independent experiments with similar outcome.

E) Western blot analysis upon transfection and treatment as indicated in A, confirming MDM2 upregulation and similar levels of PRIMPOL knock down with the different siRNAs.

F) Transfection and treatment protocol. H1299 cells were transfected with plasmids (control plasmid pCMV, expression plasmid pCMV-MDM2) and siRNA to deplete PRIMPOL (siPRIMPOL #2). For DNA fiber assays, the nascent DNA was labeled as indicated above.

G) DNA fiber assay following transfection and treatment of H1299 cells as indicated in F. A minimum of 100 fibers for each sample was quantified in two independent experiments with similar outcome.

H) Immunoblot analysis upon transfection and treatment as indicated in F, confirming MDM2 overexpression and PRIMPOL depletion.

I) Quantitative immunofluorescence analysis of γH2AX in H1299 cells upon overexpression of MDM2. Unlike in Figure 5G, EdU negative, i.e. cells that did not undergo DNA replication, were subjected to quantification. This indicated that MDM2 did not induce DNA damage in cells out of S-phase.

J) Immunoblot analysis of SJSA-1 cells upon treatment with 20μM Nutlin for 12 h, with or without RECQ1 depletion via siRNA (siRECQ1 #1), revealing no change in the DNA damage response by Nutlin treatment in the absence of RECQ1.

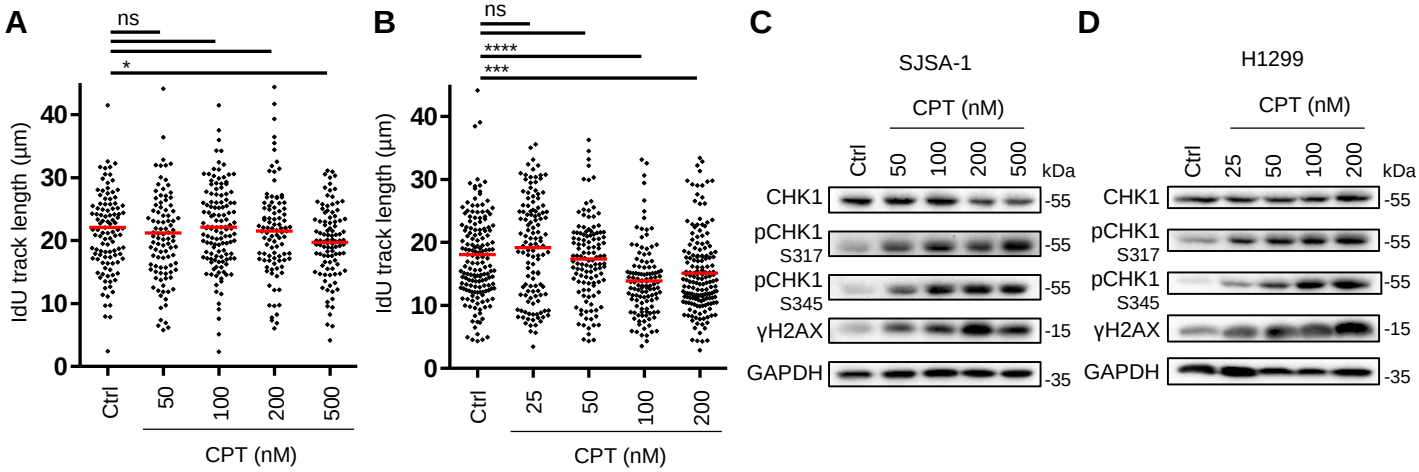

Figure S6. MDM2 accumulation antagonizes replication fork reversal. Related to Figure 6.

A, B) Fiber assay analysis of SJSA-1 and H1299 cells, respectively, treated with the indicated concentrations of CPT for 1h. More than 100 fibers for each sample were quantified in two independent experiments with similar outcome.

C, D) Immunoblot analysis of SJSA-1 and H1299 cells treated with indicated concentrations of CPT for 1h.

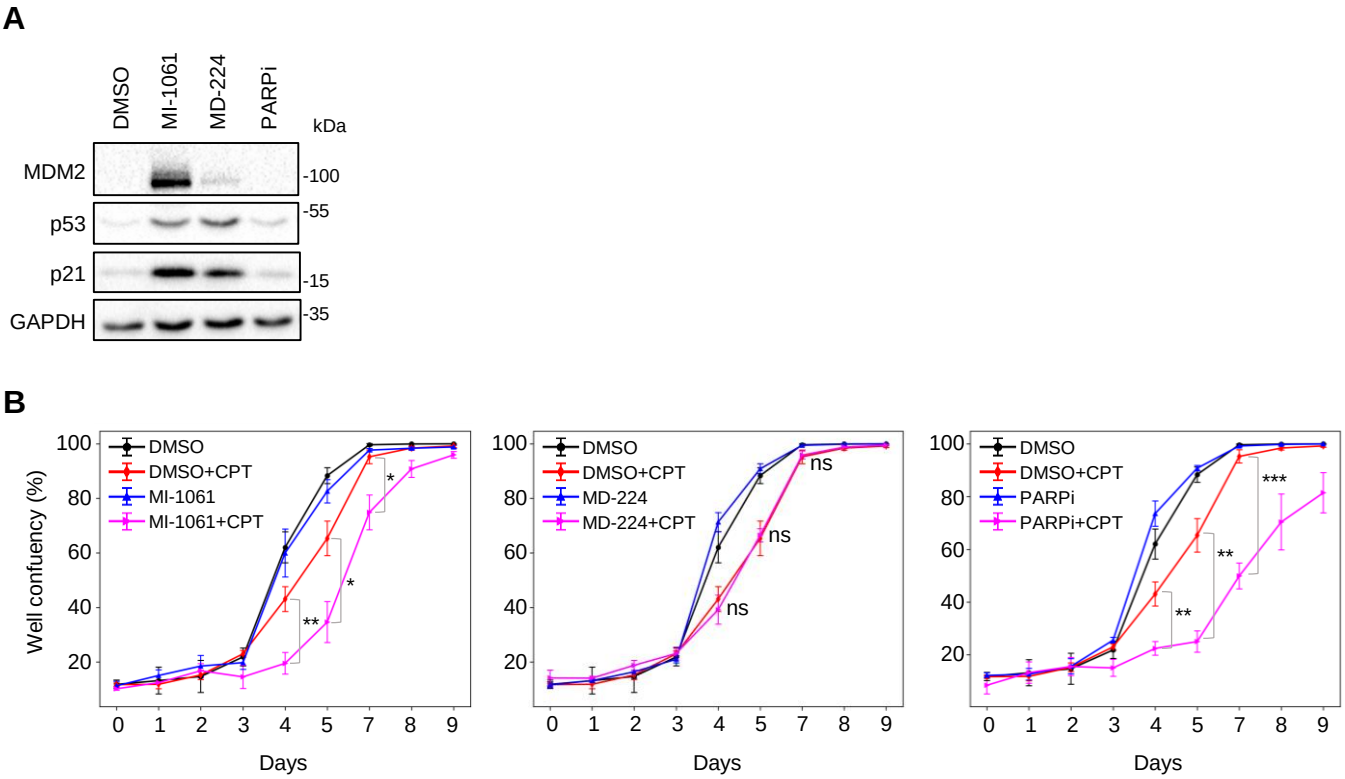

Figure S7. MDM2 enhances the accumulation of micronuclei and CPT-induced cytotoxicity. Related to Figure 7.

A) Western blot analysis of SJSA-1 cells treated according to Figure 7E and harvested right after CPT treatment. MDM2 PROTAC MD-224 depleted MDM2, while inducing p53 and its target p21 similarly to the control MI-1061.

B) Percentage of well confluency overtime. The surface of the well, in which the cells were cultivated, occupied by adherent cells was used as a readout of cellular proliferation. Mean +/- SD is represented for each time point. One of three independent experiments with three technical replicates with similar outcome is shown. Unpaired Student's t-test was used for statistical analysis: ns, not significant; *p-value≤0.05; **p-value≤0.01, ***p-value≤0.001.

5. DISCUSSION

In this study, we investigated the causes of the full-length PARP1 degradation upon p53 activation. We observed that the p53 target gene product and antagonist MDM2 is mediating PARP1 degradation. MDM2 binds and ubiquitinates PARP1, affecting its enzymatic activity and stability. We explored the functional consequences of this interaction in the context of DNA replication, reporting that MDM2 enhances replication fork progression via PARP1 inactivation. Mechanistically, inactivation of PARP1 promotes the activity of the helicase RECQ1, which mediates the resolution of reversed replication forks. In addition, the primase/polymerase PRIMPOL becomes more active, leading to the restart of DNA synthesis downstream replication blocks (Publication Figure 7H).

5.1 MDM2 interacts with PARP1 to regulate its catalytic activity

We report that p53 induction in the cell line SJSA-1 strongly reduced PARylation at a time when PARP1 levels are still unchanged (Publication Figure 1J), suggesting that MDM2 might reduce the activity of PARP1 even before destabilizing it. Experiments with the proteasome inhibitor MG132 confirmed this hypothesis; even when disabling the degradation of ubiquitinated proteins, we still observed a reduction in PAR staining upon Nutlin treatment (Publication Figure S1H). Likewise, overexpression of the MDM2 RING finger mutant (C464A), which lacks ubiquitination activity, diminished PAR levels similarly to wild type MDM2 (Publication Figures 1I, S1I). Considering that PARP1 accounts for most of the cellular PARylation (Chen et al., 2018), these results point out that MDM2 interferes both with PARP1 stability and catalytic activity. We propose that MDM2 binding to PARP1 first reduces PARylation activity, whereas prolonged MDM2 induction also leads to PARP1 degradation. This is reminiscent of how MDM2 acts on p53: it immediately reduces p53-mediated transcription, and at later time points, it destabilizes p53 (Dobbelstein et al., 1999; Henningsen et al., 2021).

PARP1 was found to interact with a number of regulatory cofactors, including the Histone PARylation factor 1 (HPF1) and the methyl transferase CARM1, which determine its amino acid specificity and DNA binding at DNA replication forks, respectively (Genois et al., 2021; Gibbs-Seymour et al., 2016; Suskiewicz et al., 2020). In addition, PARP1 interacts with the ubiquitin ligases: CHFR (Kashima et al., 2012), RNF146/Iduna (Kang et al., 2011) and TRIP12 (Gatti et al., 2020). These associate with PARP1, because they recognize and bind PAR. Being PARP1 the most abundantly PARylated protein (Hendriks et al., 2019), these E3 ubiquitin ligases are recruited very efficiently on PARP1 surface upon PARylation, mediating PARP1 proteasomal degradation. The interaction of MDM2 with PARP1 presents a rather opposite dynamic: it does not require PAR, PARylation inhibition with the PARP1/2 inhibitor olaparib did

not impair co-precipitation of MDM2 with PARP1 (Publication Figures 2B). Conversely, induction of PAR accumulation by treatment with the PARG inhibitor PDD 00017273 even decreased co-precipitation and co-localization of PARP1 and MDM2 (Publication Figures 2B–2D, S2F, and S2G).

Based on these findings, we can hypothesize that MDM2 might allosterically regulate poly(ADP-ribose) production by PARP1. PARP1 bears a regulatory allosteric domain, the helical domain (HD), which is unfolded upon DNA binding allowing NAD^+-entrance and catalytic activity. Engaging of PARP1 inhibitors in the NAD^+-binding site causes structural changes of the HD, regulating PARP1 DNA binding and retention on the chromatin, which have been shown to determine PARPi efficacy as cancer therapeutic. PARP1 inhibitors have been classified in three types based on the structural rearrangement of the HD they provoke: Type I, allosteric pro-retention on DNA that destabilizes the HD; Type II, non-allosteric that does not affect the HD; and Type III, allosteric pro-release from DNA that stabilizes the HD (Zandarashvili et al., 2020).

Similarly, MDM2 might provoke structural rearrangements of the HD affecting DNA binding and finally PARP1 enzymatic activity. In order to find this out, the following experiments would be required. Measuring the dynamics of association/dissociation from DNA using recombinant proteins *in vitro*. Alternatively, *in vivo* detection of chromatin-bound PARP1 over time upon MDM2 accumulation. Co-immunoprecipitation of MDM2 and PARP1 upon expression of different PARP1 mutants, in order to determine the residues that are involved in the interaction with MDM2. This would contribute to predicting if MDM2 could interfere with the structure of certain PARP1 domains. In order to study the impact of MDM2 on PARP1 allostery, hydrogen/deuterium exchange mass spectrometry (HXMS), combined with x-ray structures could also be used. This innovative approach has been recently established in the Prof. Ben Black's laboratory, and it would allow to directly measure the structural rearrangement of the HD upon MDM2 binding (Zandarashvili et al., 2020).

5.2 Impact of MDM2 on ADP-ribosylation

PARP1-mediated ADP-ribosylation is playing different roles in a diverse array of biological processes leading to different functional outcomes (Gupte et al., 2017; Suskiewicz et al., 2021). The different functional outcomes of PARP1 catalytic activity depend on (1) the targeted macromolecule, (2) the structural features of the ADP-ribose moiety, and (3) the conjugation site. The impact of MDM2 on each of these aspects remains to be experimentally addressed. Some hypothesis regarding MDM2 influence on these aspects are presented in the following paragraphs.

5.2.1 The impact of MDM2 on the choice of PARP1-targeted macromolecules

MDM2 could affect PARP1 preference toward different modification targets in different ways. MDM2 could recruit other proteins in close proximity of PARP1, facilitating their PARylation. MDM2 presents several interaction partners, such as the histone modifiers EZH2 (Wienken et al., 2016), RNF2/RING1B (Klusmann et al., 2018), TIP60 (Dohmesen et al., 2008; Legube et al., 2002), the repair factor NBS1, which is part of the MRN (Mre11, Rad50, Nbs1) complex (Alt et al., 2005), and the cell cycle regulator CDC25C (Giono et al., 2017). Conversely, MDM2 binding to PARP1 could antagonize the ADP-ribosylation of MDM2 binding partners.

ADP-ribosylation has been extensively studied as a protein modification. However, recent findings demonstrate that nucleic acids can also be modified. The first reported case of ADP-ribosylated nucleic acid comes from the cabbage butterfly, where the reaction is catalyzed by the DNA modifying ADP-ribosyltransferase Pierisin (Takamura-Enya et al., 2001). Following publications have shown that PARP1/2/3 can ADP-ribosylate the terminal DNA phosphate groups *in vitro* (Belousova et al., 2018; Munnur and Ahel, 2017; Talhaoui et al., 2016), while PARP10, PARP11 and PARP15 have been shown to ADP-ribosylate the terminal 5′-phosphate of RNA *in vivo* (Munnur et al., 2019). Recently, Prof. Ivan Ahel's lab has reported that the bacterial ADP-ribosyltransferase (ART) DarT is capable of modifying thymidine in single-stranded DNA (ssDNA) in human cell lines (Tromans-Coia et al., 2021). It is still unknown whether ssDNA ADP-ribosylation is an endogenous modification also in higher organisms, and which could be the ART active in human cells. However, the presence of the ADP-ribosylhydrolase TARG1, which acts as a ssDNA ADP-ribosylation negative regulator, would support the endogenous source of DNA modification in human cells (Tromans-Coia et al., 2021).

It would be intriguing to study whether PARP1 could be mediating this modification, and if MDM2 could affect PARP1 preference toward nucleic acids rather than protein substrates. Interestingly, an antibody raised against protein MAR and PAR was reported to be capable of detecting ADP-ribosylated DNA. This antibody was used for immunofluorescence staining of PAR (Publication Figure 2H), which confirmed a MDM2-dependent reduction of signal upon MDM2 overexpression. It would be relevant to further investigate whether DNA ADP-ribosylation could be detected in our system, and whether MDM2 could affect this in addition to the protein modification. This could be tested by genomic DNA isolation and Dot Blot analysis using the antibody capable of detecting DNA ADP-ribosylation.

5.2.2 The impact of MDM2 on structural features of the ADP-ribose modification

The ADP-ribose modification can present different structural features. It can consist of a single ADP-ribose (Mono(ADP-Ribose), MAR) or more ADP-ribose units (Poly(ADP-Ribose, PAR)

linked by α(1 → 2) O-glycosidic bonds that can be elongated up to about 250 units in a linear or branched fashion (Gibson and Kraus, 2012; Vyas et al., 2014). We detected the changes in ADP-ribosylation upon p53 induction or MDM2 accumulation by immunostaining, using two antibodies that are capable of recognizing both MAR and PAR. However, the cells were treated with the PARG inhibitor prior harvesting to increase PAR signal to a detectable level (Publication Figures 1J, 1I, 2H). The presence of a PARG inhibitor restrict the analysis to PAR. To gain further information about MARylation activity of PARP1 upon MDM2 accumulation, other experimental settings should be applied in order to enhance ADP-ribosylation, e.g., DNA damage induction via H_2O_2 treatment, which is known to strongly enhance MAR.

Since PARP1 has been identified for decades as a PARylation enzyme, while other members of the PARP family have been reported to act exclusively as mono(ADP-ribosyl) transferases (Vyas et al., 2014), we could imagine MDM2 to affect PARylation only. However, recently PARP1 has been show to act as mono(ADP-ribosyl) transferase in complex with HPF1. Therefore, we cannot exclude an MDM2-mediated regulation of the MARylation reactions carried out by PARP1.

5.2.3 The impact of MDM2 on the amino acid specificity of ADP-ribosylation by PARP1

Determining the amino acid that is targeted for ADP-ribosylation remained challenging for many years, due to technical reasons. For example, the development of antibodies was limited by the chemical complexity and heterogeneity of the ADP-ribose modification. The first antibody recognizing PAR was developed in 1986, and for decades was the only one available (Kawamitsu et al., 1984; Meyer and Hilz, 1986). Three major technological breakthroughs allowed the advances that have been recently made in the study of PARP1 amino acid specificity: (i) mass spectrometry-based proteomics methods for identification of endogenous ADP-ribosylation targets sites; (ii) synthesis of recombinant ADP-ribosylation substrates; (iii) generation of antibodies detecting ADP-ribose conjugated to different substrates (Longarini and Matic, 2022). These advances allowed to discover that the amino acid specificity of PARP1 is interchangeable. In particular, it was shown that the substrate specificity of PARP1/2 can be shifted from glutamate and aspartate to serine in a DNA damage context by the interaction with the cofactor HPF1 (Suskiewicz et al., 2020).

Studying whether interaction partners of PARP1 could affect amino acid specificity similar to HPF1 would greatly contribute to our understanding of the biological role of PARP1, especially in the context of DNA damage, where a transient switch toward Ser-ADP-ribosylation seems to be crucial to accomplish DNA damage repair (Longarini and Matic, 2022). Currently, the biological function of this switch in amino acid specificity remains unknown. It is also unknown whether specific DNA damage repair factors could be recruited by this specific kind of modification. It is tempting to speculate a regulatory role of MDM2 on PARP1 amino acid

specificity. Equally tempting is to consider the potential interference of MDM2 with PARP1 amino acid specificity as part of p53 oncosuppressive activity, since it could affect the DNA damage repair. In order to explore this aspect, a recently developed antibody showing preference for MAR conjugated to serine could be used (Bonfiglio et al., 2020). Additionally, to test the nature of the ADP-ribose-conjugated amino acid, cell lysates could be subjected to treatment with hydroxylamine. Hydroxylamine would remove the ADP-ribose bound to glutamate and aspartate, since they react with the ribose through the carboxyl group forming an ester. Instead, serine-bound ADP-ribose would not be affected by the treatment, since serine is linked to the ribose by O-glycosylation of the hydroxyl group. Therefore, ADP-ribose immunostaining after hydroxylamine treatment of the cell lysates could reveal the nature of the modified amino acid.

5.3 The risks of persistent PARylation

Since PARylation is involved in DNA damage repair, we might question why a tumor suppressor like p53 would reduce PARylation via MDM2 induction. However, elevated PAR has been shown to cause cytotoxicity and genomic instability (O'Sullivan et al., 2019). PARG depletion, which stabilizes PARylation, delays cellular recovery from genotoxic stress, sensitizing the cells to DNA damage inducing agents (Cortes et al., 2004; Illuzzi et al., 2014; Min et al., 2010). The fact that PARG knock out in mice is embryonic lethal further corroborates the cytotoxic impact of excessive and permanent PARylation (Koh et al., 2004). Persistent PARylation is perturbing genome integrity by a series of mechanisms. High PAR levels negatively regulate RPA foci formation on ssDNA, which remains unprotected causing DSBs accumulation (Illuzzi et al., 2014). PARP1 PARylation is inhibiting the activity of the helicase RECQ1 that mediates restart of reversed DNA replication forks (Berti et al., 2013). Consequently, stable PARylation dramatically enhances the accumulation of reversed forks and decreases DNA replication fork progression, leading to prolonged fork stalling, which results in fork collapse and DSB formation (Ray Chaudhuri et al., 2015). PARylation of the telomeric protein TRF1 disables DNA maintenance at the telomeres (Yang et al., 2017). Finally, PARylated PARP1 is released from the chromatin due to electrostatic repulsion (Aberle et al., 2020). Limiting PARylated PARP1 accumulation is required for maintaining a pool of functional PARP1. Therefore, by preventing PAR accumulation, p53 antagonizes each of these mechanisms contributing to genome stability. However, persistent p53 activation leads to prolonged MDM2 accumulation and consequent loss of PARP1, which boosts genome instability and cell death (Publication Figure 7). This could be considered as part of the p53 oncosuppressive activity, with p53 using PARP1 repression as mean for destruction of cells undergoing persistent genotoxic stress.

Additionally, PARylation can lead to a caspase-independent type of cell death known as parthanatos. Parthanatos is mediated by protein-free PAR chains that results from PARG activity as endoglycosidase. Free PAR provokes the translocation from the mitochondria to the nucleus of the apoptosis-inducing factor (AIF), which carries out large-scale fragmentation of genomic DNA and chromatin condensation, followed by cell death (Wang et al., 2011). However, PARG shows endoglycosidic digestion of PAR only in 20% of cases, while is more frequently sequentially digesting glycosidic linkages from the protein-distal end of the polymer (Braun et al., 1994). What determines the switch from exoglycosidic toward endoglycosidic digestion of PAR still remains to be defined. It is therefore hard to predict PARG mode of action in a context of p53 activation and MDM2 accumulation. It is also unknown whether the p53 pathway can directly regulate PARG enzymatic activity, but we can hypothesize that MDM2 inactivating PARP1 might to a certain extent antagonize parthanatos.

Given the MDM2-mediated reduction of PARylation, we could envision MDM2 downregulation to enhance PAR levels. This could be tested by immunostaining of PAR upon treatment with MDM2 PROTAC. In addition, it could be relevant to investigate whether the combined loss of MDM2 and PARG could synergistically enhance PAR accumulation to provoke cell death, similarly to the recently reported synergistic enhancement of cell death upon combined PARG and ARH3 depletion (Prokhorova et al., 2021a). This could have potential therapeutic applications, especially in PARP1 inhibitor-resistant tumors that retains high levels of PARylation upon PARP1 inhibitors treatment (Prokhorova et al., 2021b).

5.4 Clinical relevance of MDM2-dependent PARP1 inactivation

We report an impact of MDM2 on cellular viability upon treatment with the Topoisomerase I inhibitor CPT (Publication Figure 7F). The MDM2 antagonist MI-1061 enhanced cell death to a significantly greater extent than CPT alone, similarly to PARP1 inhibition, but the MDM2-depleting PROTAC did not (Publication Figures 7F, S7A). Thus, MDM2 contributes to cell death in the context of CPT-induced genotoxic stress. Moreover, monitoring cellular proliferation, we observed that in the presence of CPT, MDM2 strongly reduced cell growth (Publication Figure 7G, S7B). The depletion of MDM2, again, completely reverted this phenotype (Publication Figure 7G, S7B). These observations reveal MDM2 as an enhancer of CPT-induced cytotoxicity. The fact that the impact of MDM2 accumulation on cellular fitness upon CPT treatment phenocopied PARP inhibition strongly suggests that in both cases genome instability is enabled via premature fork restart. Indeed, we observed an MDM2-dependent increase in γH2AX levels that was reduced upon depletion of PRIMPOL but not RECQ1 (Publication Figures 5I, S5J), and a significant increase of micronuclei formation upon MDM2 overexpression, which was attenuated by PARP1 co-overexpression (Publication

Figure 7B). These results highlight a potential clinical relevance of MDM2 levels, particularly in tumors carrying MDM2 gene amplifications, e.g., in sarcomas (Rayburn et al., 2005).

Whether MDM2-dependent PARP1 inactivation could show synthetic lethality in a context of BRCA deficiency it is still an open question. Intriguingly, 90% of cancers with BRCA1 mutations also have mutations in the TP53 gene (Cancer Genome Atlas Research et al., 2013). This is most likely ascribable to cell cycle arrest and apoptosis induced by p53, which is activated upon BRCA loss due to DNA damage accumulation. In addition to that, upon p53 induction, MDM2-dependent PARP1 inactivation could cause the death of BRCA deficient cells, further promoting positive selection of cells carrying mutant p53, which is unable to induce the target genes expression.

Since PARP inhibitors were initially reported to be particularly active against cancers harboring defects in BRCA or other genes involved in homologous recombination (HR), DSBs have been considered the lesion sensitizing cells toward PARP inhibition (Bryant et al., 2005; Farmer et al., 2005; Helleday, 2011a). More recently, the mechanism behind the synthetic lethality of PARP inhibition and BRCA deficiency was reconsidered due to discrepancies in the experimental findings, with Olaparib-dependent cytotoxicity being ascribed to PARP1 trapping on the DNA. Trapped PARP1 was thought to act as obstacle for DNA replication, promoting fork stalling (D'Andrea, 2018; Michelena et al., 2018; Murai et al., 2012; Pommier et al., 2016). Since BRCA deficiency is known to cause newly synthetized DNA degradation at stalled replication forks, the mechanistic base of the synthetic lethality was attributed to fork stalling and consequent fork degradation (Lomonosov et al., 2003; Schlacher et al., 2011). However, this was challenged by the observation that olaparib did not slow DNA replication fork progression, but rather accelerated it (Maya-Mendoza et al., 2018), which was reproduced by our work in the context of MDM2-dependent PARP1 inactivation (Publication Figure 3).

In 2021, a study from the Prof. Sharon Cantor's lab revealed instead replication gaps to be the primary sensitizing lesion to PARP inhibition (Cong et al., 2021a). Replication ssDNA gaps, which are shown to be elevated in BRCA deficient cells, can arise from loss of functional DNA damage repair or Okazaki fragment processing. The presence of ssDNA gaps can be detected via nascent DNA labeling with nucleoside analogs, and immunofluorescence staining under non-denaturing conditions (Couch et al., 2013). This finding open the possibility of screening the patients for the presence of these lesions as diagnostic marker of sensitivity toward PARP inhibition. Based on our finding of MDM2 accumulation phenocopying PARP1 inhibition, we propose to exploit the identification of replication gaps for the assessment of response toward MDM2 antagonists. To this end, further experiments need to be performed with the aim to correlate the presence of replication gaps to the impact of MDM2 antagonists on cellular

fitness. These experiments could firstly be performed in cell lines carrying MDM2 gene amplification, which might be showing a faster inactivation of PARP1.

Another aspect to consider is the impact of MDM2-dependent PARP1 degradation on the therapeutic response toward PARP inhibitors like Olaparib. As already mentioned above, Olaparib induced cytotoxicity works at least in part through the trapping of PARP1 on the DNA. As a consequence, the activation of E3 ubiquitin ligases that mediate PARP1 degradation constrains the toxicity of Olaparib, as demonstrated for the PARP1 negative regulator TRIP12 (Gatti et al., 2020). We could speculate that the observed resistance towards PARP inhibitors in cancer cells upon p53 induction (Ireno et al., 2014) might be provoked by MDM2-mediated PARP1 degradation. Additionally, it was shown that, in U2OS cells, the loss of PARP1 MARylation on serine residues 499, 507 and 519 leads to marked sensitization to all PARP1/PARP2 inhibitors. PARP1 auto-modification seems indeed to prevent trapping, thus limiting the interaction with DNA breaks, presumably through steric and electrostatic interference (Prokhorova et al., 2021b). Assessing the impact of MDM2 on PARP1 auto-MARylation would be of paramount importance to define the impact of p53 induction and MDM2 accumulation on therapeutic efficacy of PARP inhibitors.

5.5 ADP-ribosylation of p53

P53 is a target of PARylation upon DNA damage (Kanai et al., 2007; Malanga et al., 1998; Wang et al., 1998). Thus, it is tempting to speculate that MDM2-mediated regulation of ADP-ribosylation could represent an additional indirect way for MDM2 to regulate p53. PARylation of p53 has been reported to have different functional outcomes. It blocks the p53 interaction with the nuclear export receptor CRM1 upon DNA damage, thereby favoring nuclear accumulation (Kanai et al., 2007). On top, PARylated p53 has been shown to be unable to bind to the DNA consensus sequences in the promoters of its cognate genes (Malanga et al., 1998; Simbulan-Rosenthal et al., 2001). Based on these studies, MDM2-dependent PARP1 inactivation could limit p53 PARylation, promoting p53 export from the nucleus, but also transcriptional transactivation of the target genes. In order to test this hypothesis, p53 subcellular localization should be analyzed by immunostaining, and the expression of p53 target genes should be tested by quantitative RT-PCR. In addition, it would be important to determine: (1) p53-PARylation upon MDM2 accumulation, and (2) the p53 residues targeted by PARylation.

5.5.1 Regulation of p53 PARylation by MDM2

We measured the overall levels of PAR upon Nutlin treatment in the whole cell lysates of the p53 wild type cell line SJSA-1 by immunoblot analysis (Publication Figure 1I, 1J). However, we do not know if the PARylation of p53 is affected. To further explore this aspect, p53 could

be immunoprecipitated and PAR levels could be detected after treatment with the MDM2 antagonist MI1061 to activate p53. The MDM2 PROTAC could be used in the same context to discriminate the impact of MDM2 on p53 PARylation from the direct/indirect impact of the other p53 targets. Since MDM2 interacts with PARP1 and p53 via different domains, namely the central/acidic domain and the N-terminal domain, respectively, we might speculate that MDM2 might bind both factors in a complex to repress p53 PARylation.

MDM2-PARP1 interaction might be regulated by posttranslational modifications to modulate p53 PARylation in a temporal and spatial fashion. For instance, the serine/threonine kinases ATM and ATR, which are activating p53, are also capable of targeting MDM2 and PARP1. Phosphorylation of MDM2 and/or PARP1 could promote MDM2 regulation of PARP1 boosting the transactivation of p53 target genes. Upon phosphorylation removal, p53 PARylation could be restored to prevent p53 activity as transcription faction, as part of an additional negative regulatory feedback loop. This would be in line with the intricate interplay observed between ADP-ribosylation and other kinds of posttranslational modifications, which is just starting to emerge (Prokhorova et al., 2021a). Another thing we must take into account is the high turnover of ADP-ribosylation. P53 modified molecules might indeed undergo very high turnover to keep a balance of active and inactive molecules.

Establishing the dynamics of p53 PARylation during the p53 response is of paramount importance to understand the role of this modification in p53 regulation. P53 PARylation might serve different functions in the p53 response, which might be modulated by the MDM2-PARP1 interaction, and by posttranslational modifications. One first approach to elucidate these dynamics could be to monitor the levels of PAR on p53 during different phases of the p53 response, by preforming immunoprecipitation of p53 upon different time points of Nutlin treatment in p53 proficient cell lines. The quantification of p53 targets transcripts could be used as a readout for p53 activity.

5.5.2 P53 residues targeted by PARylation

In addition to what mentioned above, the functional outcome of p53 PARylation might depend on the targeted residue. All the studies on p53 PARylation published until now use an antibody that is recognizing PAR. This is unable to discriminate PAR chains bound to different amino acids and it cannot detect MAR. Taking advantage of this antibody, the modified residues on p53 were identified to be E255, D256 and E268 (Kanai et al., 2007). However, we cannot exclude the presence of other MARylated residues that could not be detected. The newly developed substrate-specific antibodies and the possibility of synthetizing recombinant ADP-ribosylated peptides could help identifying other residues of p53 targeted by MARylation and the nature of the targeted amino acids (Longarini and Matic, 2022). Modulation of the length

of the ADP-ribose modification and of the targeted residue could allow further regulation of p53 by the MDM2-PARP1 pathway.

5.6 Role of MDM2 in the Fork Speed Regulatory Network (FSRN)

Our results confirm a critical role of PARP1 and its activity in the regulation of DNA replication fork speed (Publication Figure 3). In order to recapitulate how PARP1, PARylation and the p53-p21 axis provide a coordinated mechanism to regulate the speed of fork progression, Prof. Jiri Bartek's lab proposes a model named Fork Speed Regulatory Network (FSRN) (Maya-Mendoza et al., 2018; Merchut-Maya et al., 2019). According to this model, during unperturbed S phase PARP1, together with p53 and CtBP, forms a co-repressor complex on p21 gene promoter (Madison and Lundblad, 2010; Maya-Mendoza et al., 2018). Additionally, PARP1 directly binds p21 keeping it in an inactive state (Dutto et al., 2016). P21 strongly represses DNA replication fork progression by two main mechanisms: (i) p21 amino-terminal domain inhibits cyclin/CDK kinases, (ii) p21 carboxy-terminal domain strongly binds and inhibits PCNA (Chen et al., 1995; Luo et al., 1995). Upon DNA damage, PARP1 auto-modification causes the release of the p21 co-repressor complex. When this happens, the p53-p300 complex is recruited, leading to p21 transactivation (Madison and Lundblad, 2010; Maya-Mendoza et al., 2018; Merchut-Maya et al., 2019). At the same time, PARP1 auto-PARylation abolishes the interaction with p21. P21 can then directly interact with PCNA, blocking DNA replication (Chen et al., 1995; Luo et al., 1995). In this context, fork uncoupling provokes the accumulation of ssDNA that is coated by RPA. This activates ATR, ultimately leading to ORI firing, inhibition of replication domains activation, cell cycle arrest (Marechal and Zou, 2013). Based on this model, we can envision MDM2-mediated inactivation of PARylation favoring stabilization of the PARP1-p21 interaction, and the p21 co-repressor complexes, ultimately promoting DNA replication fork progression, which is in line with what we observed at single replication forks via DNA fiber assays (Publication Figure 3). This role of MDM2 in promoting DNA elongation via PARP1 inactivation is further supported by the observation that loss of p53 causes fork stalling, but this is disabled by concomitant PARP1 knock down (Maya-Mendoza et al., 2018). Moreover, according to our findings, PARP1 initial inactivation by MDM2 is followed by ubiquitination and proteasomal degradation (Publication Figure 1). Upon PARP1 degradation, p21 binding to the fork might be promoted with consequent slowdown of replication and cell cycle arrest. This is supported by a strong reduction of DNA elongation rate in SJSA-1 cells upon a 12 hours treatment with Nutlin, which leads to extensive PARP1 degradation (data not shown). Moreover, we might speculate that different kinds of ADP-ribosylation might affect differentially PARP1 retention in the PARP1-p21, and the p21 co-repressor complexes. For instance, MARylation could be maintained at a steady state during unperturbed S-phase. PARylation, instead, might trigger the release of PARP1 with concomitant p21 induction.

Indeed, a recent publication showed that MARylation is maintained on chromatin throughout the cell cycle, and is well tolerated, while persistent PARylation results in elevated γH2AX levels and cytotoxicity (Prokhorova et al., 2021a). Defining the impact of MDM2 on the stability of the PARP1-p21, and the p21 co-repressor complexes, would help to elucidate further the role of MDM2 in regulating p21 activity and DNA replication. Additionally, analyzing newly synthetized DNA tracks length upon p53 induction, and concomitant p21 depletion, would allow determining to which extent the suppression of p21 accumulation and activity at the forks contributes to the observed acceleration of DNA elongation upon MDM2 accumulation.

5.7 The MDM2-PARP1 axis: an extended model for p53's role in DNA replication

Considering the major role of DNA replication-associated mutations in cancer etiology (Tomasetti et al., 2017), DNA replication regulation has been hypothesized to be the main oncosuppressive activity of p53 (Gottifredi and Wiesmuller, 2018). However, full mechanistic understanding of the regulation of ongoing replication forks and cellular response to replication stress by p53 is still lacking. Therefore, this field of research has gained increasing interest in the past years, boosted by the identification of p53 localization and activity at replication forks (Gottifredi et al., 2001; Kumari et al., 2004; Roy et al., 2018).

Previous reports from our lab indicated that depletion of MDM2 is causing a decrease of fork progression in a p53 deficient background. Further studies showed controversial results and left an incomplete understanding of the molecular mechanisms at the base of p53-mediated induction of DNA synthesis (Gottifredi and Wiesmuller, 2018; Klusmann et al., 2016).

We observed an induction of nascent DNA elongation rate when p53 was activated by the MDM2 binders, Nutlin and MI-1061, in the MDM2 amplified, SJSA-1 cells, as well as in the non-transformed RPE cells. However, MDM2 specific degradation via proteolysis targeting chimera (PROTAC) reverted this effect, confirming that MDM2 is the major regulator of fork progression upon p53 activation (Publication Figure 3C). A role for p53 in the resumption of DNA synthesis upon replication stress has been shown in multiple cellular systems (Roy et al., 2018; Yeo et al., 2016). In these reports, p53 regulation of replication is independent from its transcriptional functions, as proved by the use of separation-of-function mutants. Conversely, our results provide evidence that, at least partially, the functions of p53 in the regulation of replication require transcriptional transactivation of MDM2.

These apparently discordant observations could be reconciled by the fact that p53 promotes two opposed DNA replication phenotypes that are, respectively, independent and dependent on transcriptional regulation. On one hand, p53-POLι (DNA Polymerase Iota) complexes by inducing idling cycles favors slowdown of replication through fork reversal (Hampp et al., 2016; Khare and Eckert, 2002). On the other hand, p53 enhances fork progression favoring

Translesion Synthesis (TLS) by the formation of p21-POLι complexes (Ihle et al., 2021). These two phenotypes become prominent based on the differentiation status of the cell. As recently reported by Prof. Lisa Wiesmüller's laboratory, stem cells cope with endogenous replication stress preferentially by activating the first phenotype, while differentiated cells seem to rely on the second one (Ihle et al., 2021). In the cellular systems we used, the second phenotype is prominent, confirmed by the fact that p53 activation by Nutlin treatment caused lengthening of replication tracks. Our results expand this model presenting additional mechanisms that integrate the second phenotype: p53 promotes the activity of RECQ1 and PRIMPOL by inducing MDM2 accumulation, with consequent resolution of reversed replication forks and DNA synthesis re-priming.

5.8 Regulation of DNA damage tolerance by MDM2

DNA damage tolerance mechanisms allow to overcome fork stalling to complete DNA synthesis. These include (1) fork reversal, (2) translesion synthesis, and (3) re-priming by PRIMPOL. Elucidating how these pathways are regulated by p53 and MDM2 is important to determine the response to many cancer therapeutic agents (Berti et al., 2020).

5.8.1 The role of MDM2 in fork reversal

We reported for the first time that MDM2 is antagonizing fork reversal (Pubication Figure 6). The finding that replication fork reversal prevents DNA damage accumulation in the past has led to the notion that it represents a response mechanism to replication stress, which promotes genome stability (Ray Chaudhuri et al., 2012). However, unregulated fork reversal counteracts DNA elongation, induces the formation of double-strand breaks (DSBs), and causes degradation of nascent DNA, ultimately resulting in genome instability (Krishnamoorthy et al., 2021; Quinet et al., 2017). For this reason, fork reversal is fine-tuned by many regulatory factors required to restrict it to specific replication stress conditions (Krishnamoorthy et al., 2021). PARP1 is involved in the stabilization of reversed forks by RECQ1 inactivation, while being dispensable for their formation (Berti et al., 2013). Thus, MDM2 destabilizes reversed forks by antagonizing PARP1 activity, counterbalancing the p53-POLι (DNA Polymerase Iota) complexes-mediated induction of fork reversal (Hampp et al., 2016). We can envision MDM2 regulation of fork reversal to affect cellular fitness in a context-dependent manner. Upon moderate levels of DNA damage and replication stress, p53-mediated induction of MDM2 could contribute limiting fork reversal, favoring DNA replication completion and cell survival. In a context of prolonged p53 induction caused by severe DNA damage, MDM2 would provoke untimely restart of reversed forks fueling DNA damage accumulation and cell death. This is depicting MDM2 regulation of fork reversal by PARP1 inactivation as part of p53 oncosuppressive activity.

5.8.2 MDM2 in Translesion Synthesis (TLS)

Stalled replication forks engage translesion synthesis (TLS) polymerases to bypass replication obstacles, allowing DNA synthesis completion under replication stress (Yang and Gao, 2018). TLS has been shown to be a prominent mechanism of DNA damage tolerance upon PARP inhibition (Genois et al., 2021). The impact of p53 activation on TLS is not yet clarified. Transcriptional transactivation activity of p53 has been shown to both support and repress TLS (Avkin et al., 2006; Lerner et al., 2017; Livneh, 2006). Moreover, p53 enhances the use of TLS directly at forks by the formation of p21-POLι complexes (Ihle et al., 2021). To further investigate the interplay between p53 and TLS, DNA fiber assay could be exploited. Since TLS allows forks to progress faster under stress (Nayak et al., 2020), DNA fiber assay upon MDM2 induction could be performed in cells depleted of the TLS key factors RAD18 and REV1. These experiments would help clarifying the impact of MDM2 accumulation on TLS and expand our knowledge over p53 regulation of DNA replication.

5.8.3 Impact of MDM2 on PRIMPOL-mediated re-priming

MDM2 enhances the activity of PRIMPOL, which restarting DNA synthesis downstream DNA replication roadblocks, causes the accumulation of ssDNA stretches (Publication Figure 5). Being PRIMPOL re-priming an error-prone pathway, it is subject to a tight regulatory network that is just starting to emerge. PRIMPOL protein levels are regulated by the deubiquitylase USP36 in a stress-dependent fashion (Yan et al., 2020). PRIMPOL activity is stimulated by the Polymerase δ–interacting protein 2 (PolDIP2) (Kasho et al., 2021). PRIMPOL is transcriptionally transactivated by ATR, and it is regulated through the cell cycle by phosphorylation of the kinase PLK1 (Bailey et al., 2021; Quinet et al., 2020). Recently, the laboratory of Prof. David Cortez has reported that PRIMPOL is activated by Chk1-mediated phosphorylation *in vitro* and *in vivo* (Mehta et al., 2022).

We still miss a mechanistic explanation for the enhanced PRIMPOL activity found upon MDM2 accumulation. It is unknown whether ADP-ribosylation could regulate it. Mass spectrometry or immunoprecipitation experiments in cells undergoing different kinds of genetic insults could help finding out whether PRIMPOL is subject to ADP-ribosylation, and under which conditions. However, the absence of a good antibody against PRIMPOL is still representing a technical challenge. We could speculate that PARylation could antagonize PRIMPOL activity by preventing its phosphorylation by Chk1. This would be the mechanistic base for the observed PRIMPOL activation upon PARP1 inhibition (Genois et al., 2021).

Finally, fork reversal and PRIMPOL-mediated re-priming have been reported to be alternative mechanisms antagonizing each other. Our results strongly suggest that MDM2 accumulation

tilts the balance toward re-priming at the expenses of genomic stability and cell survival (Publication Figure 7).

6. CONCLUSION

In this thesis work, we investigated the interplay of the MDM2 oncoprotein and PARP1. MDM2 is mostly known as an antagonist of the tumor suppressor protein p53. Moreover, MDM2 synthesis is enhanced by p53, thus providing a negative feedback loop. Here, we report the decrease of PARP1 levels upon p53 activation. This decrease in PARP1 depended on the proteasome and on the MDM2 oncoprotein (Publication Figures 1B, 1D, 1E). MDM2 promoted PARP1 ubiquitination, as shown by *in vitro* ubiquitination assays (Publication Figure 1H). The two proteins interacted physically, as demonstrated by co-immunoprecipitation (coIP) of purified MDM2 and PARP1, and pull down experiments using recombinant MDM2 fused to glutathione S-transferase (GST; Publication Figures 2A, S2A). The interaction was recapitulated in human cells, performing Proximity Ligation Assay (PLA) and coIP (Publication Figures 2B-G). Strikingly, MDM2 accumulation strongly reduced Poly(ADP-Ribose) (PAR) levels, suggesting an inhibitory effect of MDM2 on PARP1-mediated PARylation (Publication Figures 1I, 1J). Looking into the functional consequences of this interaction in the context of the DNA replication, we discovered that transactivation of MDM2 represents the main mechanism through which p53 enhances DNA replication fork progression (Publication Figure 3C), and this depends on the MDM2-mediated inactivation and destabilization of PARP1 (Publication Figure 3E-K). PARP1 inactivation by MDM2 promoted the restart of reversed replication forks by the helicase RECQ1 (Publication Figure 4). Indeed, we observed a profound decrease in the proportion of reversed DNA replication forks by MDM2 (Publication Figure 6). In the same context, we detected a more prominent activity of the primase/polymerase PRIMPOL, which contributed to the enhancement of the nascent DNA elongation, and the accumulation of DNA damage marks (Publication Figure 5). The MDM2-dependent enhancement of DNA replication fork progression led to increased genome instability and cell death upon treatment with the Topoisomerase I inhibitor camptothecin (Publication Figure 7). In conclusion, we report that MDM2 not only serves as an antagonist to p53; rather, it accelerates DNA replication by inactivating PARP1 and promoting the engagement of DNA damage tolerance mechanisms. Hence, the MDM2 oncoprotein not only provides negative feedback to p53 activity, but also acts as an effector of p53 to shape the progression of DNA replication forks.

7. ACKNOWLEDGMENTS

I would like to thank Prof. Dr. Matthias Dobbelstein for the opportunity to do my Ph.D. in his research laboratory. In the past four years he has supervised my research work with great enthusiasm, being always there to answer any question and ready to contribute to solve any issue. Most importantly, he has always supported me to pursue a scientific career. As never before in my life I felt encouraged to follow my dreams. He mentored me pointing out strengths and weaknesses, so that I could reach an objective view of my potential as a scientist. Together with my colleagues of the Institute of Molecular Oncology he strongly contributed to make our lab an amazing working environment. To my thesis committee members, Prof. Dr. Heidi Hahn and Prof. Dr. Argyris Papantonis– thank you very much for the past four years of annual meetings and always being there to provide feedback and valuable input for my project and career. I am also very grateful to Prof. Dr. Gunther Schneider, Prof. Dr. med. Elisabeth Hessmann and Dr. Ufuk Günesdogan for agreeing to be extended committee members.

8. REFERENCES

Aberle, L., Kruger, A., Reber, J.M., Lippmann, M., Hufnagel, M., Schmalz, M., Trussina, I., Schlesiger, S., Zubel, T., Schutz, K.*, et al.* (2020). PARP1 catalytic variants reveal branching and chain length-specific functions of poly(ADP-ribose) in cellular physiology and stress response. Nucleic Acids Res *48*, 10015-10033.

Adimoolam, S., and Ford, J.M. (2002). p53 and DNA damage-inducible expression of the xeroderma pigmentosum group C gene. Proc Natl Acad Sci U S A *99*, 12985-12990.

Aguilar-Quesada, R., Munoz-Gamez, J.A., Martin-Oliva, D., Peralta, A., Valenzuela, M.T., Matinez-Romero, R., Quiles-Perez, R., Menissier-de Murcia, J., de Murcia, G., Ruiz de Almodovar, M.*, et al.* (2007). Interaction between ATM and PARP-1 in response to DNA damage and sensitization of ATM deficient cells through PARP inhibition. BMC Mol Biol *8*, 29.

Ahel, D., Horejsi, Z., Wiechens, N., Polo, S.E., Garcia-Wilson, E., Ahel, I., Flynn, H., Skehel, M., West, S.C., Jackson, S.P.*, et al.* (2009). Poly(ADP-ribose)-dependent regulation of DNA repair by the chromatin remodeling enzyme ALC1. Science *325*, 1240-1243.

Aksoy, O., Chicas, A., Zeng, T., Zhao, Z., McCurrach, M., Wang, X., and Lowe, S.W. (2012). The atypical E2F family member E2F7 couples the p53 and RB pathways during cellular senescence. Genes Dev *26*, 1546-1557.

Alemasova, E.E., and Lavrik, O.I. (2019). Poly(ADP-ribosyl)ation by PARP1: reaction mechanism and regulatory proteins. Nucleic Acids Res *47*, 3811-3827.

Alt, J.R., Bouska, A., Fernandez, M.R., Cerny, R.L., Xiao, H., and Eischen, C.M. (2005). Mdm2 binds to Nbs1 at sites of DNA damage and regulates double strand break repair. J Biol Chem *280*, 18771-18781.
Arcaro, A., and Guerreiro, A.S. (2007). The phosphoinositide 3-kinase pathway in human cancer: genetic alterations and therapeutic implications. Curr Genomics *8*, 271-306.

Atkinson, J., and McGlynn, P. (2009). Replication fork reversal and the maintenance of genome stability. Nucleic Acids Res *37*, 3475-3492.

Avkin, S., Sevilya, Z., Toube, L., Geacintov, N., Chaney, S.G., Oren, M., and Livneh, Z. (2006). p53 and p21 regulate error-prone DNA repair to yield a lower mutation load. Mol Cell *22*, 407-413.

Azarm, K., and Smith, S. (2020). Nuclear PARPs and genome integrity. Genes Dev *34*, 285-301.

Bailey, L.J., Teague, R., Kolesar, P., Bainbridge, L.J., Lindsay, H.D., and Doherty, A.J. (2021). PLK1 regulates the PrimPol damage tolerance pathway during the cell cycle. Sci Adv *7*, eabh1004.

Baker, S.J., Fearon, E.R., Nigro, J.M., Hamilton, S.R., Preisinger, A.C., Jessup, J.M., vanTuinen, P., Ledbetter, D.H., Barker, D.F., Nakamura, Y.*, et al.* (1989). Chromosome 17 deletions and p53 gene mutations in colorectal carcinomas. Science *244*, 217-221.

Barak, Y., Gottlieb, E., Juven-Gershon, T., and Oren, M. (1994). Regulation of mdm2 expression by p53: alternative promoters produce transcripts with nonidentical translation potential. Genes Dev *8*, 1739-1749.

Bartz, S.R., Zhang, Z., Burchard, J., Imakura, M., Martin, M., Palmieri, A., Needham, R., Guo, J., Gordon, M., Chung, N.*, et al.* (2006). Small interfering RNA screens reveal enhanced cisplatin cytotoxicity in tumor cells having both BRCA network and TP53 disruptions. Mol Cell Biol *26*, 9377-9386.
Belousova, E.A., Ishchenko capital A, C., and Lavrik, O.I. (2018). Dna is a New Target of Parp3. Sci Rep *8*, 4176.

Berti, M., Ray Chaudhuri, A., Thangavel, S., Gomathinayagam, S., Kenig, S., Vujanovic, M., Odreman, F., Glatter, T., Graziano, S., Mendoza-Maldonado, R.*, et al.* (2013). Human RECQ1 promotes restart of replication forks reversed by DNA topoisomerase I inhibition. Nat Struct Mol Biol *20*, 347-354.

Berti, M., Teloni, F., Mijic, S., Ursich, S., Fuchs, J., Palumbieri, M.D., Krietsch, J., Schmid, J.A., Garcin, E.B., Gon, S.*, et al.* (2020). Sequential role of RAD51 paralog complexes in replication fork remodeling and restart. Nat Commun *11*, 3531.

Boeckler, F.M., Joerger, A.C., Jaggi, G., Rutherford, T.J., Veprintsev, D.B., and Fersht, A.R. (2008). Targeted rescue of a destabilized mutant of p53 by an in silico screened drug. Proc Natl Acad Sci U S A *105*, 10360-10365.

Bonfiglio, J.J., Leidecker, O., Dauben, H., Longarini, E.J., Colby, T., San Segundo-Acosta, P., Perez, K.A., and Matic, I. (2020). An HPF1/PARP1-Based Chemical Biology Strategy for Exploring ADP-Ribosylation. Cell *183*, 1086-1102 e1023.

Bork, P., Hofmann, K., Bucher, P., Neuwald, A.F., Altschul, S.F., and Koonin, E.V. (1997). A superfamily of conserved domains in DNA damage-responsive cell cycle checkpoint proteins. FASEB J *11*, 68-76.

Braun, S.A., Panzeter, P.L., Collinge, M.A., and Althaus, F.R. (1994). Endoglycosidic cleavage of branched polymers by poly(ADP-ribose) glycohydrolase. Eur J Biochem *220*, 369-375.

Brookes, S., Rowe, J., Ruas, M., Llanos, S., Clark, P.A., Lomax, M., James, M.C., Vatcheva, R., Bates, S., Vousden, K.H.*, et al.* (2002). INK4a-deficient human diploid fibroblasts are resistant to RAS-induced senescence. EMBO J *21*, 2936-2945.

Bryant, H.E., Schultz, N., Thomas, H.D., Parker, K.M., Flower, D., Lopez, E., Kyle, S., Meuth, M., Curtin, N.J., and Helleday, T. (2005). Specific killing of BRCA2-deficient tumours with inhibitors of poly(ADP-ribose) polymerase. Nature *434*, 913-917.

Bunz, F., Hwang, P.M., Torrance, C., Waldman, T., Zhang, Y., Dillehay, L., Williams, J., Lengauer, C., Kinzler, K.W., and Vogelstein, B. (1999). Disruption of p53 in human cancer cells alters the responses to therapeutic agents. J Clin Invest *104*, 263-269.

Bykov, V.J., Issaeva, N., Shilov, A., Hultcrantz, M., Pugacheva, E., Chumakov, P., Bergman, J., Wiman, K.G., and Selivanova, G. (2002). Restoration of the tumor suppressor function to mutant p53 by a low-molecular-weight compound. Nat Med *8*, 282-288.

Caldecott, K.W. (2008). Single-strand break repair and genetic disease. Nat Rev Genet *9*, 619-631.

Caldecott, K.W., McKeown, C.K., Tucker, J.D., Ljungquist, S., and Thompson, L.H. (1994). An interaction between the mammalian DNA repair protein XRCC1 and DNA ligase III. Mol Cell Biol *14*, 68-76.

Cancer Genome Atlas Research, N., Weinstein, J.N., Collisson, E.A., Mills, G.B., Shaw, K.R., Ozenberger, B.A., Ellrott, K., Shmulevich, I., Sander, C., and Stuart, J.M. (2013). The Cancer Genome Atlas Pan-Cancer analysis project. Nat Genet *45*, 1113-1120.

Chapman, J.R., Taylor, M.R., and Boulton, S.J. (2012). Playing the end game: DNA double-strand break repair pathway choice. Mol Cell *47*, 497-510.

Chen, J., Jackson, P.K., Kirschner, M.W., and Dutta, A. (1995). Separate domains of p21 involved in the inhibition of Cdk kinase and PCNA. Nature *374*, 386-388.

Chen, Q., Kassab, M.A., Dantzer, F., and Yu, X. (2018). PARP2 mediates branched poly ADP-ribosylation in response to DNA damage. Nat Commun *9*, 3233.

Cheng, T.H., and Cohen, S.N. (2007). Human MDM2 isoforms translated differentially on constitutive versus p53-regulated transcripts have distinct functions in the p53/MDM2 and TSG101/MDM2 feedback control loops. Mol Cell Biol *27*, 111-119.

Cong, K., Peng, M., Kousholt, A.N., Lee, W.T.C., Lee, S., Nayak, S., Krais, J., VanderVere-Carozza, P.S., Pawelczak, K.S., Calvo, J.*, et al.* (2021a). Replication gaps are a key determinant of PARP inhibitor synthetic lethality with BRCA deficiency. Mol Cell *81*, 3128-3144 e3127.

Cong, K., Peng, M., Kousholt, A.N., Lee, W.T.C., Lee, S., Nayak, S., Krais, J., VanderVere-Carozza, P.S., Pawelczak, K.S., Calvo, J.*, et al.* (2021b). Replication gaps are a key determinant of PARP inhibitor synthetic lethality with BRCA deficiency. Mol Cell *81*, 3227.

Cortes, U., Tong, W.M., Coyle, D.L., Meyer-Ficca, M.L., Meyer, R.G., Petrilli, V., Herceg, Z., Jacobson, E.L., Jacobson, M.K., and Wang, Z.Q. (2004). Depletion of the 110-kilodalton isoform of poly(ADP-ribose) glycohydrolase increases sensitivity to genotoxic and endotoxic stress in mice. Mol Cell Biol *24*, 7163-7178.

Couch, F.B., Bansbach, C.E., Driscoll, R., Luzwick, J.W., Glick, G.G., Betous, R., Carroll, C.M., Jung, S.Y., Qin, J., Cimprich, K.A.*, et al.* (2013). ATR phosphorylates SMARCAL1 to prevent replication fork collapse. Genes Dev *27*, 1610-1623.

Crawford, K., Bonfiglio, J.J., Mikoc, A., Matic, I., and Ahel, I. (2018). Specificity of reversible ADP-ribosylation and regulation of cellular processes. Crit Rev Biochem Mol Biol *53*, 64-82.

D'Andrea, A.D. (2018). Mechanisms of PARP inhibitor sensitivity and resistance. DNA Repair (Amst) *71*, 172-176.

Dantzer, F., de La Rubia, G., Menissier-De Murcia, J., Hostomsky, Z., de Murcia, G., and Schreiber, V. (2000). Base excision repair is impaired in mammalian cells lacking Poly(ADP-ribose) polymerase-1. Biochemistry *39*, 7559-7569.

Dantzer, F., Schreiber, V., Niedergang, C., Trucco, C., Flatter, E., De La Rubia, G., Oliver, J., Rolli, V., Menissier-de Murcia, J., and de Murcia, G. (1999). Involvement of poly(ADP-ribose) polymerase in base excision repair. Biochimie *81*, 69-75.

Das, B.B., Huang, S.Y., Murai, J., Rehman, I., Ame, J.C., Sengupta, S., Das, S.K., Majumdar, P., Zhang, H., Biard, D.*, et al.* (2014). PARP1-TDP1 coupling for the repair of topoisomerase I-induced DNA damage. Nucleic Acids Res *42*, 4435-4449.

Dawicki-McKenna, J.M., Langelier, M.F., DeNizio, J.E., Riccio, A.A., Cao, C.D., Karch, K.R., McCauley, M., Steffen, J.D., Black, B.E., and Pascal, J.M. (2015). PARP-1 Activation Requires Local Unfolding of an Autoinhibitory Domain. Mol Cell *60*, 755-768.

DeLeo, A.B., Jay, G., Appella, E., Dubois, G.C., Law, L.W., and Old, L.J. (1979). Detection of a transformation-related antigen in chemically induced sarcomas and other transformed cells of the mouse. Proc Natl Acad Sci U S A *76*, 2420-2424.

Dobbelstein, M., Wienzek, S., Konig, C., and Roth, J. (1999). Inactivation of the p53-homologue p73 by the mdm2-oncoprotein. Oncogene *18*, 2101-2106.

Dohmesen, C., Koeppel, M., and Dobbelstein, M. (2008). Specific inhibition of Mdm2-mediated neddylation by Tip60. Cell Cycle *7*, 222-231.

Donehower, L.A., Harvey, M., Slagle, B.L., McArthur, M.J., Montgomery, C.A., Jr., Butel, J.S., and Bradley, A. (1992). Mice deficient for p53 are developmentally normal but susceptible to spontaneous tumours. Nature *356*, 215-221.

Donehower, L.A., and Lozano, G. (2009). 20 years studying p53 functions in genetically engineered mice. Nat Rev Cancer *9*, 831-841.

Dungrawala, H., Rose, K.L., Bhat, K.P., Mohni, K.N., Glick, G.G., Couch, F.B., and Cortez, D. (2015). The Replication Checkpoint Prevents Two Types of Fork Collapse without Regulating Replisome Stability. Mol Cell *59*, 998-1010.

Dutto, I., Sukhanova, M., Tillhon, M., Cazzalini, O., Stivala, L.A., Scovassi, A.I., Lavrik, O., and Prosperi, E. (2016). p21CDKN1A Regulates the Binding of Poly(ADP-Ribose) Polymerase-1 to DNA Repair Intermediates. PLoS One *11*, e0146031.

El-Khamisy, S.F., Masutani, M., Suzuki, H., and Caldecott, K.W. (2003). A requirement for PARP-1 for the assembly or stability of XRCC1 nuclear foci at sites of oxidative DNA damage. Nucleic Acids Res *31*, 5526-5533.

El-Khamisy, S.F., Saifi, G.M., Weinfeld, M., Johansson, F., Helleday, T., Lupski, J.R., and Caldecott, K.W. (2005). Defective DNA single-strand break repair in spinocerebellar ataxia with axonal neuropathy-1. Nature *434*, 108-113.

Eliyahu, D., Michalovitz, D., Eliyahu, S., Pinhasi-Kimhi, O., and Oren, M. (1989). Wild-type p53 can inhibit oncogene-mediated focus formation. Proc Natl Acad Sci U S A *86*, 8763-8767.

Eliyahu, D., Raz, A., Gruss, P., Givol, D., and Oren, M. (1984). Participation of p53 cellular tumour antigen in transformation of normal embryonic cells. Nature *312*, 646-649.

Essers, J., Theil, A.F., Baldeyron, C., van Cappellen, W.A., Houtsmuller, A.B., Kanaar, R., and Vermeulen, W. (2005). Nuclear dynamics of PCNA in DNA replication and repair. Mol Cell Biol *25*, 9350-9359.

Fan, J., Wilson, P.F., Wong, H.K., Urbin, S.S., Thompson, L.H., and Wilson, D.M., 3rd (2007). XRCC1 down-regulation in human cells leads to DNA-damaging agent hypersensitivity, elevated sister chromatid exchange, and reduced survival of BRCA2 mutant cells. Environ Mol Mutagen *48*, 491-500.

Fang, S., Jensen, J.P., Ludwig, R.L., Vousden, K.H., and Weissman, A.M. (2000). Mdm2 is a RING finger-dependent ubiquitin protein ligase for itself and p53. J Biol Chem *275*, 8945-8951.

Farmer, H., McCabe, N., Lord, C.J., Tutt, A.N., Johnson, D.A., Richardson, T.B., Santarosa, M., Dillon, K.J., Hickson, I., Knights, C.*, et al.* (2005). Targeting the DNA repair defect in BRCA mutant cells as a therapeutic strategy. Nature *434*, 917-921.

Fields, S., and Jang, S.K. (1990). Presence of a potent transcription activating sequence in the p53 protein. Science *249*, 1046-1049.

Finlay, C.A., Hinds, P.W., and Levine, A.J. (1989). The p53 proto-oncogene can act as a suppressor of transformation. Cell *57*, 1083-1093.

Fortin, A., Cregan, S.P., MacLaurin, J.G., Kushwaha, N., Hickman, E.S., Thompson, C.S., Hakim, A., Albert, P.R., Cecconi, F., Helin, K.*, et al.* (2001). APAF1 is a key transcriptional target for p53 in the regulation of neuronal cell death. J Cell Biol *155*, 207-216.

Galbiati, F., Volonte, D., Liu, J., Capozza, F., Frank, P.G., Zhu, L., Pestell, R.G., and Lisanti, M.P. (2001). Caveolin-1 expression negatively regulates cell cycle progression by inducing G(0)/G(1) arrest via a p53/p21(WAF1/Cip1)-dependent mechanism. Mol Biol Cell *12*, 2229-2244.

Gatti, M., Imhof, R., Huang, Q., Baudis, M., and Altmeyer, M. (2020). The Ubiquitin Ligase TRIP12 Limits PARP1 Trapping and Constrains PARP Inhibitor Efficiency. Cell Rep *32*, 107985.

Genois, M.M., Gagne, J.P., Yasuhara, T., Jackson, J., Saxena, S., Langelier, M.F., Ahel, I., Bedford, M.T., Pascal, J.M., Vindigni, A.*, et al.* (2021). CARM1 regulates replication fork speed and stress response by stimulating PARP1. Mol Cell *81*, 784-800 e788.

Gibbs-Seymour, I., Fontana, P., Rack, J.G.M., and Ahel, I. (2016). HPF1/C4orf27 Is a PARP-1-Interacting Protein that Regulates PARP-1 ADP-Ribosylation Activity. Mol Cell *62*, 432-442.

Gibson, B.A., and Kraus, W.L. (2012). New insights into the molecular and cellular functions of poly(ADP-ribose) and PARPs. Nat Rev Mol Cell Biol *13*, 411-424.

Giono, L.E., Resnick-Silverman, L., Carvajal, L.A., St Clair, S., and Manfredi, J.J. (2017). Mdm2 promotes Cdc25C protein degradation and delays cell cycle progression through the G2/M phase. Oncogene *36*, 6762-6773.

Goldberg, Z., Vogt Sionov, R., Berger, M., Zwang, Y., Perets, R., Van Etten, R.A., Oren, M., Taya, Y., and Haupt, Y. (2002). Tyrosine phosphorylation of Mdm2 by c-Abl: implications for p53 regulation. EMBO J *21*, 3715-3727.

Gottifredi, V., Shieh, S., Taya, Y., and Prives, C. (2001). p53 accumulates but is functionally impaired when DNA synthesis is blocked. Proc Natl Acad Sci U S A *98*, 1036-1041.

Gottifredi, V., and Wiesmuller, L. (2018). The Tip of an Iceberg: Replication-Associated Functions of the Tumor Suppressor p53. Cancers (Basel) *10*.

Grasberger, B.L., Lu, T., Schubert, C., Parks, D.J., Carver, T.E., Koblish, H.K., Cummings, M.D., LaFrance, L.V., Milkiewicz, K.L., Calvo, R.R.*, et al.* (2005). Discovery and cocrystal structure of benzodiazepinedione HDM2 antagonists that activate p53 in cells. J Med Chem *48*, 909-912.

Gupte, R., Liu, Z., and Kraus, W.L. (2017). PARPs and ADP-ribosylation: recent advances linking molecular functions to biological outcomes. Genes Dev *31*, 101-126.

Haince, J.F., Kozlov, S., Dawson, V.L., Dawson, T.M., Hendzel, M.J., Lavin, M.F., and Poirier, G.G. (2007). Ataxia telangiectasia mutated (ATM) signaling network is modulated by a novel poly(ADP-ribose)-dependent pathway in the early response to DNA-damaging agents. J Biol Chem *282*, 16441-16453.

Haince, J.F., McDonald, D., Rodrigue, A., Dery, U., Masson, J.Y., Hendzel, M.J., and Poirier, G.G. (2008). PARP1-dependent kinetics of recruitment of MRE11 and NBS1 proteins to multiple DNA damage sites. J Biol Chem *283*, 1197-1208.

Hampp, S., Kiessling, T., Buechle, K., Mansilla, S.F., Thomale, J., Rall, M., Ahn, J., Pospiech, H., Gottifredi, V., and Wiesmuller, L. (2016). DNA damage tolerance pathway involving DNA polymerase iota and the tumor suppressor p53 regulates DNA replication fork progression. Proc Natl Acad Sci U S A *113*, E4311-4319.

Hanzlikova, H., Kalasova, I., Demin, A.A., Pennicott, L.E., Cihlarova, Z., and Caldecott, K.W. (2018). The Importance of Poly(ADP-Ribose) Polymerase as a Sensor of Unligated Okazaki Fragments during DNA Replication. Mol Cell *71*, 319-331 e313.

Harper, J.W., Elledge, S.J., Keyomarsi, K., Dynlacht, B., Tsai, L.H., Zhang, P., Dobrowolski, S., Bai, C., Connell-Crowley, L., Swindell, E.*, et al.* (1995). Inhibition of cyclin-dependent kinases by p21. Mol Biol Cell *6*, 387-400.

Hatakeyama, K., Nemoto, Y., Ueda, K., and Hayaishi, O. (1986). Purification and characterization of poly(ADP-ribose) glycohydrolase. Different modes of action on large and small poly(ADP-ribose). J Biol Chem *261*, 14902-14911.

Haupt, Y., Maya, R., Kazaz, A., and Oren, M. (1997). Mdm2 promotes the rapid degradation of p53. Nature *387*, 296-299.

Helleday, T. (2011a). DNA repair as treatment target. Eur J Cancer *47 Suppl 3*, S333-335.

Helleday, T. (2011b). The underlying mechanism for the PARP and BRCA synthetic lethality: clearing up the misunderstandings. Mol Oncol *5*, 387-393.

Hendriks, I.A., Larsen, S.C., and Nielsen, M.L. (2019). An Advanced Strategy for Comprehensive Profiling of ADP-ribosylation Sites Using Mass Spectrometry-based Proteomics. Mol Cell Proteomics *18*, 1010-1026.

Henningsen, K.M., Manzini, V., Magerhans, A., Gerber, S., and Dobbelstein, M. (2021). MDM2-Driven Ubiquitination Rapidly Removes p53 from Its Cognate Promoters. Biomolecules *12*.

Hermeking, H., Lengauer, C., Polyak, K., He, T.C., Zhang, L., Thiagalingam, S., Kinzler, K.W., and Vogelstein, B. (1997). 14-3-3sigma is a p53-regulated inhibitor of G2/M progression. Mol Cell *1*, 3-11.

Hoch, N.C., Hanzlikova, H., Rulten, S.L., Tetreault, M., Komulainen, E., Ju, L., Hornyak, P., Zeng, Z., Gittens, W., Rey, S.A.*, et al.* (2017). XRCC1 mutation is associated with PARP1 hyperactivation and cerebellar ataxia. Nature *541*, 87-91.

Hochegger, H., Dejsuphong, D., Fukushima, T., Morrison, C., Sonoda, E., Schreiber, V., Zhao, G.Y., Saberi, A., Masutani, M., Adachi, N.*, et al.* (2006). Parp-1 protects homologous recombination from interference by Ku and Ligase IV in vertebrate cells. EMBO J *25*, 1305-1314.

Honda, R., Tanaka, H., and Yasuda, H. (1997). Oncoprotein MDM2 is a ubiquitin ligase E3 for tumor suppressor p53. FEBS Lett *420*, 25-27.

Hu, Y., Petit, S.A., Ficarro, S.B., Toomire, K.J., Xie, A., Lim, E., Cao, S.A., Park, E., Eck, M.J., Scully, R.*, et al.* (2014). PARP1-driven poly-ADP-ribosylation regulates BRCA1 function in homologous recombination-mediated DNA repair. Cancer Discov *4*, 1430-1447.

Ihle, M., Biber, S., Schroeder, I.S., Blattner, C., Deniz, M., Damia, G., Gottifredi, V., and Wiesmuller, L. (2021). Impact of the interplay between stemness features, p53 and pol iota on replication pathway choices. Nucleic Acids Res *49*, 7457-7475.

Illuzzi, G., Fouquerel, E., Ame, J.C., Noll, A., Rehmet, K., Nasheuer, H.P., Dantzer, F., and Schreiber, V. (2014). PARG is dispensable for recovery from transient replicative stress but required to prevent detrimental accumulation of poly(ADP-ribose) upon prolonged replicative stress. Nucleic Acids Res *42*, 7776-7792.

Ireno, I.C., Wiehe, R.S., Stahl, A.I., Hampp, S., Aydin, S., Troester, M.A., Selivanova, G., and Wiesmuller, L. (2014). Modulation of the poly (ADP-ribose) polymerase inhibitor response and DNA recombination in breast cancer cells by drugs affecting endogenous wild-type p53. Carcinogenesis *35*, 2273-2282.

Iwashita, A., Hattori, K., Yamamoto, H., Ishida, J., Kido, Y., Kamijo, K., Murano, K., Miyake, H., Kinoshita, T., Warizaya, M.*, et al.* (2005). Discovery of quinazolinone and quinoxaline derivatives as potent and selective poly(ADP-ribose) polymerase-1/2 inhibitors. FEBS Lett *579*, 1389-1393.

Jenkins, J.R., Rudge, K., and Currie, G.A. (1984). Cellular immortalization by a cDNA clone encoding the transformation-associated phosphoprotein p53. Nature *312*, 651-654.

Junttila, M.R., Karnezis, A.N., Garcia, D., Madriles, F., Kortlever, R.M., Rostker, F., Brown Swigart, L., Pham, D.M., Seo, Y., Evan, G.I.*, et al.* (2010). Selective activation of p53-mediated tumour suppression in high-grade tumours. Nature *468*, 567-571.

Kallen, J., Goepfert, A., Blechschmidt, A., Izaac, A., Geiser, M., Tavares, G., Ramage, P., Furet, P., Masuya, K., and Lisztwan, J. (2009). Crystal Structures of Human MdmX (HdmX) in Complex with p53 Peptide Analogues Reveal Surprising Conformational Changes. J Biol Chem *284*, 8812-8821.

Kamijo, T., Weber, J.D., Zambetti, G., Zindy, F., Roussel, M.F., and Sherr, C.J. (1998). Functional and physical interactions of the ARF tumor suppressor with p53 and Mdm2. Proc Natl Acad Sci U S A *95*, 8292-8297.

Kanai, M., Hanashiro, K., Kim, S.H., Hanai, S., Boulares, A.H., Miwa, M., and Fukasawa, K. (2007). Inhibition of Crm1-p53 interaction and nuclear export of p53 by poly(ADP-ribosyl)ation. Nat Cell Biol *9*, 1175-1183.

Kang, H.C., Lee, Y.I., Shin, J.H., Andrabi, S.A., Chi, Z., Gagne, J.P., Lee, Y., Ko, H.S., Lee, B.D., Poirier, G.G.*, et al.* (2011). Iduna is a poly(ADP-ribose) (PAR)-dependent E3 ubiquitin ligase that regulates DNA damage. Proc Natl Acad Sci U S A *108*, 14103-14108.

Kashima, L., Idogawa, M., Mita, H., Shitashige, M., Yamada, T., Ogi, K., Suzuki, H., Toyota, M., Ariga, H., Sasaki, Y.*, et al.* (2012). CHFR protein regulates mitotic checkpoint by targeting PARP-1 protein for ubiquitination and degradation. J Biol Chem *287*, 12975-12984.

Kasho, K., Stojkovic, G., Velazquez-Ruiz, C., Martinez-Jimenez, M.I., Doimo, M., Laurent, T., Berner, A., Perez-Rivera, A.E., Jenninger, L., Blanco, L.*, et al.* (2021). A unique arginine cluster in PolDIP2 enhances nucleotide binding and DNA synthesis by PrimPol. Nucleic Acids Res *49*, 2179-2191.

Kawamitsu, H., Hoshino, H., Okada, H., Miwa, M., Momoi, H., and Sugimura, T. (1984). Monoclonal antibodies to poly(adenosine diphosphate ribose) recognize different structures. Biochemistry *23*, 3771-3777.

Khare, V., and Eckert, K.A. (2002). The proofreading 3'-->5' exonuclease activity of DNA polymerases: a kinetic barrier to translesion DNA synthesis. Mutat Res *510*, 45-54.

Kim, M.Y., Zhang, T., and Kraus, W.L. (2005). Poly(ADP-ribosyl)ation by PARP-1: 'PAR-laying' NAD+ into a nuclear signal. Genes Dev *19*, 1951-1967.

King, B.S., Cooper, K.L., Liu, K.J., and Hudson, L.G. (2012). Poly(ADP-ribose) contributes to an association between poly(ADP-ribose) polymerase-1 and xeroderma pigmentosum complementation group A in nucleotide excision repair. J Biol Chem *287*, 39824-39833.

Klusmann, I., Rodewald, S., Muller, L., Friedrich, M., Wienken, M., Li, Y., Schulz-Heddergott, R., and Dobbelstein, M. (2016). p53 Activity Results in DNA Replication Fork Processivity. Cell Rep *17*, 1845-1857.

Klusmann, I., Wohlberedt, K., Magerhans, A., Teloni, F., Korbel, J.O., Altmeyer, M., and Dobbelstein, M. (2018). Chromatin modifiers Mdm2 and RNF2 prevent RNA:DNA hybrids that impair DNA replication. Proc Natl Acad Sci U S A *115*, E11311-E11320.

Kobet, E., Zeng, X., Zhu, Y., Keller, D., and Lu, H. (2000). MDM2 inhibits p300-mediated p53 acetylation and activation by forming a ternary complex with the two proteins. Proc Natl Acad Sci U S A *97*, 12547-12552.

Koh, D.W., Lawler, A.M., Poitras, M.F., Sasaki, M., Wattler, S., Nehls, M.C., Stoger, T., Poirier, G.G., Dawson, V.L., and Dawson, T.M. (2004). Failure to degrade poly(ADP-ribose) causes increased sensitivity to cytotoxicity and early embryonic lethality. Proc Natl Acad Sci U S A *101*, 17699-17704.

Kortlever, R.M., Higgins, P.J., and Bernards, R. (2006). Plasminogen activator inhibitor-1 is a critical downstream target of p53 in the induction of replicative senescence. Nat Cell Biol *8*, 877-884.

Kostic, M., Matt, T., Martinez-Yamout, M.A., Dyson, H.J., and Wright, P.E. (2006). Solution structure of the Hdm2 C2H2C4 RING, a domain critical for ubiquitination of p53. J Mol Biol *363*, 433-450.

Kranz, D., and Dobbelstein, M. (2006). Nongenotoxic p53 activation protects cells against S-phase-specific chemotherapy. Cancer Res *66*, 10274-10280.

Kranz, D., Dohmesen, C., and Dobbelstein, M. (2008). BRCA1 and Tip60 determine the cellular response to ultraviolet irradiation through distinct pathways. J Cell Biol *182*, 197-213.

Krastev, D.B., Slabicki, M., Paszkowski-Rogacz, M., Hubner, N.C., Junqueira, M., Shevchenko, A., Mann, M., Neugebauer, K.M., and Buchholz, F. (2011). A systematic RNAi synthetic interaction screen reveals a link between p53 and snoRNP assembly. Nat Cell Biol *13*, 809-818.

Kress, M., May, E., Cassingena, R., and May, P. (1979). Simian virus 40-transformed cells express new species of proteins precipitable by anti-simian virus 40 tumor serum. J Virol *31*, 472-483.

Krietsch, J., Rouleau, M., Pic, E., Ethier, C., Dawson, T.M., Dawson, V.L., Masson, J.Y., Poirier, G.G., and Gagne, J.P. (2013). Reprogramming cellular events by poly(ADP-ribose)-binding proteins. Mol Aspects Med *34*, 1066-1087.

Krishnamoorthy, A., Jackson, J., Mohamed, T., Adolph, M., Vindigni, A., and Cortez, D. (2021). RADX prevents genome instability by confining replication fork reversal to stalled forks. Mol Cell *81*, 3007-3017 e3005.

Kubbutat, M.H., Jones, S.N., and Vousden, K.H. (1997). Regulation of p53 stability by Mdm2. Nature *387*, 299-303.

Kumari, A., Schultz, N., and Helleday, T. (2004). p53 protects from replication-associated DNA double-strand breaks in mammalian cells. Oncogene *23*, 2324-2329.

Kussie, P.H., Gorina, S., Marechal, V., Elenbaas, B., Moreau, J., Levine, A.J., and Pavletich, N.P. (1996). Structure of the MDM2 oncoprotein bound to the p53 tumor suppressor transactivation domain. Science *274*, 948-953.

Lai, K.P., Leong, W.F., Chau, J.F., Jia, D., Zeng, L., Liu, H., He, L., Hao, A., Zhang, H., Meek, D.*, et al.* (2010). S6K1 is a multifaceted regulator of Mdm2 that connects nutrient status and DNA damage response. EMBO J *29*, 2994-3006.

Lane, D.P. (1992). Cancer. p53, guardian of the genome. Nature *358*, 15-16.

Lane, D.P., and Crawford, L.V. (1979). T antigen is bound to a host protein in SV40-transformed cells. Nature *278*, 261-263.

Langelier, M.F., Planck, J.L., Roy, S., and Pascal, J.M. (2011). Crystal structures of poly(ADP-ribose) polymerase-1 (PARP-1) zinc fingers bound to DNA: structural and functional insights into DNA-dependent PARP-1 activity. J Biol Chem *286*, 10690-10701.

Langelier, M.F., Planck, J.L., Roy, S., and Pascal, J.M. (2012). Structural basis for DNA damage-dependent poly(ADP-ribosyl)ation by human PARP-1. Science *336*, 728-732.

Langelier, M.F., Ruhl, D.D., Planck, J.L., Kraus, W.L., and Pascal, J.M. (2010). The Zn3 domain of human poly(ADP-ribose) polymerase-1 (PARP-1) functions in both DNA-dependent poly(ADP-ribose) synthesis activity and chromatin compaction. J Biol Chem *285*, 18877-18887.

Langelier, M.F., Zandarashvili, L., Aguiar, P.M., Black, B.E., and Pascal, J.M. (2018). NAD(+) analog reveals PARP-1 substrate-blocking mechanism and allosteric communication from catalytic center to DNA-binding domains. Nat Commun *9*, 844.

Larsen, S.C., Hendriks, I.A., Lyon, D., Jensen, L.J., and Nielsen, M.L. (2018). Systems-wide Analysis of Serine ADP-Ribosylation Reveals Widespread Occurrence and Site-Specific Overlap with Phosphorylation. Cell Rep *24*, 2493-2505 e2494.

Ledermann, J.A., and Pujade-Lauraine, E. (2019). Olaparib as maintenance treatment for patients with platinum-sensitive relapsed ovarian cancer. Ther Adv Med Oncol *11*, 1758835919849753.

Legube, G., Linares, L.K., Lemercier, C., Scheffner, M., Khochbin, S., and Trouche, D. (2002). Tip60 is targeted to proteasome-mediated degradation by Mdm2 and accumulates after UV irradiation. EMBO J *21*, 1704-1712.

Lerner, L.K., Francisco, G., Soltys, D.T., Rocha, C.R., Quinet, A., Vessoni, A.T., Castro, L.P., David, T.I., Bustos, S.O., Strauss, B.E.*, et al.* (2017). Predominant role of DNA polymerase eta and p53-dependent translesion synthesis in the survival of ultraviolet-irradiated human cells. Nucleic Acids Res *45*, 1270-1280.

Leung, A.K. (2014). Poly(ADP-ribose): an organizer of cellular architecture. J Cell Biol *205*, 613-619.
Leung, A.K.L. (2020). Poly(ADP-ribose): A Dynamic Trigger for Biomolecular Condensate Formation. Trends Cell Biol *30*, 370-383.

Levine, A.J. (2019). The many faces of p53: something for everyone. J Mol Cell Biol *11*, 524-530.
Levine, A.J., and Oren, M. (2009). The first 30 years of p53: growing ever more complex. Nat Rev Cancer *9*, 749-758.

Li, M., and Yu, X. (2013). Function of BRCA1 in the DNA damage response is mediated by ADP-ribosylation. Cancer Cell *23*, 693-704.

Li, T., Kon, N., Jiang, L., Tan, M., Ludwig, T., Zhao, Y., Baer, R., and Gu, W. (2012). Tumor suppression in the absence of p53-mediated cell-cycle arrest, apoptosis, and senescence. Cell *149*, 1269-1283.

Li, Y., Saini, P., Sriraman, A., and Dobbelstein, M. (2015). Mdm2 inhibition confers protection of p53-proficient cells from the cytotoxic effects of Wee1 inhibitors. Oncotarget *6*, 32339-32352.

Li, Y., Yang, J., Aguilar, A., McEachern, D., Przybranowski, S., Liu, L., Yang, C.Y., Wang, M., Han, X., and Wang, S. (2019). Discovery of MD-224 as a First-in-Class, Highly Potent, and Efficacious Proteolysis Targeting Chimera Murine Double Minute 2 Degrader Capable of Achieving Complete and Durable Tumor Regression. J Med Chem *62*, 448-466.

Lin, A.W., Barradas, M., Stone, J.C., van Aelst, L., Serrano, M., and Lowe, S.W. (1998). Premature senescence involving p53 and p16 is activated in response to constitutive MEK/MAPK mitogenic signaling. Genes Dev *12*, 3008-3019.

Linares, L.K., Hengstermann, A., Ciechanover, A., Muller, S., and Scheffner, M. (2003). HdmX stimulates Hdm2-mediated ubiquitination and degradation of p53. Proc Natl Acad Sci U S A *100*, 12009-12014.

Lindstrom, M.S., Jin, A., Deisenroth, C., White Wolf, G., and Zhang, Y. (2007). Cancer-associated mutations in the MDM2 zinc finger domain disrupt ribosomal protein interaction and attenuate MDM2-induced p53 degradation. Mol Cell Biol *27*, 1056-1068.

Linke, K., Mace, P.D., Smith, C.A., Vaux, D.L., Silke, J., and Day, C.L. (2008). Structure of the MDM2/MDMX RING domain heterodimer reveals dimerization is required for their ubiquitylation in trans. Cell Death Differ *15*, 841-848.

Linzer, D.I., and Levine, A.J. (1979). Characterization of a 54K dalton cellular SV40 tumor antigen present in SV40-transformed cells and uninfected embryonal carcinoma cells. Cell *17*, 43-52.
Liu, G., and Chen, X. (2006). DNA polymerase eta, the product of the xeroderma pigmentosum variant gene and a target of p53, modulates the DNA damage checkpoint and p53 activation. Mol Cell Biol *26*, 1398-1413.

Liu, X., Yue, P., Khuri, F.R., and Sun, S.Y. (2004). p53 upregulates death receptor 4 expression through an intronic p53 binding site. Cancer Res *64*, 5078-5083.

Livneh, Z. (2006). Keeping mammalian mutation load in check: regulation of the activity of error-prone DNA polymerases by p53 and p21. Cell Cycle *5*, 1918-1922.

Loizou, J.I., El-Khamisy, S.F., Zlatanou, A., Moore, D.J., Chan, D.W., Qin, J., Sarno, S., Meggio, F., Pinna, L.A., and Caldecott, K.W. (2004). The protein kinase CK2 facilitates repair of chromosomal DNA single-strand breaks. Cell *117*, 17-28.

Lomonosov, M., Anand, S., Sangrithi, M., Davies, R., and Venkitaraman, A.R. (2003). Stabilization of stalled DNA replication forks by the BRCA2 breast cancer susceptibility protein. Genes Dev *17*, 3017-3022.

Longarini, E.J., and Matic, I. (2022). The fast-growing business of Serine ADP-ribosylation. DNA Repair (Amst) *118*, 103382.

Lord, C.J., and Ashworth, A. (2017). PARP inhibitors: Synthetic lethality in the clinic. Science *355*, 1152-1158.

Lu, X., Ma, O., Nguyen, T.A., Jones, S.N., Oren, M., and Donehower, L.A. (2007). The Wip1 Phosphatase acts as a gatekeeper in the p53-Mdm2 autoregulatory loop. Cancer Cell *12*, 342-354.

Luijsterburg, M.S., de Krijger, I., Wiegant, W.W., Shah, R.G., Smeenk, G., de Groot, A.J.L., Pines, A., Vertegaal, A.C.O., Jacobs, J.J.L., Shah, G.M.*, et al.* (2016). PARP1 Links CHD2-Mediated Chromatin Expansion and H3.3 Deposition to DNA Repair by Non-homologous End-Joining. Mol Cell *61*, 547-562.

Luijsterburg, M.S., Lindh, M., Acs, K., Vrouwe, M.G., Pines, A., van Attikum, H., Mullenders, L.H., and Dantuma, N.P. (2012). DDB2 promotes chromatin decondensation at UV-induced DNA damage. J Cell Biol *197*, 267-281.

Luo, Y., Hurwitz, J., and Massague, J. (1995). Cell-cycle inhibition by independent CDK and PCNA binding domains in p21Cip1. Nature *375*, 159-161.

Madison, D.L., and Lundblad, J.R. (2010). C-terminal binding protein and poly(ADP)ribose polymerase 1 contribute to repression of the p21(waf1/cip1) promoter. Oncogene *29*, 6027-6039.

Mak, J.P.Y., Ma, H.T., and Poon, R.Y.C. (2020). Synergism between ATM and PARP1 Inhibition Involves DNA Damage and Abrogating the G2 DNA Damage Checkpoint. Mol Cancer Ther *19*, 123-134.

Malanga, M., Pleschke, J.M., Kleczkowska, H.E., and Althaus, F.R. (1998). Poly(ADP-ribose) binds to specific domains of p53 and alters its DNA binding functions. J Biol Chem *273*, 11839-11843.

Malkin, D., Li, F.P., Strong, L.C., Fraumeni, J.F., Jr., Nelson, C.E., Kim, D.H., Kassel, J., Gryka, M.A., Bischoff, F.Z., Tainsky, M.A.*, et al.* (1990). Germ line p53 mutations in a familial syndrome of breast cancer, sarcomas, and other neoplasms. Science *250*, 1233-1238.

Mansilla, S.F., Bertolin, A.P., Bergoglio, V., Pillaire, M.J., Gonzalez Besteiro, M.A., Luzzani, C., Miriuka, S.G., Cazaux, C., Hoffmann, J.S., and Gottifredi, V. (2016). Cyclin Kinase-independent role of p21(CDKN1A) in the promotion of nascent DNA elongation in unstressed cells. Elife *5*.

Mansilla, S.F., Soria, G., Vallerga, M.B., Habif, M., Martinez-Lopez, W., Prives, C., and Gottifredi, V. (2013). UV-triggered p21 degradation facilitates damaged-DNA replication and preserves genomic stability. Nucleic Acids Res *41*, 6942-6951.

Marechal, A., and Zou, L. (2013). DNA damage sensing by the ATM and ATR kinases. Cold Spring Harb Perspect Biol *5*.

Marintchev, A., Robertson, A., Dimitriadis, E.K., Prasad, R., Wilson, S.H., and Mullen, G.P. (2000). Domain specific interaction in the XRCC1-DNA polymerase beta complex. Nucleic Acids Res *28*, 2049-2059.

Marteijn, J.A., Lans, H., Vermeulen, W., and Hoeijmakers, J.H. (2014). Understanding nucleotide excision repair and its roles in cancer and ageing. Nat Rev Mol Cell Biol *15*, 465-481.

Mattia, M., Gottifredi, V., McKinney, K., and Prives, C. (2007). p53-Dependent p21 mRNA elongation is impaired when DNA replication is stalled. Mol Cell Biol *27*, 1309-1320.

Maya-Mendoza, A., Moudry, P., Merchut-Maya, J.M., Lee, M., Strauss, R., and Bartek, J. (2018). High speed of fork progression induces DNA replication stress and genomic instability. Nature *559*, 279-284.
Maya, R., Balass, M., Kim, S.T., Shkedy, D., Leal, J.F., Shifman, O., Moas, M., Buschmann, T., Ronai, Z., Shiloh, Y.*, et al.* (2001). ATM-dependent phosphorylation of Mdm2 on serine 395: role in p53 activation by DNA damage. Genes Dev *15*, 1067-1077.

Mayo, L.D., Turchi, J.J., and Berberich, S.J. (1997). Mdm-2 phosphorylation by DNA-dependent protein kinase prevents interaction with p53. Cancer Res *57*, 5013-5016.

Mehta, A., and Haber, J.E. (2014). Sources of DNA double-strand breaks and models of recombinational DNA repair. Cold Spring Harb Perspect Biol *6*, a016428.

Mehta, K.P.M., Thada, V., Zhao, R., Krishnamoorthy, A., Leser, M., Lindsey Rose, K., and Cortez, D. (2022). CHK1 phosphorylates PRIMPOL to promote replication stress tolerance. Sci Adv *8*, eabm0314.

Melero, J.A., Stitt, D.T., Mangel, W.F., and Carroll, R.B. (1979). Identification of new polypeptide species (48-55K) immunoprecipitable by antiserum to purified large T antigen and present in SV40-infected and -transformed cells. Virology *93*, 466-480.

Menendez, D., Inga, A., and Resnick, M.A. (2009). The expanding universe of p53 targets. Nat Rev Cancer *9*, 724-737.

Merchut-Maya, J.M., Bartek, J., and Maya-Mendoza, A. (2019). Regulation of replication fork speed: Mechanisms and impact on genomic stability. DNA Repair (Amst) *81*, 102654.

Meyer, T., and Hilz, H. (1986). Production of anti-(ADP-ribose) antibodies with the aid of a dinucleotide-pyrophosphatase-resistant hapten and their application for the detection of mono(ADP-ribosyl)ated polypeptides. Eur J Biochem *155*, 157-165.

Michalovitz, D., Halevy, O., and Oren, M. (1990). Conditional inhibition of transformation and of cell proliferation by a temperature-sensitive mutant of p53. Cell *62*, 671-680.

Michelena, J., Lezaja, A., Teloni, F., Schmid, T., Imhof, R., and Altmeyer, M. (2018). Analysis of PARP inhibitor toxicity by multidimensional fluorescence microscopy reveals mechanisms of sensitivity and resistance. Nat Commun *9*, 2678.

Min, W., Cortes, U., Herceg, Z., Tong, W.M., and Wang, Z.Q. (2010). Deletion of the nuclear isoform of poly(ADP-ribose) glycohydrolase (PARG) reveals its function in DNA repair, genomic stability and tumorigenesis. Carcinogenesis *31*, 2058-2065.

Miyashita, T., and Reed, J.C. (1995). Tumor suppressor p53 is a direct transcriptional activator of the human bax gene. Cell *80*, 293-299.

Momand, J., Zambetti, G.P., Olson, D.C., George, D., and Levine, A.J. (1992). The mdm-2 oncogene product forms a complex with the p53 protein and inhibits p53-mediated transactivation. Cell *69*, 1237-1245.

Morgan, W.F., and Cleaver, J.E. (1982). 3-Aminobenzamide synergistically increases sister-chromatid exchanges in cells exposed to methyl methanesulfonate but not to ultraviolet light. Mutat Res *104*, 361-366.

Muller, M., Wilder, S., Bannasch, D., Israeli, D., Lehlbach, K., Li-Weber, M., Friedman, S.L., Galle, P.R., Stremmel, W., Oren, M.*, et al.* (1998). p53 activates the CD95 (APO-1/Fas) gene in response to DNA damage by anticancer drugs. J Exp Med *188*, 2033-2045.

Munnur, D., and Ahel, I. (2017). Reversible mono-ADP-ribosylation of DNA breaks. FEBS J *284*, 4002-4016.

Munnur, D., Bartlett, E., Mikolcevic, P., Kirby, I.T., Rack, J.G.M., Mikoc, A., Cohen, M.S., and Ahel, I. (2019). Reversible ADP-ribosylation of RNA. Nucleic Acids Res *47*, 5658-5669.

Munsch, D., Watanabe-Fukunaga, R., Bourdon, J.C., Nagata, S., May, E., Yonish-Rouach, E., and Reisdorf, P. (2000). Human and mouse Fas (APO-1/CD95) death receptor genes each contain a p53-responsive element that is activated by p53 mutants unable to induce apoptosis. J Biol Chem *275*, 3867-3872.

Murai, J., Huang, S.Y., Das, B.B., Renaud, A., Zhang, Y., Doroshow, J.H., Ji, J., Takeda, S., and Pommier, Y. (2012). Trapping of PARP1 and PARP2 by Clinical PARP Inhibitors. Cancer Res *72*, 5588-5599.

Nakano, K., and Vousden, K.H. (2001). PUMA, a novel proapoptotic gene, is induced by p53. Mol Cell *7*, 683-694.

Nayak, S., Calvo, J.A., Cong, K., Peng, M., Berthiaume, E., Jackson, J., Zaino, A.M., Vindigni, A., Hadden, M.K., and Cantor, S.B. (2020). Inhibition of the translesion synthesis polymerase REV1 exploits replication gaps as a cancer vulnerability. Sci Adv *6*, eaaz7808.

Neelsen, K.J., and Lopes, M. (2015). Replication fork reversal in eukaryotes: from dead end to dynamic response. Nat Rev Mol Cell Biol *16*, 207-220.

Nishikimi, M., Ogasawara, K., Kameshita, I., Taniguchi, T., and Shizuta, Y. (1982). Poly(ADP-ribose) synthetase. The DNA binding domain and the automodification domain. J Biol Chem *257*, 6102-6105.

O'Sullivan, J., Tedim Ferreira, M., Gagne, J.P., Sharma, A.K., Hendzel, M.J., Masson, J.Y., and Poirier, G.G. (2019). Emerging roles of eraser enzymes in the dynamic control of protein ADP-ribosylation. Nat Commun *10*, 1182.

Oikawa, A., Tohda, H., Kanai, M., Miwa, M., and Sugimura, T. (1980). Inhibitors of poly(adenosine diphosphate ribose) polymerase induce sister chromatid exchanges. Biochem Biophys Res Commun *97*, 1311-1316.

Oliner, J.D., Pietenpol, J.A., Thiagalingam, S., Gyuris, J., Kinzler, K.W., and Vogelstein, B. (1993). Oncoprotein MDM2 conceals the activation domain of tumour suppressor p53. Nature *362*, 857-860.

Orta, M.L., Hoglund, A., Calderon-Montano, J.M., Dominguez, I., Burgos-Moron, E., Visnes, T., Pastor, N., Strom, C., Lopez-lazaro, M., and Helleday, T. (2014). The PARP inhibitor Olaparib disrupts base excision repair of 5-aza-2'-deoxycytidine lesions. Nucleic Acids Res *42*, 9108-9120.

Pachkowski, B.F., Tano, K., Afonin, V., Elder, R.H., Takeda, S., Watanabe, M., Swenberg, J.A., and Nakamura, J. (2009). Cells deficient in PARP-1 show an accelerated accumulation of DNA single strand breaks, but not AP sites, over the PARP-1-proficient cells exposed to MMS. Mutat Res *671*, 93-99.

Palazzo, L., Leidecker, O., Prokhorova, E., Dauben, H., Matic, I., and Ahel, I. (2018). Serine is the major residue for ADP-ribosylation upon DNA damage. Elife *7*.

Palazzo, L., Suskiewicz, M.J., and Ahel, I. (2021). Serine ADP-ribosylation in DNA-damage response regulation. Curr Opin Genet Dev *71*, 106-113.

Pandey, N., and Black, B.E. (2021). Rapid Detection and Signaling of DNA Damage by PARP-1. Trends Biochem Sci *46*, 744-757.

Parada, L.F., Land, H., Weinberg, R.A., Wolf, D., and Rotter, V. (1984). Cooperation between gene encoding p53 tumour antigen and ras in cellular transformation. Nature *312*, 649-651.

Pearson, M., Carbone, R., Sebastiani, C., Cioce, M., Fagioli, M., Saito, S., Higashimoto, Y., Appella, E., Minucci, S., Pandolfi, P.P.*, et al.* (2000). PML regulates p53 acetylation and premature senescence induced by oncogenic Ras. Nature *406*, 207-210.

Pines, A., Vrouwe, M.G., Marteijn, J.A., Typas, D., Luijsterburg, M.S., Cansoy, M., Hensbergen, P., Deelder, A., de Groot, A., Matsumoto, S.*, et al.* (2012). PARP1 promotes nucleotide excision repair through DDB2 stabilization and recruitment of ALC1. J Cell Biol *199*, 235-249.

Pommier, Y., O'Connor, M.J., and de Bono, J. (2016). Laying a trap to kill cancer cells: PARP inhibitors and their mechanisms of action. Sci Transl Med *8*, 362ps317.

Pouliot, J.J., Yao, K.C., Robertson, C.A., and Nash, H.A. (1999). Yeast gene for a Tyr-DNA phosphodiesterase that repairs topoisomerase I complexes. Science *286*, 552-555.

Price, B.D., and D'Andrea, A.D. (2013). Chromatin remodeling at DNA double-strand breaks. Cell *152*, 1344-1354.

Prokhorova, E., Agnew, T., Wondisford, A.R., Tellier, M., Kaminski, N., Beijer, D., Holder, J., Groslambert, J., Suskiewicz, M.J., Zhu, K.*, et al.* (2021a). Unrestrained poly-ADP-ribosylation provides insights into chromatin regulation and human disease. Mol Cell *81*, 2640-2655 e2648.

Prokhorova, E., Zobel, F., Smith, R., Zentout, S., Gibbs-Seymour, I., Schutzenhofer, K., Peters, A., Groslambert, J., Zorzini, V., Agnew, T.*, et al.* (2021b). Serine-linked PARP1 auto-modification controls PARP inhibitor response. Nat Commun *12*, 4055.

Quinet, A., Lemacon, D., and Vindigni, A. (2017). Replication Fork Reversal: Players and Guardians. Mol Cell *68*, 830-833.

Quinet, A., Tirman, S., Jackson, J., Svikovic, S., Lemacon, D., Carvajal-Maldonado, D., Gonzalez-Acosta, D., Vessoni, A.T., Cybulla, E., Wood, M.*, et al.* (2020). PRIMPOL-Mediated Adaptive Response Suppresses Replication Fork Reversal in BRCA-Deficient Cells. Mol Cell *77*, 461-474 e469.

Ray-Coquard, I., Blay, J.Y., Italiano, A., Le Cesne, A., Penel, N., Zhi, J., Heil, F., Rueger, R., Graves, B., Ding, M.*, et al.* (2012). Effect of the MDM2 antagonist RG7112 on the P53 pathway in patients with MDM2-amplified, well-differentiated or dedifferentiated liposarcoma: an exploratory proof-of-mechanism study. Lancet Oncol *13*, 1133-1140.

Ray Chaudhuri, A., Ahuja, A.K., Herrador, R., and Lopes, M. (2015). Poly(ADP-ribosyl) glycohydrolase prevents the accumulation of unusual replication structures during unperturbed S phase. Mol Cell Biol *35*, 856-865.

Ray Chaudhuri, A., Hashimoto, Y., Herrador, R., Neelsen, K.J., Fachinetti, D., Bermejo, R., Cocito, A., Costanzo, V., and Lopes, M. (2012). Topoisomerase I poisoning results in PARP-mediated replication fork reversal. Nat Struct Mol Biol *19*, 417-423.

Ray Chaudhuri, A., and Nussenzweig, A. (2017). The multifaceted roles of PARP1 in DNA repair and chromatin remodelling. Nat Rev Mol Cell Biol *18*, 610-621.

Rayburn, E., Zhang, R., He, J., and Wang, H. (2005). MDM2 and human malignancies: expression, clinical pathology, prognostic markers, and implications for chemotherapy. Curr Cancer Drug Targets *5*, 27-41.

Raycroft, L., Wu, H.Y., and Lozano, G. (1990). Transcriptional activation by wild-type but not transforming mutants of the p53 anti-oncogene. Science *249*, 1049-1051.

Reynolds, P., Cooper, S., Lomax, M., and O'Neill, P. (2015). Disruption of PARP1 function inhibits base excision repair of a sub-set of DNA lesions. Nucleic Acids Res *43*, 4028-4038.

Robles, A.I., Bemmels, N.A., Foraker, A.B., and Harris, C.C. (2001). APAF-1 is a transcriptional target of p53 in DNA damage-induced apoptosis. Cancer Res *61*, 6660-6664.

Robu, M., Shah, R.G., Petitclerc, N., Brind'Amour, J., Kandan-Kulangara, F., and Shah, G.M. (2013). Role of poly(ADP-ribose) polymerase-1 in the removal of UV-induced DNA lesions by nucleotide excision repair. Proc Natl Acad Sci U S A *110*, 1658-1663.

Roninson, I.B. (2002). Oncogenic functions of tumour suppressor p21(Waf1/Cip1/Sdi1): association with cell senescence and tumour-promoting activities of stromal fibroblasts. Cancer Lett *179*, 1-14.

Rose, M., Burgess, J.T., O'Byrne, K., Richard, D.J., and Bolderson, E. (2020). PARP Inhibitors: Clinical Relevance, Mechanisms of Action and Tumor Resistance. Front Cell Dev Biol *8*, 564601.

Roth, J., Dobbelstein, M., Freedman, D.A., Shenk, T., and Levine, A.J. (1998). Nucleo-cytoplasmic shuttling of the hdm2 oncoprotein regulates the levels of the p53 protein via a pathway used by the human immunodeficiency virus rev protein. EMBO J *17*, 554-564.

Rotter, V., Witte, O.N., Coffman, R., and Baltimore, D. (1980). Abelson murine leukemia virus-induced tumors elicit antibodies against a host cell protein, P50. J Virol *36*, 547-555.

Rouault, J.P., Falette, N., Guehenneux, F., Guillot, C., Rimokh, R., Wang, Q., Berthet, C., Moyret-Lalle, C., Savatier, P., Pain, B.*, et al.* (1996). Identification of BTG2, an antiproliferative p53-dependent component of the DNA damage cellular response pathway. Nat Genet *14*, 482-486.

Roy, S., Tomaszowski, K.H., Luzwick, J.W., Park, S., Li, J., Murphy, M., and Schlacher, K. (2018). p53 orchestrates DNA replication restart homeostasis by suppressing mutagenic RAD52 and POLtheta pathways. Elife *7*.

Ruscetti, T., Lehnert, B.E., Halbrook, J., Le Trong, H., Hoekstra, M.F., Chen, D.J., and Peterson, S.R. (1998). Stimulation of the DNA-dependent protein kinase by poly(ADP-ribose) polymerase. J Biol Chem *273*, 14461-14467.

Schilling, T., Schleithoff, E.S., Kairat, A., Melino, G., Stremmel, W., Oren, M., Krammer, P.H., and Muller, M. (2009). Active transcription of the human FAS/CD95/TNFRSF6 gene involves the p53 family. Biochem Biophys Res Commun *387*, 399-404.

Schlacher, K., Christ, N., Siaud, N., Egashira, A., Wu, H., and Jasin, M. (2011). Double-strand break repair-independent role for BRCA2 in blocking stalled replication fork degradation by MRE11. Cell *145*, 529-542.

Schultz, N., Lopez, E., Saleh-Gohari, N., and Helleday, T. (2003). Poly(ADP-ribose) polymerase (PARP-1) has a controlling role in homologous recombination. Nucleic Acids Res *31*, 4959-4964.

Schwertman, P., Bekker-Jensen, S., and Mailand, N. (2016). Regulation of DNA double-strand break repair by ubiquitin and ubiquitin-like modifiers. Nat Rev Mol Cell Biol *17*, 379-394.

Setton, J., Zinda, M., Riaz, N., Durocher, D., Zimmermann, M., Koehler, M., Reis-Filho, J.S., and Powell, S.N. (2021). Synthetic Lethality in Cancer Therapeutics: The Next Generation. Cancer Discov *11*, 1626-1635.

Shibue, T., Takeda, K., Oda, E., Tanaka, H., Murasawa, H., Takaoka, A., Morishita, Y., Akira, S., Taniguchi, T., and Tanaka, N. (2003). Integral role of Noxa in p53-mediated apoptotic response. Genes Dev *17*, 2233-2238.

Shivakumar, C.V., Brown, D.R., Deb, S., and Deb, S.P. (1995). Wild-type human p53 transactivates the human proliferating cell nuclear antigen promoter. Mol Cell Biol *15*, 6785-6793.

Shvarts, A., Steegenga, W.T., Riteco, N., van Laar, T., Dekker, P., Bazuine, M., van Ham, R.C., van der Houven van Oordt, W., Hateboer, G., van der Eb, A.J*., et al.* (1996). MDMX: a novel p53-binding protein with some functional properties of MDM2. EMBO J *15*, 5349-5357.

Simbulan-Rosenthal, C.M., Rosenthal, D.S., Luo, R.B., Samara, R., Jung, M., Dritschilo, A., Spoonde, A., and Smulson, M.E. (2001). Poly(ADP-ribosyl)ation of p53 in vitro and in vivo modulates binding to its DNA consensus sequence. Neoplasia *3*, 179-188.

Skalniak, L., Twarda-Clapa, A., Neochoritis, C.G., Surmiak, E., Machula, M., Wisniewska, A., Labuzek, B., Ali, A.M., Krzanik, S., Dubin, G*., et al.* (2019). A fluorinated indole-based MDM2 antagonist selectively inhibits the growth of p53(wt) osteosarcoma cells. FEBS J *286*, 1360-1374.

Slade, D., Dunstan, M.S., Barkauskaite, E., Weston, R., Lafite, P., Dixon, N., Ahel, M., Leys, D., and Ahel, I. (2011). The structure and catalytic mechanism of a poly(ADP-ribose) glycohydrolase. Nature *477*, 616-620.

Smith, A.E., Smith, R., and Paucha, E. (1979). Characterization of different tumor antigens present in cells transformed by simian virus 40. Cell *18*, 335-346.

Spagnolo, L., Barbeau, J., Curtin, N.J., Morris, E.P., and Pearl, L.H. (2012). Visualization of a DNA-PK/PARP1 complex. Nucleic Acids Res *40*, 4168-4177.

Srdanovic, S., Wolter, M., Trinh, C.H., Ottmann, C., Warriner, S.L., and Wilson, A.J. (2022). Understanding the interaction of 14-3-3 proteins with hDMX and hDM2: a structural and biophysical study. FEBS J *289*, 5341-5358.

Srivastava, S., Zou, Z.Q., Pirollo, K., Blattner, W., and Chang, E.H. (1990). Germ-line transmission of a mutated p53 gene in a cancer-prone family with Li-Fraumeni syndrome. Nature *348*, 747-749.

Stehelin, D., Varmus, H.E., Bishop, J.M., and Vogt, P.K. (1976). DNA related to the transforming gene(s) of avian sarcoma viruses is present in normal avian DNA. Nature *260*, 170-173.

Strom, C.E., Johansson, F., Uhlen, M., Szigyarto, C.A., Erixon, K., and Helleday, T. (2011). Poly (ADP-ribose) polymerase (PARP) is not involved in base excision repair but PARP inhibition traps a single-strand intermediate. Nucleic Acids Res *39*, 3166-3175.

Sugasawa, K. (2019). Mechanism and regulation of DNA damage recognition in mammalian nucleotide excision repair. Enzymes *45*, 99-138.

Suskiewicz, M.J., Palazzo, L., Hughes, R., and Ahel, I. (2021). Progress and outlook in studying the substrate specificities of PARPs and related enzymes. FEBS J *288*, 2131-2142.

Suskiewicz, M.J., Zobel, F., Ogden, T.E.H., Fontana, P., Ariza, A., Yang, J.C., Zhu, K., Bracken, L., Hawthorne, W.J., Ahel, D.*, et al.* (2020). HPF1 completes the PARP active site for DNA damage-induced ADP-ribosylation. Nature *579*, 598-602.

Takamura-Enya, T., Watanabe, M., Totsuka, Y., Kanazawa, T., Matsushima-Hibiya, Y., Koyama, K., Sugimura, T., and Wakabayashi, K. (2001). Mono(ADP-ribosyl)ation of 2'-deoxyguanosine residue in DNA by an apoptosis-inducing protein, pierisin-1, from cabbage butterfly. Proc Natl Acad Sci U S A *98*, 12414-12419.

Takimoto, R., and El-Deiry, W.S. (2000). Wild-type p53 transactivates the KILLER/DR5 gene through an intronic sequence-specific DNA-binding site. Oncogene *19*, 1735-1743.

Talhaoui, I., Lebedeva, N.A., Zarkovic, G., Saint-Pierre, C., Kutuzov, M.M., Sukhanova, M.V., Matkarimov, B.T., Gasparutto, D., Saparbaev, M.K., Lavrik, O.I.*, et al.* (2016). Poly(ADP-ribose) polymerases covalently modify strand break termini in DNA fragments in vitro. Nucleic Acids Res *44*, 9279-9295.

Tan, T., and Chu, G. (2002). p53 Binds and activates the xeroderma pigmentosum DDB2 gene in humans but not mice. Mol Cell Biol *22*, 3247-3254.

Tanaka, H., Arakawa, H., Yamaguchi, T., Shiraishi, K., Fukuda, S., Matsui, K., Takei, Y., and Nakamura, Y. (2000). A ribonucleotide reductase gene involved in a p53-dependent cell-cycle checkpoint for DNA damage. Nature *404*, 42-49.

Teloni, F., and Altmeyer, M. (2016). Readers of poly(ADP-ribose): designed to be fit for purpose. Nucleic Acids Res *44*, 993-1006.

Tomasetti, C., Li, L., and Vogelstein, B. (2017). Stem cell divisions, somatic mutations, cancer etiology, and cancer prevention. Science *355*, 1330-1334.

Tromans-Coia, C., Sanchi, A., Moeller, G.K., Timinszky, G., Lopes, M., and Ahel, I. (2021). TARG1 protects against toxic DNA ADP-ribosylation. Nucleic Acids Res *49*, 10477-10492.

Truong, L.N., Li, Y., Shi, L.Z., Hwang, P.Y., He, J., Wang, H., Razavian, N., Berns, M.W., and Wu, X. (2013). Microhomology-mediated End Joining and Homologous Recombination share the initial end resection step to repair DNA double-strand breaks in mammalian cells. Proc Natl Acad Sci U S A *110*, 7720-7725.

Vaitsiankova, A., Burdova, K., Sobol, M., Gautam, A., Benada, O., Hanzlikova, H., and Caldecott, K.W. (2022). PARP inhibition impedes the maturation of nascent DNA strands during DNA replication. Nat Struct Mol Biol *29*, 329-338.

Valente, L.J., Gray, D.H., Michalak, E.M., Pinon-Hofbauer, J., Egle, A., Scott, C.L., Janic, A., and Strasser, A. (2013). p53 efficiently suppresses tumor development in the complete absence of its cell-cycle inhibitory and proapoptotic effectors p21, Puma, and Noxa. Cell Rep *3*, 1339-1345.

Vassilev, L.T. (2007). MDM2 inhibitors for cancer therapy. Trends Mol Med *13*, 23-31.

Vassilev, L.T., Vu, B.T., Graves, B., Carvajal, D., Podlaski, F., Filipovic, Z., Kong, N., Kammlott, U., Lukacs, C., Klein, C.*, et al.* (2004). In vivo activation of the p53 pathway by small-molecule antagonists of MDM2. Science *303*, 844-848.

Vodenicharov, M.D., Sallmann, F.R., Satoh, M.S., and Poirier, G.G. (2000). Base excision repair is efficient in cells lacking poly(ADP-ribose) polymerase 1. Nucleic Acids Res *28*, 3887-3896.

Vogelstein, B., Lane, D., and Levine, A.J. (2000). Surfing the p53 network. Nature *408*, 307-310.

Vyas, S., Matic, I., Uchima, L., Rood, J., Zaja, R., Hay, R.T., Ahel, I., and Chang, P. (2014). Family-wide analysis of poly(ADP-ribose) polymerase activity. Nat Commun *5*, 4426.

Wade, M., Li, Y.C., and Wahl, G.M. (2013). MDM2, MDMX and p53 in oncogenesis and cancer therapy. Nature reviews. Cancer *13*, 83-96.

Wang, X., Ohnishi, K., Takahashi, A., and Ohnishi, T. (1998). Poly(ADP-ribosyl)ation is required for p53-dependent signal transduction induced by radiation. Oncogene *17*, 2819-2825.

Wang, X.W., Zhan, Q., Coursen, J.D., Khan, M.A., Kontny, H.U., Yu, L., Hollander, M.C., O'Connor, P.M., Fornace, A.J., Jr., and Harris, C.C. (1999). GADD45 induction of a G2/M cell cycle checkpoint. Proc Natl Acad Sci U S A *96*, 3706-3711.

Wang, Y., Kim, N.S., Haince, J.F., Kang, H.C., David, K.K., Andrabi, S.A., Poirier, G.G., Dawson, V.L., and Dawson, T.M. (2011). Poly(ADP-ribose) (PAR) binding to apoptosis-inducing factor is critical for PAR polymerase-1-dependent cell death (parthanatos). Sci Signal *4*, ra20.

Whitehouse, C.J., Taylor, R.M., Thistlethwaite, A., Zhang, H., Karimi-Busheri, F., Lasko, D.D., Weinfeld, M., and Caldecott, K.W. (2001). XRCC1 stimulates human polynucleotide kinase activity at damaged DNA termini and accelerates DNA single-strand break repair. Cell *104*, 107-117.

Wienken, M., Dickmanns, A., Nemajerova, A., Kramer, D., Najafova, Z., Weiss, M., Karpiuk, O., Kassem, M., Zhang, Y., Lozano, G.*, et al.* (2016). MDM2 Associates with Polycomb Repressor Complex 2 and Enhances Stemness-Promoting Chromatin Modifications Independent of p53. Mol Cell *61*, 68-83.

Wilson, S.H., and Kunkel, T.A. (2000). Passing the baton in base excision repair. Nat Struct Biol *7*, 176-178.

Wohlberedt, K., Klusmann, I., Derevyanko, P.K., Henningsen, K., Choo, J., Manzini, V., Magerhans, A., Giansanti, C., Eischen, C.M., Jochemsen, A.G.*, et al.* (2020). Mdm4 supports DNA replication in a p53-independent fashion. Oncogene *39*, 4828-4843.

Xie, L., Gazin, C., Park, S.M., Zhu, L.J., Debily, M.A., Kittler, E.L., Zapp, M.L., Lapointe, D., Gobeil, S., Virbasius, C.M.*, et al.* (2012). A synthetic interaction screen identifies factors selectively required for proliferation and TERT transcription in p53-deficient human cancer cells. PLoS Genet *8*, e1003151.

Yan, Y., Xu, Z., Huang, J., Guo, G., Gao, M., Kim, W., Zeng, X., Kloeber, J.A., Zhu, Q., Zhao, F.*, et al.* (2020). The deubiquitinase USP36 Regulates DNA replication stress and confers therapeutic resistance through PrimPol stabilization. Nucleic Acids Res *48*, 12711-12726.

Yang, G., Liu, C., Chen, S.H., Kassab, M.A., Hoff, J.D., Walter, N.G., and Yu, X. (2018). Super-resolution imaging identifies PARP1 and the Ku complex acting as DNA double-strand break sensors. Nucleic Acids Res *46*, 3446-3457.

Yang, L., Sun, L., Teng, Y., Chen, H., Gao, Y., Levine, A.S., Nakajima, S., and Lan, L. (2017). Tankyrase1-mediated poly(ADP-ribosyl)ation of TRF1 maintains cell survival after telomeric DNA damage. Nucleic Acids Res *45*, 3906-3921.

Yang, W., and Gao, Y. (2018). Translesion and Repair DNA Polymerases: Diverse Structure and Mechanism. Annu Rev Biochem *87*, 239-261.

Yang, Y.G., Cortes, U., Patnaik, S., Jasin, M., and Wang, Z.Q. (2004). Ablation of PARP-1 does not interfere with the repair of DNA double-strand breaks, but compromises the reactivation of stalled replication forks. Oncogene *23*, 3872-3882.

Yeo, C.Q.X., Alexander, I., Lin, Z., Lim, S., Aning, O.A., Kumar, R., Sangthongpitag, K., Pendharkar, V., Ho, V.H.B., and Cheok, C.F. (2016). p53 Maintains Genomic Stability by Preventing Interference between Transcription and Replication. Cell Rep *15*, 132-146.

Zandarashvili, L., Langelier, M.F., Velagapudi, U.K., Hancock, M.A., Steffen, J.D., Billur, R., Hannan, Z.M., Wicks, A.J., Krastev, D.B., Pettitt, S.J.*, et al.* (2020). Structural basis for allosteric PARP-1 retention on DNA breaks. Science *368*.

Zauberman, A., Flusberg, D., Haupt, Y., Barak, Y., and Oren, M. (1995). A functional p53-responsive intronic promoter is contained within the human mdm2 gene. Nucleic Acids Res *23*, 2584-2592.

Zhang, Y., Wolf, G.W., Bhat, K., Jin, A., Allio, T., Burkhart, W.A., and Xiong, Y. (2003). Ribosomal protein L11 negatively regulates oncoprotein MDM2 and mediates a p53-dependent ribosomal-stress checkpoint pathway. Mol Cell Biol *23*, 8902-8912.

Zhu, J., Zhou, W., Jiang, J., and Chen, X. (1998). Identification of a novel p53 functional domain that is necessary for mediating apoptosis. J Biol Chem *273*, 13030-13036.